UNIVERSITÀ DEGLI STUDI DI PADOVA

CORSO DI LAUREA MAGISTRALE IN INGEGNERIA ELETTRICA

TESI DI LAUREA MAGISTRALE

Analysis and possible improvements of a Rogowski transducer for current measurements in a lightning laboratory for aerospace applications

Studio di un trasduttore Rogowski e possibili soluzioni per misure di corrente in un laboratorio di alte tensioni per prove in ambito aeronautico

RELATORE: PROF. ROBERTO TURRI
DIPARTIMENTO DI INGEGNERIA INDUSTRIALE

CORRELATORE: PROF. MANU HADDAD
SCHOOL OF ENGINEERING, CARDIFF UNIVERSITY

LAUREANDO: FRANCESCO SINDICO

ANNO ACCADEMICO 2013-2014

Contents

Abstract Scopo di questo lavoro di analizzare e testare un trasduttore basato su sonda Rogowski per la misura di impulsi di corrente di fulmine oltre i 100kA. L'obiettivo di implementare il trasduttore nel Data acquisition System del Morgan Botti Laboratory (Cardiff). Vengono proposte soluzioni per incrementare il SNR del segnale misurato mediante filtraggio numerico ed elettronico. Dai risultati si osserva la la dipendenza delle forme d'onda misurate dal tipo di sonda e dalla posizione nel circuito. Si studiano possibili interferenze derivate dal circuito di generazione dell'impulso.

Introduzione Il laboratorio Morgan-Botti (Cardiff, Regno Unito) si prefigge lo scopo di impiegare circuiti RLC per simulare le correnti di fulmine, secondo gli standard aeronautici EUROCAE ED14, ED84 e ED105.
In questo modo sarà possibile studiare gli effetti (diretti e indiretti) del fulmine sui materiali e componenti in fase di adozione sugli aeromobili di nuova concezione. In particolare, nel Laboratorio si studieranno i meccanismi di conduzione, degrad azione e cedimento dei materiali compositi a seguito di scariche cerauniche. Il Laboratorio sarà d'ausilio nella progettazione di componenti in fibra di carbonio capaci di minimizzare gli effetti del fulmine.

Questa tesi analizza le problematiche connesse alla misurazione dell'impulso di corrente di tipo D (secondo ED84) mediante l'utilizzo di una sonda Rogowski. L'obiettivo è dunque di contribuire al miglioramento del sistema di acquisizione dati (Data Acquisition System) di cui il Laboratorio ha bisogno per il suo funzionamento e per l'esecuzione dei test sui materiali aeronautici.

Il problema da affrontare è l'esecuzione di misure di buona qualità (basso SNR e limitati disturbi) in un contesto di rumore elettromagnetico, verosimilmente causato dalle componenti elettriche del laboratorio che generano l'impulso di corrente. I componenti del circuito (banco di condensatori, resistenze e induttori, principalmente) sono caratterizzati da elevate variazioni di tensione (oltre 55kV in poche decine di microsecondi) e di corrente, oltre che da correnti elevate (fino a 100kA). In particolare:

- vengono descritti i possibili meccanismi di accoppiamento del rumore con il trasduttore e le criticità della sonda Rogowski rispetto ai disturbi esterni.
- vengono testate due sonde commerciali Rocoil ed analizzati i risultati ottenuti nel dominio del tempo e della frequenza. I test sono eseguiti in diverse posizioni del circuito e al variare del livello di carica del banco di condensatori.
- si ricorre al filtraggio numerico in MATLAB del segnale pot-misura per incrementare il SNR e si propongono soluzioni di ottimizzazione delle mis-

ure: si progetta un filtro elettronico da postporre allo stadio integratore del trasduttore.

- la forma d'onda filtrata viene confrontata con una 'forma d'onda ideale' ottenuta mediante simulazione numerica del circuito RC di generazione del Laboratorio, per assicurarsi che rispetti gli standard ED-84.

Abstract Problems related to the measurement of high current lightning pulse in a noisy environment are investigated, to improve the Data Acquisition System of Morgan Botti Lightning Laboratory. A transducer based on Rogowski coil and passive RC integrator is tested. Solutions are proposed to enhance SNR, including numerical and electronic filtering. Results show that measurements are affected by type of coil used, its position in the circuit and by an initial disturb. Hypothesis on its origin are made.

Introduction Morgan-Botti Lightning Laboratory (Cardiff, UK) was built to use RLC circuits to simulate lightning currents, according to the aeronautical standards EUROCAE ED14, ED84 and ED105.
This will make it possible to study the effects (direct and indirect) of lightning on materials and components, which are being adopted in newly developed aircrafts. In particular, the purpose of the laboratory will be to study the conduction, degradation and failure mechanisms in composite materials, as a result of lightning discharges. A further aim is also to be helpful in the design of components made of carbon fibre which are capable of minimizing the effects of lightning.

This work analyses the problems related to the measurement of the current pulse D waveform (second ED84) through the use of a Rogowski probe. The objective is therefore to contribute to the improvement of the data acquisition system (DAS) whose laboratory needs for its operation and for the execution of tests on aerospace materials.

The problem to be addressed is to obtain good quality (low SNR and limited interference) measurements in an environment dominated by electromagnetic noise, probably caused by the electrical components of the laboratory that generate the current pulse. The components of the circuit (bank of capacitors, resistors and inductors, mainly) are characterized by high voltage variations (over 55kV in a few tens of microseconds) and current variations, as well as high currents (up to 100kA).

In particular:

- The thesis describes the possible mechanisms of noise coupling with the transducer and the criticality of the Rogowski probe with respect to the external disturbs.
- two commercial Rocoil probes and results are analysed in the time domain and frequency domain. The tests are performed in different locations of the circuit with respect to the charge level of the capacitor bank.

- numerical filtering in MATLAB of measured signal is performed, in order to increase the SNR. Solutions are proposed to optimize measurements with the design of an electronic filter.
- the filtered waveform is compared with an 'ideal waveform' obtained by numerical simulation of the RC circuit for generating the Laboratory to ensure that they comply with the standard ED-84.

Chapter 1

The Morgan Botti Lightning Laboratory

Classically, protection systems in the aerospace industry are designed for worst-case scenario. Hence, in a bid to ensure adequate lightning protection and flight safety for next-generation carbon composite airborne vehicles, Cardiff University in collaboration with aircraft manufacturer, EADS, and the Welsh Government, has established a lightning simulation and research facility, called the Morgan-Botti Lightning Laboratory (MBLL). MBLL has been designed to generate full-threat current waveforms in accordance with international aeronautical standards EUROCAE - ED14, ED84, and ED 105. It is envisaged that this controlled lightning, when combined with advanced diagnostics, will be focused to develop and enhance electrical performance of carbon composite materials. This laboratory employs RLC control circuits during the discharge of capacitor banks to generate desired component waveforms. When fully developed, the capabilities of this robust facility would be significantly relevant for robust research in any of the following areas:

- Direct effect of lightning strikes on aerospace materials and components
- Effect of lightning currents on power system components including wind turbines
- Direct effect of lightning strikes on aerospace materials and components
- Conduction mechanisms, degradation effects and failure mechanisms of carbon composite materials under lightning strike currents
- Discharge phenomena and electric and magnetic field distributions in carbon composite materials and components under lightning strikes

- Characterisation of degradation phenomena in carbon composite materials under the combined mechanical and lightning current stresses
- Development of optimized designs for carbon composite materials and components for airborne vehicles
- Investigate performance of coating and paints in combination with carbon composite materials

Presently, the D-waveform generator is in operation, and installations are underway for B and C generators. The A-component generator remains a futuristic consideration as two more capacitors have yet to be sourced.

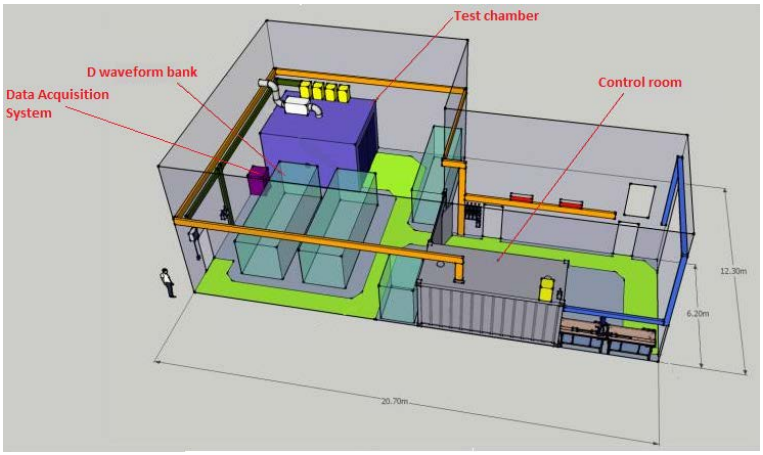

Figure 1.1: Morgan-Botti Laboratory Layout

1.1 The D Waveform Generator

[2] According to ED-84, the D-current component represents a subsequent stroke in a negative cloud to ground strike, and is given mathematically by the double exponential equation:

$$i(t) = I_0 * (e^{-\alpha t} - e^{-\beta t}) \tag{1.1}$$

where:
$I_0 = 19405A$
$\alpha = 22708s^{-1}$
$\beta = 1294530s^{-1}$
Clearly, the picture reveals the peak current amplitude will be 100kA ($\pm$10%),

Peak	100 kA
Rise time [10 % - 90 %]	1.42 μ s
Peak di/dt	1.4 x $10^1$1 A/s
Rise time to 100%	3.18 μ s
Fall time to 50%	34.5 μ s
Action Integral (within 500 μ s)	0.25 x 10^6 A^2s

and ED-84 specifies the rise time shall not exceed $25\mu s$, with and action integral of $0.25 * 10^6 A^2 s$ ($\pm 20\%$). The time duration to 1% of peak value should be less than $500\mu s$. Thus,this is the ideal D current component for analytical purposes.

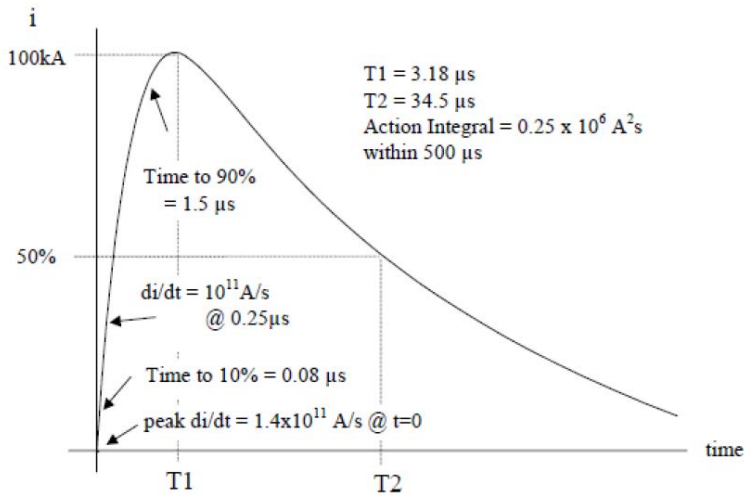

Figure 1.2: D waveform

To achieve this, a 60kV 20kW charger charges three series connected D bank capacitors, each rated at 20kV, 200F. Subsequently, the capacitor bank is discharged through a test sample, which is fitted firmly to the mounting plate of a test rig within an enclosed test chamber, using a pneumatic spark gap trigger to achieve excellent personnel safety.

In practice, the Dbank generator incorporates three sub-assemblies of series-connected 0.09375 Ω resistors with 36 200F capacitors, linked in series using long flat aluminium bars. These GAEP castor oil impregnated capacitors are rated at 20kV and have Direct Current (DC) life of about 100 hours. The battery life is about 3000 charge/discharged cycles. Each capacitor has a single bushing having estimated equivalent series inductance of 40nH. Also, the rated voltage reversal is 20% and maximum peak current rating is about 150kA, while the rated energy is

roughly 50kJ. Several HV 12.7cm diameter Linear Disc Resistors, each valued at 0.125Ω ±10%, are combined uniquely to give an equivalent of 0.09375 Ω. This is achieved by connecting six discs in series across eight parallel branches.

Figure 1.3: External view of the Laboratory

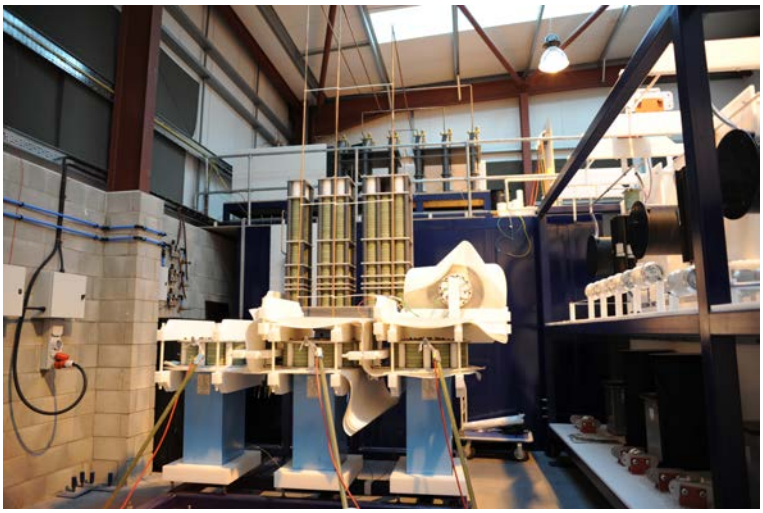

Figure 1.4: Internal view of the Laboratory

Chapter 2

Current transducer

2.1 Data acquisition system (DAS)

The D-waveform is measured using a set of instruments that are placed inside a steel enclosure, as seen in 2.1. Main purpose of the enclosure is to protect instruments from EM interferences (radiated, coupling or conducted). It is grounded in two points. Every instrument is then internally connected through a common rail to the aluminium plate which acts as a common reference ground point.

The data acquisition system (DAS) resides near the test chamber and houses:

- one rack-mounted National Instrument (NI) single PXI chassis
- a breakout board
- Rocoil integrator
- UPS module (APC Smart UPS 1500)

The PXI unit, dubbed Gargamel, has the following modules:

- Chassis: PXI-1031 (4 slot with 400W PSU)
- Controller: PXI-8108 (2.53GHz Dual Core)
- Module: PXI-5105 (60 MS/s, 12-Bit, 8-Channel Digitizer/Oscilloscope)
- Module: PXI-6251 (Multichannel ADC, DAC and DIO)

The NI-PXI chassis is linked to the control room through fibre optic conductors to avoid electrical interferences.

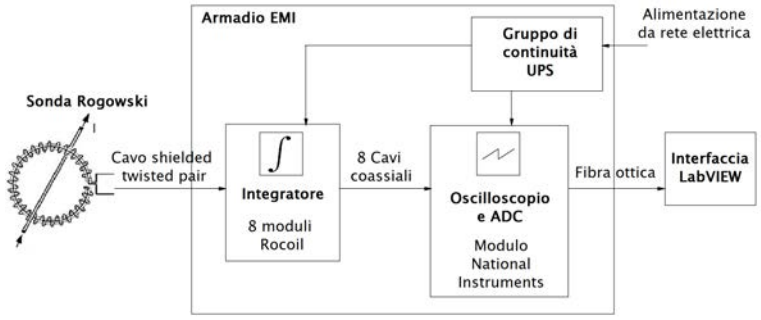

Figure 2.1: DAS simplified scheme

2.2 Current transducer

The current transducer used at MBLL is based on Rogowski coil and it is composed by the following elements:

- Rogowski coil
- Shielded twisted pair cable
- Integrator (passive and active amplifier)

The whole transducer is represented in 2.2. The circuit of the integrator is:

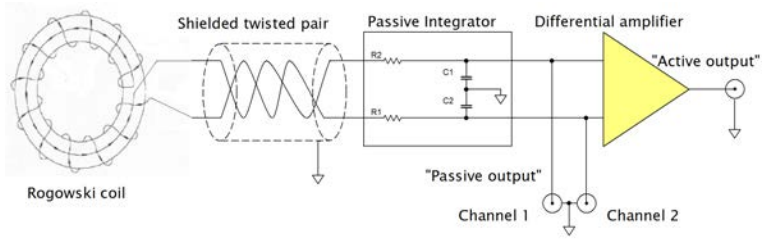

Figure 2.2: Rogowski coil transducer

2.2.1 Rogowski coil

A Rogowski coil is a current transformer. It consists in an air-cored toroidal coil through which the current to be measured circulates. Ampere's law states that the line integral of the magnetic field H around a single closed path is equal to the current enclosed. Mathematically, it is expressed as follows:[11]

$$i = \oint \vec{H} \vec{dl} \tag{2.1}$$

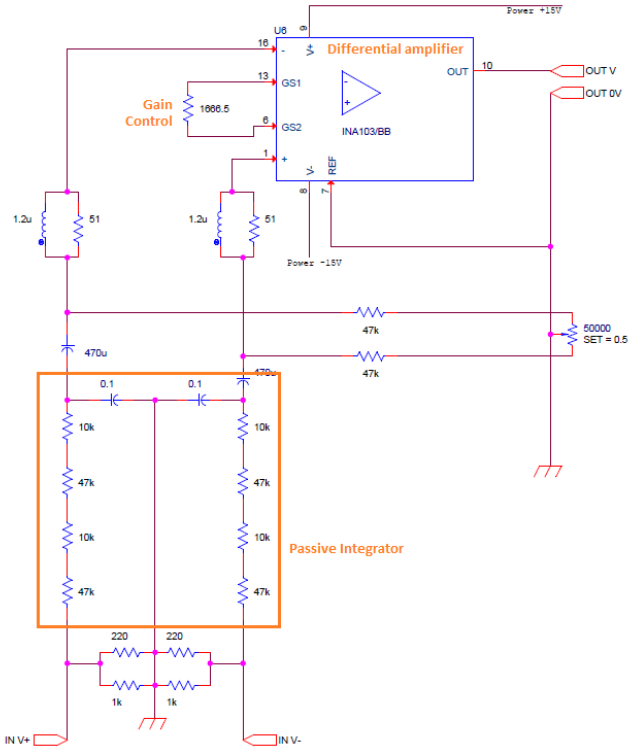

Figure 2.3: Integrator circuit, passive RC and active amplifier

where:
i is the current enclosed,
H is the magnetic field
dl is the infinitesimal element of path length.
The Faraday-Lenz law describes the generation of an emf by a changing magnetic field (Faraday's law) and the fact that if this emf appears in a closed circuit, the induced current is always in such a direction as to oppose the change that produces it (Lenz's law). For an alternating current the voltage output from the coil is given by the rate of change of flux.

In an infinitesimal element of path length dl the magnetic flux linking the section $\vec{dS}$ is $d\phi$, which is obtained integrating the magnetic field $\vec{B}$ in the area $\vec{dS}$, provided the diameter of the turns is small. The induced voltage in dl is calculated as the rate of change of the flux: [11]

$$v_{dl} = -\frac{d\phi}{dt} = -\frac{d}{dt}(\int_A \vec{B}d\vec{A}) = -\frac{d}{dt}(\int_A \mu_0\vec{H}d\vec{A}) = -\mu_0 S\frac{dH}{dt}\cos\alpha \qquad (2.2)$$

The flux linking the whole coil is given integrating along the coil, knowing that the number of turns per unit of length n is constant. From there, the total induced

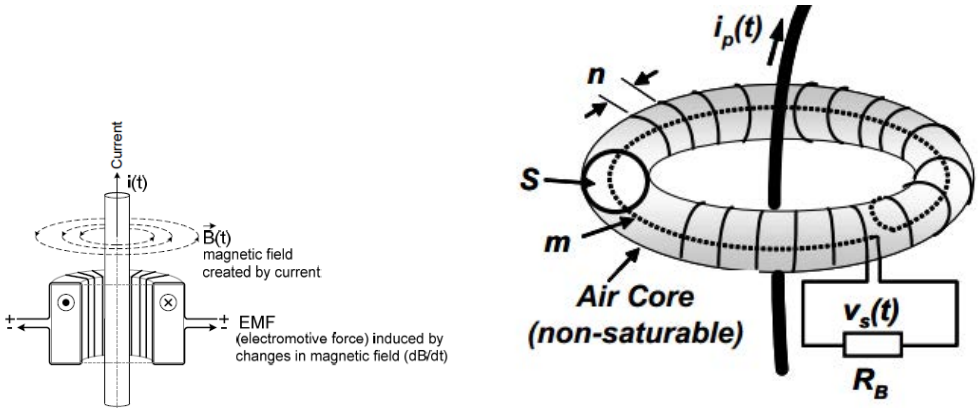

Figure 2.4: Rogowski coil

voltage can be determined.[11]

$$v_{coil} = \int_0^l (v_{dl} n dl) = -\mu_0 Sn \int_0^l \frac{dH}{dt} \cos\alpha dl = -\mu_0 Sn \frac{d}{dt} \int_0^l H \cos\alpha dl = -\mu_0 Sn \frac{di}{dt} \tag{2.3}$$

$$v_{coil} = -M \frac{di}{dt} \tag{2.4}$$

$$M = \mu_0 Sn \tag{2.5}$$

where μ_0 is the air permeability, A is the turn area and n is the number of turns per unit length.

The formulas are obtained with the following hypothesis that allow M=constant:

- constant winding density (n=constant)
- constant coil cross-section (S=constant)
- winding cross-section is perpendicular to the middle line $\cos\alpha = 1$

The problem with mass-producing coils is that their output voltage is susceptible a variety of manufacturing variations in the production of the coil. Designers have typically configured their systems such that the amplifier and integrator are calibrated to match the properties of the coil. Using this configuration, the entire assembly (coil, integrator and amplifier) must be treated as a single, field-replaceable assembly. [15]

2.2.2 Where the measure is taken

The Rogowski coil is placed on the HV bushing linking the variable resistor stack and the test chamber, via eight 50 mm2 H01N2-D welding cables at both input and return paths. The coil is wrapped around the flat aluminium bar used as return from test chamber.

2.2.3 Integrator

A current transducer, Rogowski coil, is placed around return conductors to measure the waveform of the current that flows across the test sample. The Rogowski coil is a one-built system with shielded twisted pair cable and integrator module. The integrator is provided with those following modules:

- 7 modules marked as 'Others'. These are used with coils FK-6330 to FK-6337.
- 1 module marked as 'Main'. This is used with coils FK-6328 and 6329 and measure the D waveform current from return conductors.
- 2 modules marked as 'LT4000-T'. These were designed as an interface for the LEM LT-4000T Current transducer, not used now.

Each module is made of a passive integrator (RC) and a differential amplifier. Advantages of using differential amplification and more detailed characteristics of the integrator can be found in the following sections. The two sockets marked 'PASSIVE OUTPUT' are the direct output of the passive integrator before it is processed by the differential amplifier. This is in differential form so the signal is between the centre pins of the two BNC connectors. There is also a single BNC connector marked 'OUTPUT' which is the output of the amplifier. Each module can switch between two different sensitivities (the switching is made inserting resistors in series) and gain. This gain control is made directly on the pins of the differential amplifier.[6]

A total of 7 Coaxial Cables (BNCs) connectors then link the OUTPUTs of the Rocoil integrators with the PXI-5105 Oscilloscope inputs. 6 of them come from "Others" module and 1 from "Main". This last one is normally used to trigger the oscilloscope.

The oscilloscope is then linked through optic cables to Control Room where data and signal elaboration are made.

Table 2.1: Outputs of the ”Main” module

PASSIVE OUTPUT	Sensitivity setting	Gain setting	kA/V
	LO	/	1000
	HI	/	500
ACTIVE OUTPUT			
	LO	LO	100
	HI	LO	50
	LO	HI	40
	HI	HI	20

Table 2.2: Outputs of the ”Others” modules

PASSIVE OUTPUT	Sensitivity setting	Gain setting	kA/V
	LO	/	500
	HI	/	250
ACTIVE OUTPUT			
	LO	LO	50
	HI	LO	25
	LO	HI	20
	HI	HI	10

2.2.4 Equations for equivalent circuit of transducer

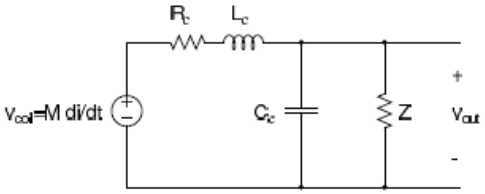

Figure 2.5: Rogowski coil equivalent circuit

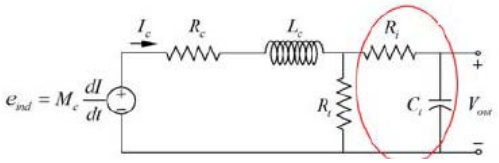

Figure 2.6: Rogowski coil and passive integrator equivalent circuit

The output voltage of the Rogowski coil is:

$$v_{out_{coil}}(t) = M\frac{dI_{ext}(t)}{dt} - L\frac{di(t)}{dt} - Ri(t) \tag{2.6}$$

At the "passive output" just after the passive integrator we have:

$$v_{in}(t) = Ri(t) + v_{out}(t) \tag{2.7}$$

$$i(t) = C\frac{dv_{out}(t)}{dt} \tag{2.8}$$

$$v_{in}(t) = RC\frac{dv_{out}(t)}{dt} + v_{out}(t) \tag{2.9}$$

$$RC\frac{dv_{out}(t)}{dt} = v_{in}(t) - v_{out}(t) \tag{2.10}$$

$$\frac{dv_{out}(t)}{dt} = \frac{1}{RC}(v_{in}(t) - v_{out}(t)) \tag{2.11}$$

$$v_{out}(t) = \frac{1}{RC}\int_0^t (v_{in} - v_{out})dt + v_{out}(0) \tag{2.12}$$

With the capacitor initially discharged: $v_{out}(0) = 0$. If we consider that $v_{out}(t) << v_{in}(t)$, that is equivalent to say that $v_{out}(t) << v_R(t)$ and $R >> X_C$ then: [**?**]

$$v_{out}(t) = \frac{1}{RC}\int_0^t v_{in}dt \tag{2.13}$$

$$v_{out}(t) = \frac{1}{RC}\int_0^t v_{out_{coil}}dt \tag{2.14}$$

The passive integrator is actually a low-pass filter.

2.3 DAS Power Supply

All instrumentation inside DAS needs to be powered from UPS. This UPS is connected to an external power supply cable that enters the cabinet of the DAS. At this point also a surge arrester and a filter are located.

- Surge arrester - To protect from over voltages
- Filter (EPCOS B84142-B25-R)- To filter conducted electrical noise from power supply mains.
- UPS - To ensure power continuity in case of failure of power supply from mains.

2.4 Noise in the measured signal

At normal operation, the waveform shown is the one below. It's clear the presence of a noise with an approximative duration of ... μs and a peak value that goes between V and V. A second test was performed with the DAS only powered

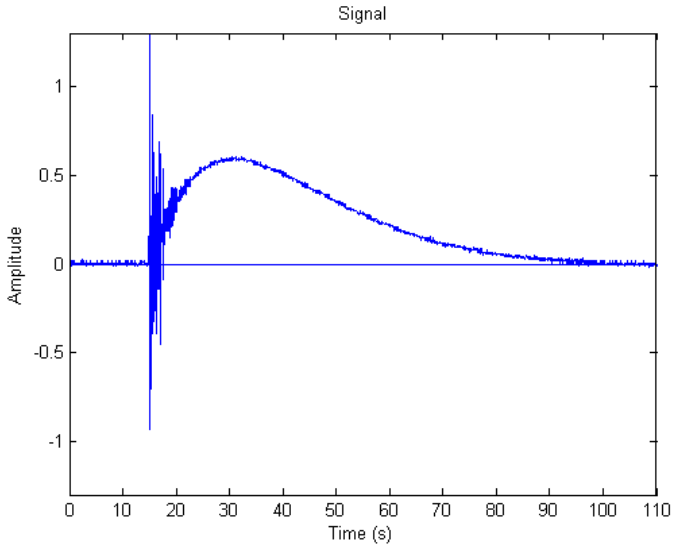

Figure 2.7: D waveform measured with power from main line

by UPS to isolate the circuit from any conducted interferences from ground loops from main power supply. A third test was made to evaluate the effects of the noise conducted from the power line. So, the Rogowski was disconnected leaving only the main line supply. The last test was made to evaluate the shielding performance

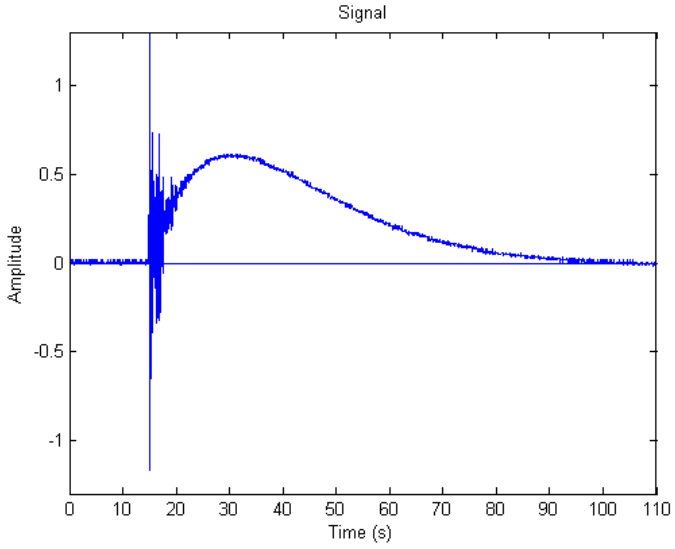

Figure 2.8: D waveform with DAS powered by UPS

of the DAS against conducted and radiated EM interferences. This was done with the instruments powered by internal UPS and no Rocoil connection. o the system was connected only to ground plate in two points. The results showed no significant interferences.

From the previous tests we can make those conclusions:

- The DAS is a complex structure with many instruments interconnected in various ways: signal reference conductors, ground connectors and power conductors. So that, multiple ways of conducting noise exist.
- A very small part of the noise is conducted through the main power supply, but the system is not affected by significant noise when neither Rogowski coil neither the main power supply are connected. The DAS is so a well screened system.
- The attention should be focused on the Rogowski coil. Purpose of next tests will be to analyse Rogowski coil susceptibility. To do this, a simpler system will be built (without significant ground loops).

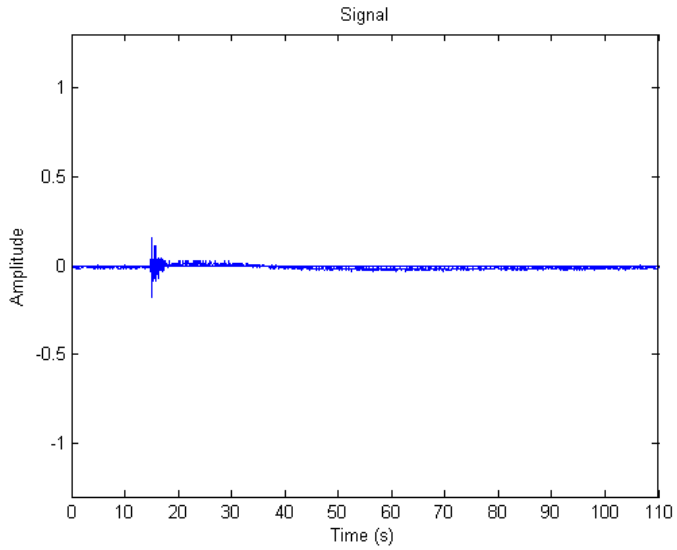

Figure 2.9: Effects of noise

Chapter 3

System weaknesses against noise and disturbs

3.1 Noise and disturbs

- According to [16], disturbs are theorically deterministic phenomena because their origin should be known. In many cases, unfortunately, their origin is complex and they can be the result of multiple causes or multiple coupling mechanisms so they may be treated as probabilistic phenomena. In the Rogowski transducer, multiple coupling mechanisms are possible and they are analysed in this chapter. The main source of this kind of phenomena is probably the circuit that generates the D waveform, even if we don't have a certain idea of which components are responsible for generating disturbs.

- Noise is surely a probabilistic phenomena. Examples of noise are:

  1. Thermal noise: Thermodynamic origin, associated to dissipative phenomena. Especially into resistors. It has a constant power spectral density.
  2. Shot noise: Thermoelectric, photoelectronic phenomena. Especially into transistors.
  3. Flicker noise: Electronic components. Its power spectral density is inversely proportional to frequency.

  We notice that noise is especially linked to circuit and its electronic components.

Radiated noise	Electric fields coupling
Conducted noise	Ground loops
Working conditions	Magnetic coupling, Coil not working in ideal assumptions

3.2 Noise in passive electronic components

There is no thermal noise associated to ideal conservative components, such as capacitors and inductors. In real components, this noise is negligible because this noise is associated to dissipative phenomena which are very small in those components. It is associated to real part of their impedance which is very small. [16] In non- conservative components, such as resistors, the noise is defined as follows with its power spectral density (PSD):

$$S = 4kTR \tag{3.1}$$

where

- S = the noise Power Spectral Density
- k = Boltzmans constant (1.3810-23)
- T = temperature in Kelvin (Room temp = 27 C = 300 K)
- R = resistance

Real resistors may contain also flicker noise.

3.3 Disturbs coupling mechanisms

The environment in which the Rogowski coil is placed is made by a complexity of potential noise sources with both low-frequencies and high-frequencies components.
This is combined with the fact that the Rogowski coil operates far from its ideal conditions, where some of the constitutive assumptions are made.

3.3.1 Radiated noise

There are three main coupling mechanisms that can result in noise propagation to Rogowski coil and cable:

1. Capacitive coupling (Electric Field Interference) (near-field interference)

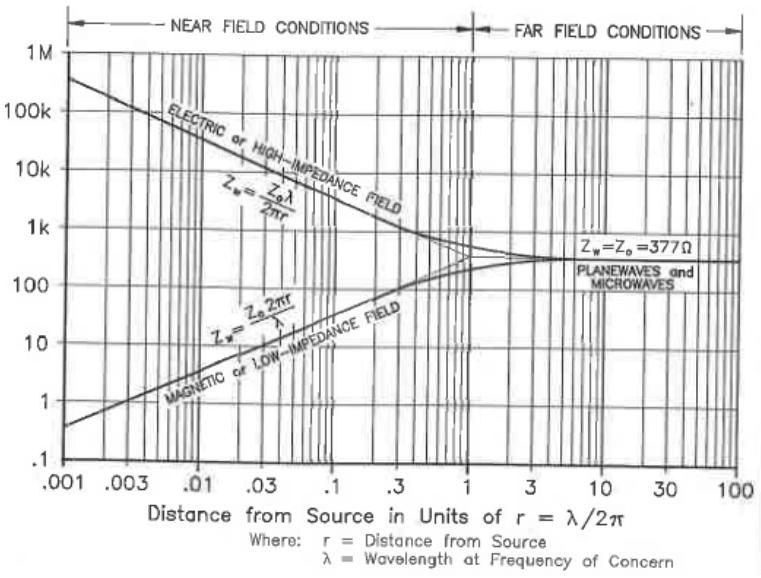

Figure 3.1: Dependence on distance

2. Inductive coupling (Magnetic Field Interference) (near-field interference)
3. Electromagnetic radiation coupling (far-field interference)

Those coupling mechanisms depends so on the distance from the source and the frequency of the noise:

Dependence on distance from source According to [14], if r=distance from source of the interference, λ=wavelength of the interference

- Near field condition when $r < \frac{\lambda}{2\pi}$
- Far field condition when $r > \frac{\lambda}{2\pi}$

Dependence on wave impedance According to [14], regardless of the type of interference, there is a characteristic impedance associated with it. The characteristic, or wave impedance of a field is determined by $Z = \frac{E_\theta}{H_\phi}$.

- In near field: the wave-impedance is determined by the nature of the interference and its distance from the source
  - If the interference source is high-current and low-voltage (for example, a loop antenna or a power-line transformer), the field is predominately

magnetic. This could be the case of the cables running close to the Rogowski coil. The ingoing and the return conductor are effectively a loop antenna for magnetic fields.

– If the source is low-current and high-voltage (for example, a rod antenna or a high-speed digital switching circuit), then the field is predominately electric. This is the case of the metallic parts placed close to the Rogowski that can exhibit a voltage drop when due to various induction mechanisms, and the metallic plate placed under the floor.

- In far field: $Z = Z_0 = 377\Omega$ with Z_0 the characteristic (wave impedance) of free space

3.3.2 Capacitive electrostatic coupling

Rogowski coils are susceptible to voltage pick-up through capacitive coupling onto the Rogowski coil winding. The time varying electrical field of an external system produces time varying charges in the disturbed system. The flow of the displacement currents can be modelled in an equivalent circuit by stray capacitances, which connect the two systems and cause the disturbing voltages. [10]

$\frac{dV}{dt} \rightarrow MutualcapacitanceM \rightarrow i_{noise}$
(Example: 1V/ns produces 1mA/pF)
Tha main source for capacitive coupling coul be the steel plate buried at few centimetres in the floor. It has the function of

Factors that influence capacitive coupling are:[10]

- Distance of the source noise. The steel plate is buried under the floor at a distance of around 1.5m from the Rogowski coil. However, several other metallic components are present all around, like cable racks and metallic walls which could be inevitably charged due to contact with ground plane.

- Entity of the voltage difference between the two circuits (noise source and Rogowski). No informations are available.

- Rapid variation in time of noise signals and with large high frequency content.

We report here a theorical representation of the capacitive coupling made by [7]. According to this study, the effect of a capacitive coupling with a metallic conductor nearby can be modelized with distributed stray capacitance.

As a consequence of the presence of C_x (which is in parallel to C', the circuit could not be correctly damped. And $\frac{dV}{dt}$ could produce the "ringing" disturb.

The simple lumped parameter model is useful in so far that it enables a relatively easy assessment to be made but it only provides a very approximate prediction of the Rogowski transducer behaviour to a step dV/dt. [7]

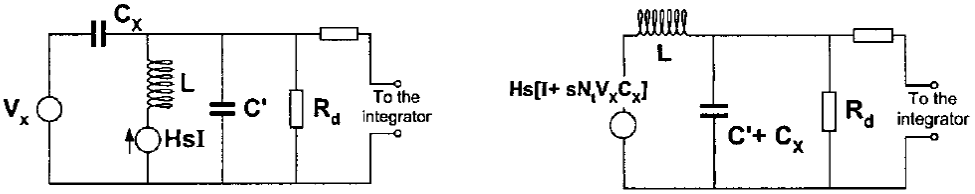

Figure 3.2: Capacitive coupling - simplified model

In reality, stray capacitance is distributed along all the coil wire.

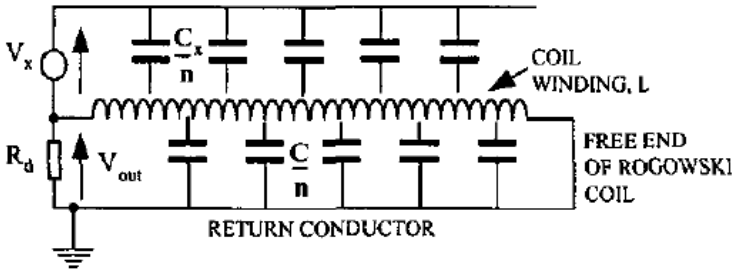

Figure 3.3: Capacitive coupling with distributed stray capacitance

Capacitive crosstalk from an adjacent ground The cable runs close to the ground steel plate buried just under the floor. (See "Grounding of the lab" for further details). It's likely possible that in this ground plate potential develops with the subsequent capacitive crosstalk with the screen and the inner twisted conductors.

3.3.3 Inductive coupling

A time varying external current $i_1(t)$, like the one that flows in the ingoing conductors, generates a magnetic field $B(t)$, which induces a disturbing voltage $u_{dist(t}$ in the neighbour Rogowski coil. In an equivalent circuit model this may be described by a coupling of both circuits via a coupling inductance M. The voltage $u_{dist(t}$ generates a common mode current $i_2(t)$, which itself generates a

magnetic field to weaken the external field. The current $i_2(t)$ is superimposed on the currents of the disturbed system and leads to the noised signal we measure. The coupling of magnetic fields of the different systems can be modelled by an equivalent circuit model by mutual inductances of the coupled circuits.[1][12]

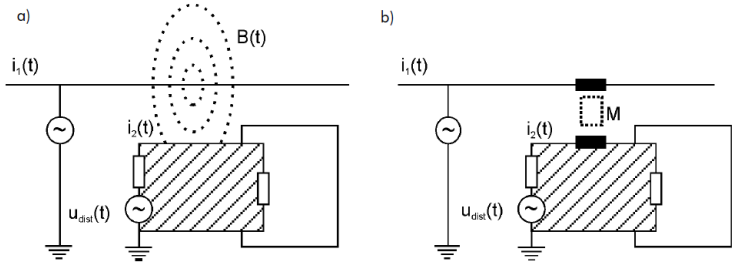

Figure 3.4: Field model and circuit representation

According to [10], the strength of the coupling depends mainly on three parameters:

- the strength of the disturbing current. The interested currents in the ingoing conductors are the classical D-waveform with a peak value of 100kA when the capacitors are fully charged (55kV, 300mA).
- the distance of source and drain. The Rogowski is really close to the ingoing conductors.The distance between them and the coil is approximatively 10 cm.
- the frequency of the disturbing field.

To give an idea of the possible peak magnetic field produced by nearby by:

$$B_0 = \frac{\mu_0 * I}{2 * \pi * d} \tag{3.2}$$

This is with the hypothesis of a rectilinear conductor and of infinite length, with a peak current I of 50 kA. If the approximate distance d of the Rogowski coil is 10 cm, then the magnetic field peak would be of

$$\mu_0 = 4 * \pi * 10^{-7} B_0 = \frac{4 * \pi * 10^{-7} * 50000}{2 * \pi * 0.5} = 0.1T \tag{3.3}$$

Induction in the screen of the screened twisted pair cable . External electromagnetic field could induce noise currents in the screen of the twisted pair cable. Those currents are variable and the subsequent electric flux will induce CM currents (ICM) equal in magnitude and phase on both twisted conductors simultaneously.[4] The electromagnetic field could likely come from the ingoing and return conductors of the test chamber or be generated by ”noise sources” like the close switch. (See ”Rogowski coil” and ”Noise” for further details).

3.3.4 Magnetic pick-up of the coil

According to coil specifications [15], the pick-up is normally less than 1%. This value is obtained through a quality test, in which the coil is usually placed a distance of one diameter away from the conductor as shown in 3.5. The coil is then turned in all orientations to find the maximum pick-up.

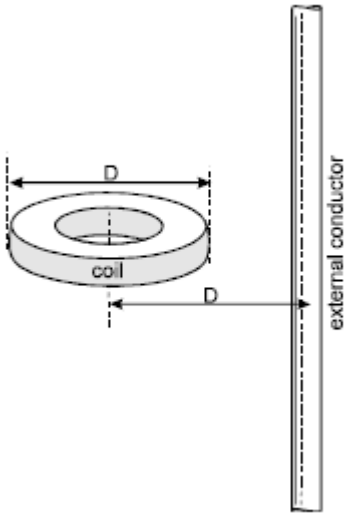

Figure 3.5: Test for inductive pickup

Unfortunately, the coil is not working within the ideal assumptions that it is built for. Consequently, magnetic pickup from near magnetic fields is possible:

1. **Internal flux cancellation** Theorically, the Rogowski coil should be sensitive only to magnetic fields produced by internal conductors placed normal to the section area A1 formed by its shape turn. Those fields are represented by vectors normal to cross section area of each loop A2. However,the progression of the main spiral winding itself makes the device into a one-turn

search coil sensitive to magnetic fields directed normal to surface A1.[12] The purpose of the return loop, which runs inside the main spiral, is to compensate this unwanted magnetic pick up. In fact, if we consider A3 as the area encircled by return conductor, we'll see that an external magnetic field V2 would be directed in opposite directions in A1 and A3. To ensure flux cancellation is necessary that A1=A3 $A_1 = A_3 = \phi * c^2$, where c is the position of return loop conductor. So:

$$c^2 = (3 * p^2 + 3 * q^2 + 2 * p * q)/8 \tag{3.4}$$

So, if the p=11 and q=9, the optimal position for return conductor would be c=10.025. This is slightly different from the actual position in the Rocoil, which is $c = \frac{p+q}{2}$. This difference causes a flux cancellation error and exposes the coil to pickup of external magnetic fields which are normal to area A1.
Unfortunately, the correct radius of return-loop is of little help because the interfering field is spatially non-uniform. Therefore in general there is no 'right' position for return-loops that deals with all situations. While one-off remedies are conceivable for measurement where the Rogowski has a fixed shape and permanent location, the situation with floppy Rogowskis is hopeless, if there is a single return-loop.[12] There is however a possible solution with multiple-spiral and multiple-return devices and research on these is in progress.
Cancellation failure is most likely found when a Rogowski encloses one conductor that runs near another, like in the case we're studying.

2. **Orthogonality to conductor** Another situation could occur when the measured conductor is not exactly normal to Rogowski coil loop area A1; so the magnetic field is not completely normal to A2 areas but can have components normal to A1 too. Unfortunately, theory supposes that the coil is normal to the measured conductor, but especially with floppy Rogowski that hypothesis is not assured. [3]

3. **Circularity of coil and conductor shape** It is a consequence of the following factors.

4. **Uniformity of coil parameters** Not uniform turn density of Rogowski coil (like non uniform spacing between adjacent turns, gaps or overlaps in the winding) or variation of area of the turn can affect Rogowski immunity to external magnetic pickup. [3] The junction of the two parts of the coil can be influent too. To reduce coil sensitivity to external magnetic fields is

important to ensure correct alignment of the two ends of the coil and the reduction of the gap in the junction. For this purpose, flexible coils have plastic end fittings to ensure that the ends are aligned correctly.[15] Those Rogowski are provided with a pushed together system in which the ends are located together simply by pushing them together until they click.[12] Unfortunately, this method gives good rejection of cross-talk from adjacent conductors which are parallel to the conductor being measured but is less good for more complex magnetic fields.

5. **Positional accuracy**. Due to small variations in the winding density and coil cross sectional area the transducer output varies slightly depending on the position of the current in the Rogowski coil and also the size of the current conductor relative to the coil. According to the constructor [4], if the conductor is moved from the central position by a distance equal to 0.5 x the coil radius the output will change by less than 1

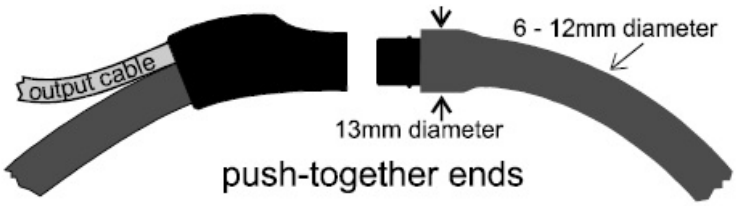

Figure 3.6: Detail of Rogowski ends

3.3.5 Ground Loops

The DAS is characterized by a series of complex connections which involve different type of purposes.

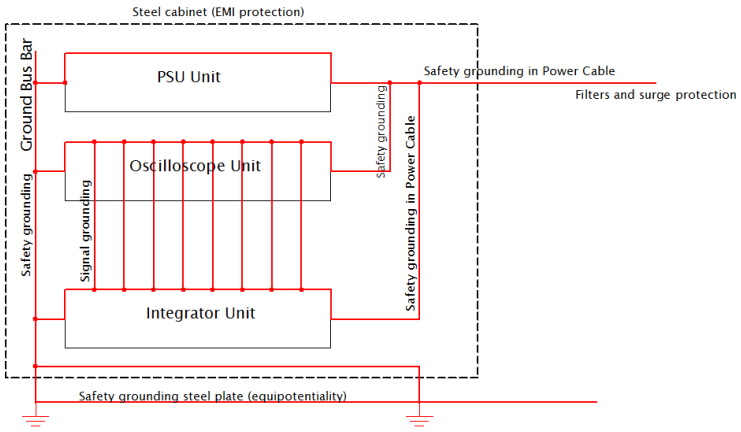

Figure 3.7: Ground loops in the DAS

3.4 Using of Differential-amplifier

Differential-ended circuits. Our Rogowski coil is connected to integrator using a differential-ended circuit. In it, two equal but opposite signals are transmitted on two complementary send lines (the two conductors of twisted pair), V_{rx+} and V_{rx-}. The differential receiver responds only to the voltage difference between the signals on its inputs, $\delta V_{in} = V_{rx+} - V_{rx-}$. If we consider the voltage on each of the conductors to be relative to the reference potential on the SRS V_{ref}, the receiver's output will be relative to δV_{in}:

$$V_{out} = f(\delta V_{in}) = f[(V_{rx+} - V_{ref}) - (V_{rx-} - V_{ref})] = f(V_{rx+} - V_{rx-}) \tag{3.5}$$

Clearly, the input voltage is independent of the reference potential, V_{ref}, present across the SRS.[4]
Let's consider the figure in which the "Driver" is the Rogowski coil, the "Receiver" is the amplifier of the integrator module and the conductors between are the ones of the twisted pair. If a noise voltage V_N is present(appearing as common-mode interference voltage), then is it equally introduced onto both the send and return conductors simultaneously. The receiver responds only to the difference, δV_{in}^N, between the voltages present on both lines. The noise present on both co inductors has, therefore, no effect on the receiver's response:

$$V_{in}^N = (\delta V_{in}) = [(V_{rx+} - (V_{ref} + V^N)) - (V_{rx-} - (V_{ref} + V^N))] = (V_{rx+} - V_{rx-}) \tag{3.6}$$

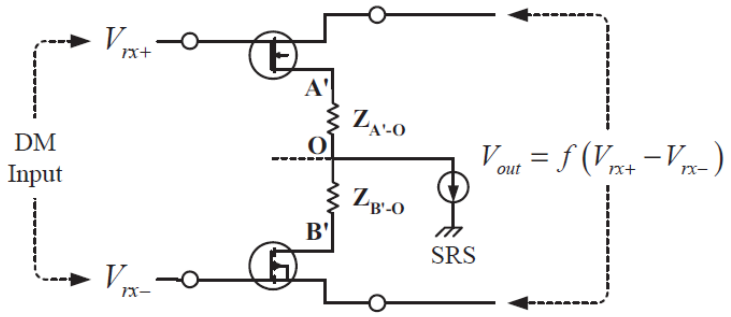

Figure 3.8: Differential signalling

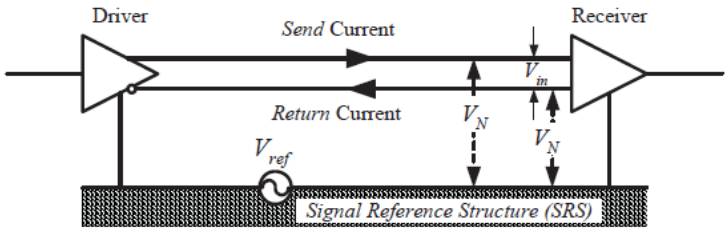

Figure 3.9: Differential signalling with noise

Imbalance in the differential amplifier (DM-to-CM) In the differential amplifier in the integrator module, the differential input signal between ports A and B, as well as the output signals between ports C and D, should ideally be equal in amplitude and opposite in phase. The driver has also a 'center tap' (O) constituting a 'virtual ground,' grounded to the reference structure (the ground common point inside the box where also oscilloscope is grounded). Ideally, the output at C-D should be a result of the input differential signal only, rejecting CM currents between its inputs. In 'real world' (nonideal) balanced devices, the gain to the CM input (V_{A0} and V_{B0}) is non-zero. Therefore, a DM input will result in some undesired CM signal at its output: DM to CM conversion takes place.[4]

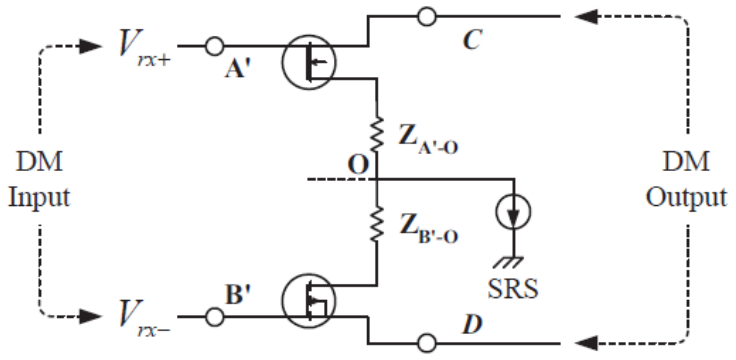

Figure 3.10: DIfferential amplifier unbalance

3.5 Theory of Common Mode (CM) and Differential Mode Noise (DM)

If we refer to 2.8, a signal source produces a current which flows to the load and than back through the return conductor. The Rogowski coil is the source in which the variation of the inducting magnetic field over time produces a current I_s. This current flows to the load (resistive, inductive and capacitive components of the filter)through one conductor of twisted pair. Then comes back through the other conductor of the shielded twisted pair.

1. **Differential Mode Noise (DM)**; A source of DM Noise will induce a current I_DM circulating in the same direction of I_s and superimposing on it as seen in 3.5

    - DM Currents have the same magnitude and their phase difference is 180 degrees in all current-carrying signal and return conductors alike.

2. **Common Mode Noise (CM)**; A source of Cm Noise will induce a current I_CM which flows in the same direction in both conductors. This current comes back to the source through stray capacitance to ground, as seen in 3.5

    - CM Currents have the same magnitude and are in phase in all current-carrying signal and return conductors alike.
    - Unlike differential currents, the exact path of common-mode currents is difficult to predict [4]. This path is not the circuit itself but are unintentional paths in metallic structures.

By definition:

$$\begin{cases} I_1 = I_{CM} + I_{DM} \\ I_2 = I_{CM} - I_{DM} \end{cases} \tag{3.7}$$

$$\begin{cases} I_{CM} = \frac{I_1 + I_2}{2} \\ I_{DM} = \frac{I_1 - I_2}{2} \end{cases} \tag{3.8}$$

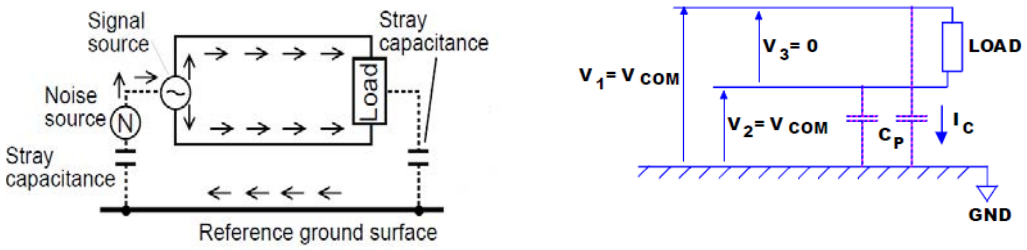

Figure 3.11: CM Noise

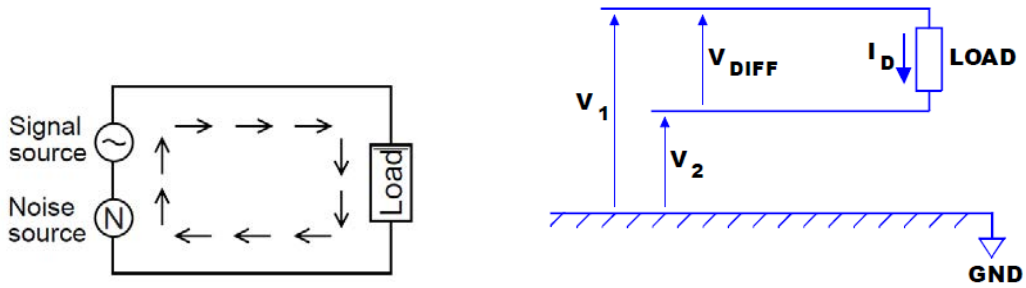

Figure 3.12: DM Noise

3.5.1 Theory of differential measurement

Examples of differential measuring:

- The differential Rogowski coil (DRC) consists of two inversely arranged wound coils with neutral return conductor. Accordingly, for a differential measurement only one measuring procedure is necessary.
- In PCB coils, two windings are wound in opposite directions to reduce magnetic pick-up from nearby conductors.

Chapter 4

Test of the transducer

4.1 Purpose of the tests

The ultimate goals of the studies would be to

1. Distinguish the real measured signal from the noise superimposed in current transducer during measurement process.
2. Understand if the transient appearing in the D waveform is due to superimposed noise only or is it produced with the current itself. In this second case, it could mean the necessity to re project partly or entirely the circuit that generates the D impulse.

To obtain this:

- Signal was taken directly from the output of passive integrator, without the amplifier. We tried to simplify at the maximum possible the circuit, taking the measurement as 'close as possible' to the coil.
- Signal was numerically filtered to extract the bandwidth of the coil (according to a model) and enhancing the SNR.
- System was protected to contain radiated and conducted noise from outside, using proper cable and instrumentation shielding.
- Three coils (FK-6328 , FK-6330 and FK-6330S) were compared to investigate their ability to correctly reproduce the D waveform.

Other purposes were:

- Investigate the noise characteristics (frequency) and make first hypothesis on its origin.

- Propose concrete solutions to optimize the current measurement in terms of noise shielding and signal quality.

On the side of the measurement system, to obtain a clean D-waveform is important to:

- Characterize and limit interferences that the Rogowski coil can pick up.
- Limit pick ups in coaxial cable
- Assure that the instrumentation (integrator, oscilloscope and others) is well screened from interferences.

4.2 Description of instrumentation

The optimized transducer is very similar to the one seen in the Data Acquisition System:

- 1 Rogowski coil
- 1 Shielded twisted pair cable
- 1 Integrator module (passive and active amplifier)
- 1 Tektronix TDS300C oscilloscope

The picture describes it: Measurements were taken at the Passive output. Mea-

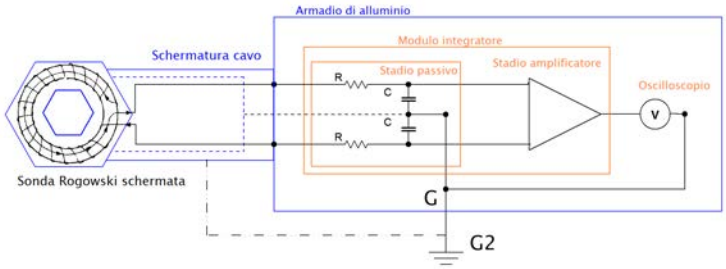

Figure 4.1: Scheme of transducer

sured directly at the end of the RC circuit. The measured voltages are: $(V_A - V_0) - (V_B - V_0) = V_{AB}$ and $(V_C - V_0) - (V_D - V_0) = V_{CD}$ In the pictures the 'V' is the voltage measurement made with the oscilloscope.

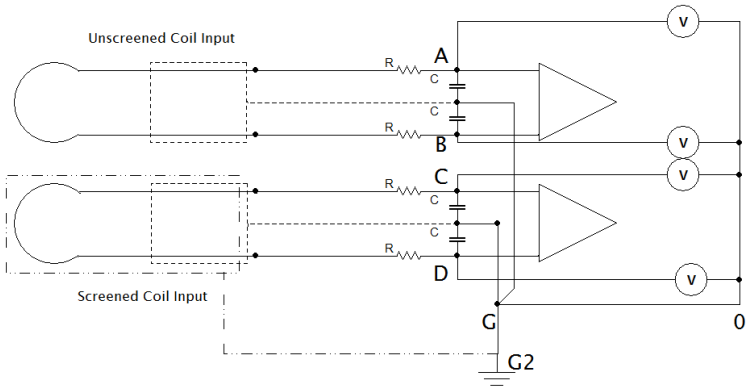

Figure 4.2: Passive output measurement

-	Coil used	Capacitors charge level
Test 1	FK-6328 FK-6330	55, 40, 30, 20 kV
Test 2	Fk-6330 (2)	55, 40, 30, 20 kV
Test 3	FK-6330 FK-6330S	55, 40, 30, 20 kV
Test 4	FK-6328	55, 30 kV

4.3 Tested coils

In the test three three different types of Rogowski coil were tested:

The voltage is the one at which the three series capacitor bank are charged, to obtain different peaks of current. Capacitor bank was charged at 40 and 55 kV at 300mA to produce the D waveform impulse. No sample was inserted and the two electrodes in the test chamber were short circuited. So that, the Rogowski coil placed on return conductors, measured exactly the D waveform impulse produced.

- For the connecting cable between coil and enclosure: Connecting cable was double-screened and the outer screen was connected to the instrumentation box at one side, and left free at other side. The screen was a steel rectangular guide where cables were inserted.

	Type	*Dcoil* [cm]	*Dcable* [mm]
FK-6328	Floppy shaped coil	100	6.5
FK-6330	Floppy shaped coil	30	6.5
FK-6330S	Screened floppy shaped coil	30	6.5

- For the input point of cables entering the instrumentation enclosure: 1) Cable entered the enclosure in one point only. In this way, high level circulating currents flowing in the long cables in many industrial situations will flow from cable to cable via connector panel or backplate edge via screen terminations or filters mounted in that area, and will not flow in the rest of the cabinet or backplate structure where they might upset the electronic structures. 2)At the entering point, the steel cable guide was soldered externally to the metallic instrumentation enclosure, while the cable entered the enclosure itself. The screen of the twisted pair cable was grounded to the enclosure as depicted in figure.

- For cables inside instrumentation enclosure: 1)All cables were run close to the enclosure chassis to avoid coupling with external fields. 2)No cables were run close to the aperture of the structure as the localized fields around this point could be high.

4.3.1 Test 1

Coils are placed as in figure, to compare the output from one with the one from another, at the same time. One coil, FK-6328, is placed as normal, around return conductors from test chamber (6 cables). The other coil, FK-6330, is placed inside test chamber around the return conductor. The two outputs are then taken to the instrumentation box via twisted pair screened cables, as described in figure. Both transducers are grounded externally to the test chamber.

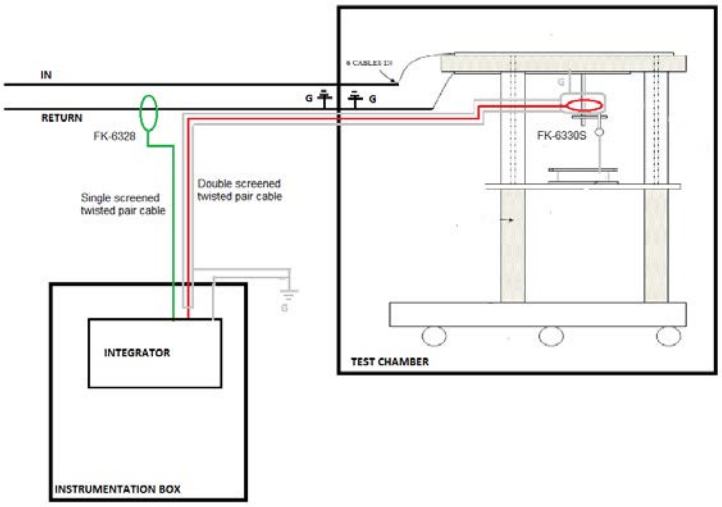

Figure 4.3: Test 1 description

4.3.2 Test 2

One coil is placed outside (FK-6330 (A)) and the other inside the test chamber (FK-6330 (B)). The first coil is grounded outside the test chamber, the other is grounded inside. Signals are taken from coil to integrator via twisted pair cables.

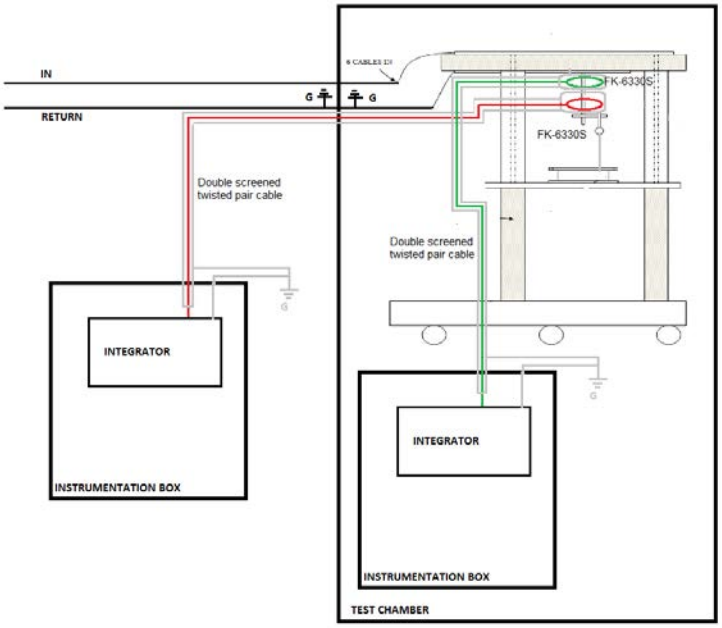

Figure 4.4: Test 2 description

4.3.3 Test 3

As described in figure, is the same as Configuration B with the only difference that coil FK-6330 is replaced with screened coil FK-6330S. Both instrumentations are connected to ground internally in the test chamber and not externally. Coils are connected to instrumentations via twisted pair cables.

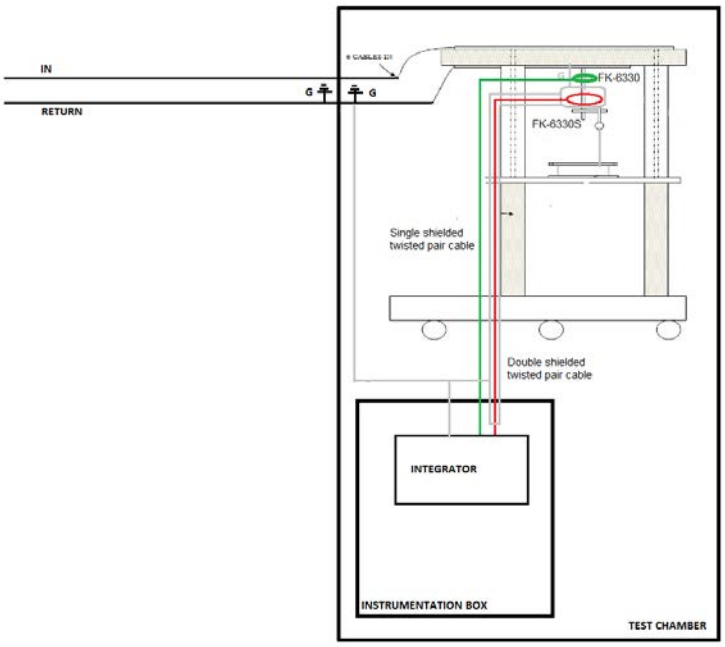

Figure 4.5: Test 3 description

In this configuration, the coil FK-6330S was used. It is identical to the FK-6330 with the exception of having a steel screen around it. The screen is a steel hexagon with inner slot to avoid pick up of wanted magnetic field from conductor and electric fields. Its main purpose should be to reduce the electric (capacitive) and magnetic (inductive) coupling as well as electromagnetic radiated coupling. The Rogowski is placed inside.

4.3.4 Test 4

The coil FK-6328 is placed around the 6 return cables from test chamber. Instrumentation is grounded outside test chamber. The coil is then connected to instrumentation via 2m twisted pair screened cable, as seen in the picture.

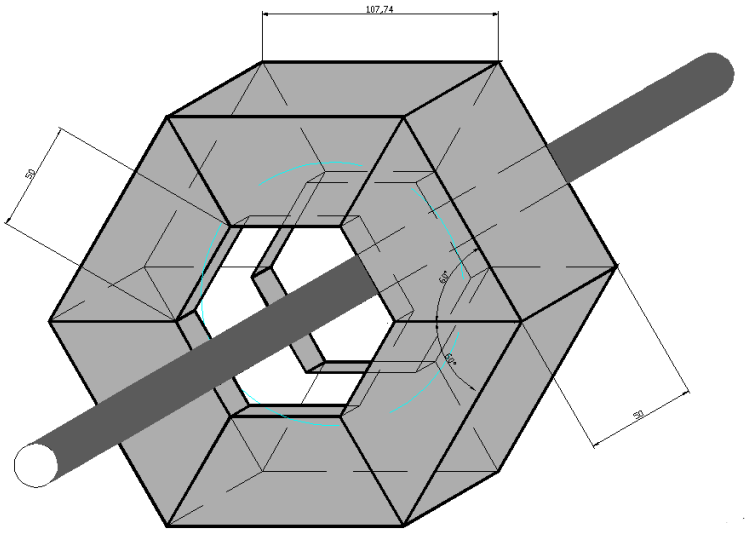

Figure 4.6: Screen for coil FK-6330S

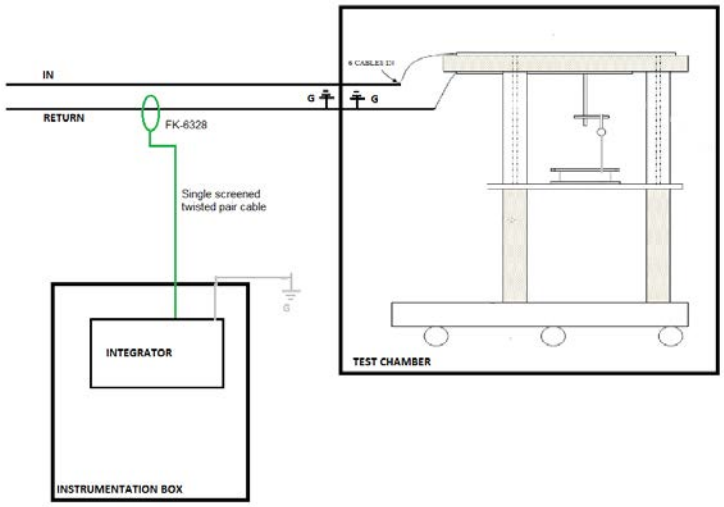

Figure 4.7: Test 4 description

4.4 Considerations on earth connections

Zoning and enclosure All the instrumentation is enclosed inside a proper EMC box, which

- Provides and demarcates a zone of increased EMI protection, preventing

radiated field coupling to and from the internal equipment

- Provides a local earth reference for internal equipment

Absence of external power:

- In test where only passive RC integrator is needed, no power is provided. This reduces the risk of external noise coupling.
- Only in tests that involve measurements from active amplifier, the system is powered by internal batteries. The oscilloscope is powered by his own internal batteries. In the box a battery is placed and connected to a DC/DC converter which provides 30V DC supply for the integrator module (active amplifier). This configuration assures that no ground loop is formed with the power supply and that no currents can flow through the earth conductor, affecting the measurements.

Test for analysing coupling with external noise With the following test the coupling between instruments and external noise from radiated EM fields was tested. The test was made with all the instrumentation operative and placed in the box. However, no input was connected to integrator. Results showed no noise in the signal and this indicated that the instrumentation (excluding coil and Rogowski) was sufficiently shielded from radiated noise.

Earth connections There are different type of grounding systems:

1. **Functional earth:** In order for an electrical circuit to interface correctly with other equipment, there must be a means both of relating voltages in one equipment to those in another and preventing adjacent but galvanically separate circuits from floating. [14]

   - Integrator circuit: The integrator circuit requires a signal reference for both passive RC circuit and active amplifier to work properly. The reference is represented by the chassis of the module and is also available in two pins in the rear din connector for connection to functional earth.
   - Oscilloscope: Is provided with a plug that requires connection using a proper output cable to the functional earth.

   Signal circuits of equipment should normally be specified for a maximum common mode voltage, which will be the voltage that appears between different parts of a functionally-earthed system. [14]

Inside the enclosure, the local earth reference for internal equipment is provided by the chassis itself. That is critical to the effectiveness of the metal enclosure, whether or not this enclosure is deliberately intended as a shield. Enclosure must have the lowest possible transfer impedance to the internal circuits and equipment so it does not couple with circuits. In this case, rectangular enclosure is one of best [14][11].
Actually, the oscilloscope earth conductor and the integrator module earth din are wired to a common stud placed on the enclosure wall. Wires are common $1mm^2$ section and are as shorter as possible.

2. **EMC Earth:** Has the sole purpose of ensuring that interfering voltages are low enough compared to the desired signal that incorrect operation or excessive emission does not occur. It has no explicit operational or safety function. It must work on wide frequency range and usually takes advantage of distributed structural components that are part of the whole system (chassis members, enclosure panels and so on). The value of an EMC earth is directly related to the physical geometry.[14]
In our case, the EMC earth system contains:

   - Cable screens (see 'External cable screening')
   - Metallic enclosure that contains all instrumentation
   - SRPP plane
   - Wired connections from cable screened and enclosure to SRPP plane

   They are all described further below.

3. **Safety earth:** Purpose of safety earth is to guarantee personnel safety under fault conditions. The IEE Wiring regulations define "earthing" as connection of the exposed conductive parts of an installation to the main earthing terminal of the installation. Earthing ensures the provision of a low impedance path in which current may flow under fault conditions. Exposed conductive parts are those conductive which may be touched and may become live in case of a fault. Equipotential bonding ensure they are maintained at the same potential. [14].

   - Integrator: Functional earth absolves the same function as safety earth. Inside PCB, two EPCOS electrode arresters M51-C90X [5] connect the signal path to earth path to ensure protection of active amplifier against over voltages.
   - Oscilloscope: According to the specifications [13], safety earth should be provided even if the oscilloscope is in use with batteries, through

Parameter	Description
L	Self inductance of the coil
M	Mutual inductance to a single conductor threading the coil
R	Internal resistance of the coil
C	Self-capacitance including lead capacitance.
Rd	Optimum damping resistance (integrator module)

the provided protective earth stud on the rear of the apparatus. The manual says that the oscilloscope can be used without safety ground connection for measured signals below 42 V peak. However the connection is made to the functional ground through that stud.

System reference potential plane (SRPP) The equipment cabinet (as many others components in the laboratory) is placed directly on this floor with insulating feet, and RF bonded to the SRPP in the floor at one corner, using a $2.5mm^2$ wire. The SRPP is a three dimensional equipotential earth-bonding, called System Reference Potential Plane (SRPP), which requires a bonding mat. The SRPP is used for safety, functional, and EMC earthing all at the same time. By creating it it is possible to achieve the various aims of safety, signal integrity, equipment reliability and EM which are seen as being in conflict. [11]
The bonding mat is a seamless metal plane under the entire system block, made from aluminium sheets from substantial thickness, all of them seam-welded to each other along all their mating edges. The SRPP is placed directly under the laboratory floor in the high voltage area only, with dimensions of 12.30m x 12.30m. SRPP bonds also every piece of structural and non structural metalwork together, to make a very highly interconnected system which is then connected to the lightning protection system (LPS) at ground level, with four

4.5 Filter details

4.5.1 Transfer function of damped coil

According to Rocoil specifications, the coil can be modelized with a RLC circuit with the following characteristics.

A normal Rogowski is represented by the circuit in Figure where: The self capacitance is between the coil winding and the return conductor.

A voltage source proportional to the variation of the current in the measured conductor $v_{in} = MsI = M\frac{dI}{dt}$ is applied on the circuit and makes it act like a reso-

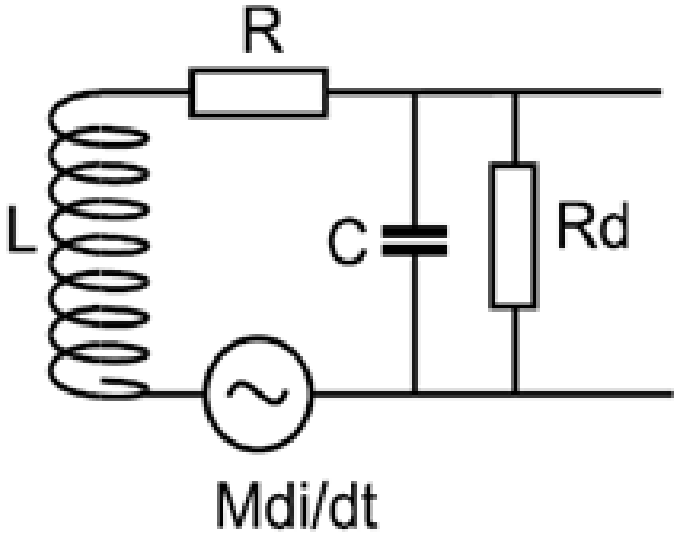

Figure 4.8: Equivalent circuit of damped coil

nant RLC circuit.

An important property of this circuit is its ability to resonate at a specific frequency, the resonance frequency, $\omega_0 = 2\pi f_0$. Resonance occurs when the circuit continues to exhibit an output (i.e. oscillates) different from zero even when the input signal has terminated. Resonance occurs because energy is stored in two different ways: in an electric field as the capacitor is charged and in a magnetic field as current flows through the inductor. Energy can be transferred from one to the other within the circuit and this can be oscillatory.
The transfer function of the coil can be obtained as follows:

$$v_{in} - L\frac{di}{dt} - Ri = v_{out} \tag{4.1}$$

$$i = i_c + i_{Rd} = C\frac{dv_{out}}{dt} + \frac{1}{Rd}v_{out} \tag{4.2}$$

$$v_{in} = M\frac{di_a}{dt} \tag{4.3}$$

So

$$v_{out} = M\frac{di_a}{dt} - LC\frac{d^2v_{out}}{dt^2} - \frac{L}{Rd}\frac{dv_{out}}{dt} - RC\frac{dv_{out}}{dt} - \frac{R}{Rd}v_{out} \tag{4.4}$$

$$v_{out} = Msi_a - LCs^2v_{out} - \frac{L}{Rd}sv_{out} - RCsv_{out} - \frac{R}{Rd}v_{out} \tag{4.5}$$

$$Msi_a = v_{out}(LCs^2 + \frac{L}{Rd}s + RCs + \frac{R}{Rd} + 1) \tag{4.6}$$

$$\frac{i_a}{v_{out}} = \frac{(LCs^2 + \frac{L}{Rd}s + RCs + \frac{R}{Rd} + 1)}{Ms} \tag{4.7}$$

$$\frac{v_{out}}{i_a} = \frac{Ms}{(LCs^2 + \frac{L}{Rd}s + RCs + \frac{R}{Rd} + 1)} \tag{4.8}$$

$$\boxed{G_{coil}(s) = \frac{Ms}{(LCs^2 + \frac{L}{Rd}s + RCs + \frac{R}{Rd} + 1)}} \tag{4.9}$$

$$\boxed{G_{coil}(s) = \frac{M\frac{Rd}{Rd+R}s}{(\frac{LCRd}{R+Rd})s^2 + (\frac{L}{Rd+R} + \frac{RCRd}{Rd+R})s + 1}} \tag{4.10}$$

$$\boxed{G_{coil}(s) = \frac{M\frac{Rd}{Rd+R}s}{(\frac{1}{\omega_n^2})s^2 + (\frac{2\sigma}{\omega_n})s + 1}} \tag{4.11}$$

Where

$$\boxed{\omega_n = \sqrt{\frac{R+Rd}{LCRd}}} \tag{4.12}$$

4.5.2 Transfer function of damped coil and integrator

Integrator circuit appears as follows.
Its transfer function is the one of a simple lowpass filter:

$$v_{in} - R_1 i = v_{out} \tag{4.13}$$

$$i = C_1\frac{dv_{out}}{dt} \tag{4.14}$$

So

$$v_{in} - R_1C_1\frac{dv_{out}}{dt} = v_{out} \tag{4.15}$$

$$v_{in} = v_{out}(1 + R_1C_1s) \tag{4.16}$$

$$\frac{v_{out}}{v_{in}} = \frac{1}{(1 + R_1C_1s)} \tag{4.17}$$

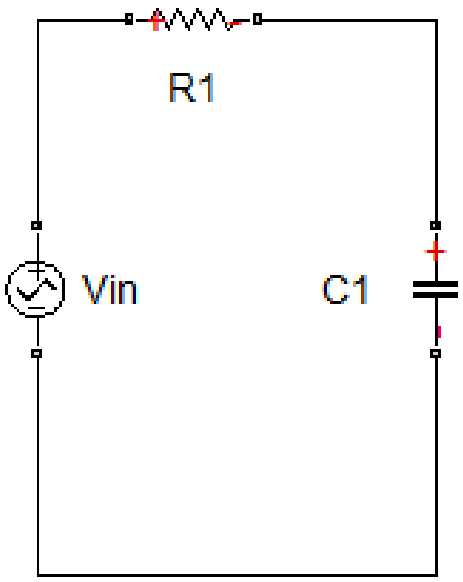

Figure 4.9: Circuit of RC passive integrator

$$\boxed{G_{RC}(s) = \frac{1}{(1+R_1C_1s)}} \tag{4.18}$$

$$\boxed{\tau = R_1C_1} \tag{4.19}$$

the time constant of integrator RC circuit

$$\boxed{\frac{1}{\tau}} \tag{4.20}$$

the natural pulsation of RC integrator circuit.

The complete circuit (tf coil + tf RC integrator) can be described as follows

$$\boxed{G(s) = G_{coil}(s) * G_{RC}(s)} \tag{4.21}$$

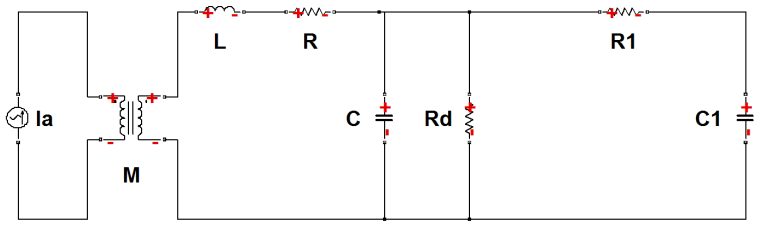

Figure 4.10: Circuit of RC passive integrator and coil

As described in previous chapter, under particular circumstances, the RC circuit acts as an integrator. Those are the following:

$$\frac{v_{out}}{v_{in}} = \frac{1}{1+sR_1C_1} \tag{4.22}$$

$$i = C_1 s v_{out} \tag{4.23}$$

$$\frac{i}{v_{in}} = \frac{C_1 s}{1+sR_1C_1} \tag{4.24}$$

$$i = \frac{v_{in}}{R_1 + \frac{1}{C_1 s}} \tag{4.25}$$

Consider the output across the capacitor at high frequency so that

$$\omega \gg \frac{1}{R_1 C_1} \tag{4.26}$$

$$\omega C_1 \gg \frac{1}{R_1} \tag{4.27}$$

So

$$i \simeq \frac{v_{in}}{R_1} \tag{4.28}$$

But

$$v_{C_1} = \frac{1}{C_1}\int i\mathrm{d}t \tag{4.29}$$

$$v_{C_1} \simeq \frac{1}{R_1 C_1}\int v_{in}\mathrm{d}t \tag{4.30}$$

4.6 Filter design

Transfer function has been inserted into MATLAB code to produce a Bode diagram and a frequency response plot, as follows. Those are the data for the two

Parameter	Unit	FK-6328	FK-6330
L	mH	0.0047	0.0129
M	μH	0.0082	0.0225
R	Ω	2	2
C	pF	713	372
Rd	Ω	70	150

-	Unit	Value
R1	Ω	114e3
C1	μF	8.7

coil used: According to specifications, the capacitance C is calculated for our 2 metres lead cable. The effect of extending the lead is to add capacitance at about 120 - 160pF / m.
According to Rocoil, the specified values of self capacitance and inductance can vary with a factor of 2.

The RC integrator has the following values:
The corresponding G(s) for the systems are: For the FK-6328:

$$G_{coil}(s) = \frac{8.2 * 10^{-9} s}{5.744 * 10^{-13} s^2 + 1.583 * 10^{-6} s + 1.177} \tag{4.31}$$

$$G_{RC}(s) = \frac{1}{\tau s + 1} = \frac{1}{0.9918 s + 1} \tag{4.32}$$

$$G(s) = G_{coil}(s) * G_{RC}(s) \tag{4.33}$$

$$G(s) = \frac{8.2 * 10^{-9} s}{5.697 * 10^{-13} s^3 + 2.57 * 10^{-6} s^2 + 1.168 s + 1.177} \tag{4.34}$$

$$f_{c2} = 0.250 MHz \tag{4.35}$$

$$\omega_{n1} = 0.161 Hz \tag{4.36}$$

$$\omega_{n2} = 0.228 MHz \tag{4.37}$$

For FK-6330:

$$G_{coil}(s) = \frac{2.25 * 10^{-8} s}{5.744 * 10^{-13} s^2 + 1.602 * 10^{-6} s + 1.227} \tag{4.38}$$

$$G_{RC}(s) = \frac{1}{\tau s + 1} = \frac{1}{0.9918s + 1} \tag{4.39}$$

$$G(s) = G_{coil}(s) * G_{RC}(s) \tag{4.40}$$

$$G(s) = \frac{2.25 * 10^{-8} s}{5.697 * 10^{-13} s^3 + 1.589 * 10^{-6} s^2 + 1.217s + 1.227} \tag{4.41}$$

$$\omega_{n1} = 0.161Hz \tag{4.42}$$

$$\omega_{n2} = 0.233MHz \tag{4.43}$$

$$f_{c2} = 0.253MHz \tag{4.44}$$

With the following frequency response diagrams:

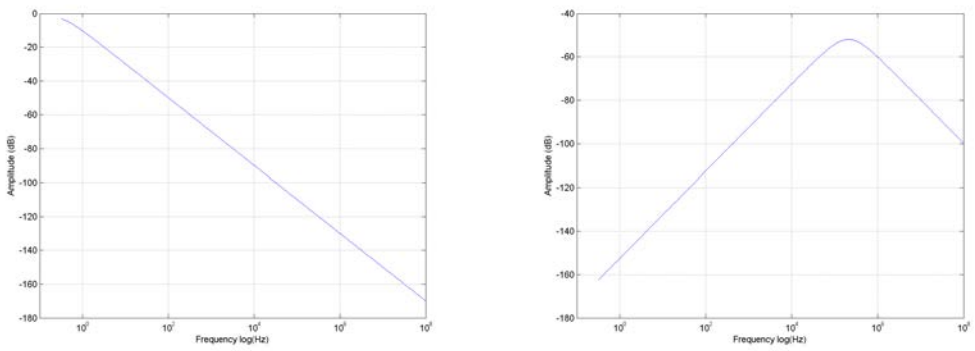

Figure 4.11: RC integrator and coil magnitude response FK-6328

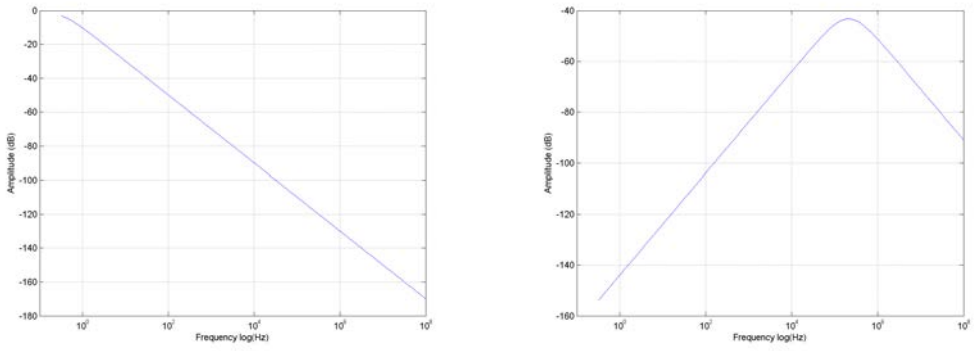

Figure 4.12: RC integrator and coil magnitude response FK-6330

The obtained response diagram (Bode plot) can be obtained by the 'sum' of the two previous ones.

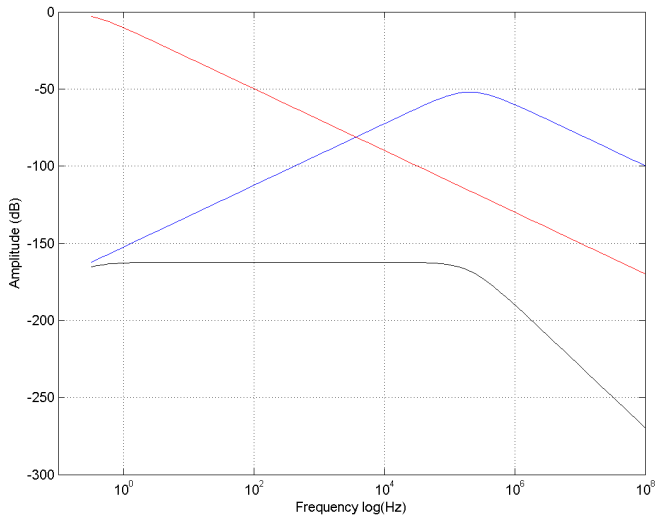

Figure 4.13: Magnitude response for FK-6328 as sum of coil and RC responses

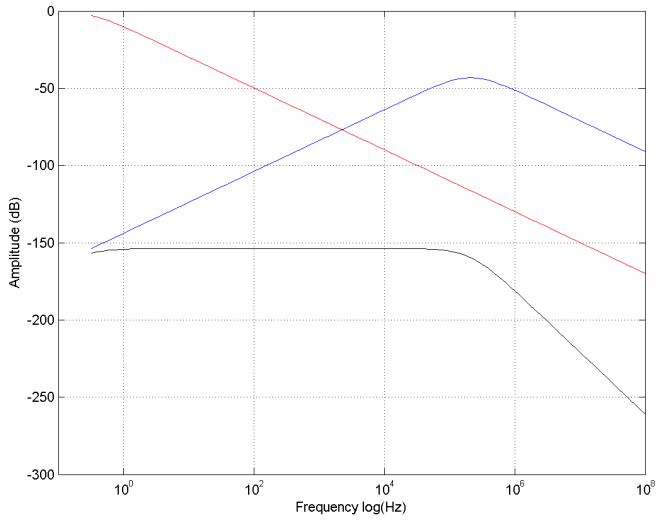

Figure 4.14: Magnitude response for FK-6330 as sum of coil and RC responses

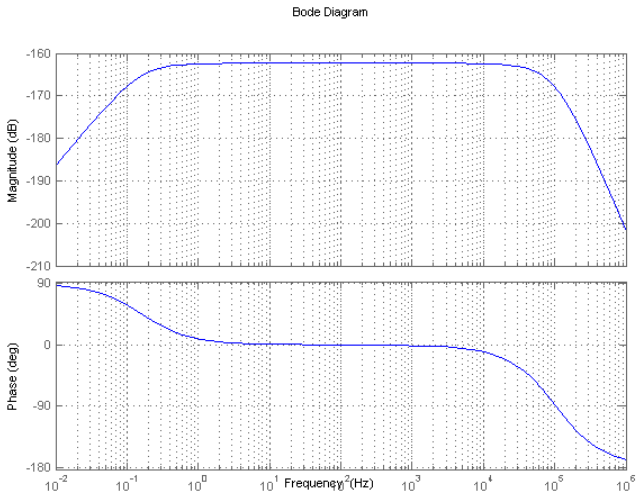

Figure 4.15: Bode diagram of FK-6328

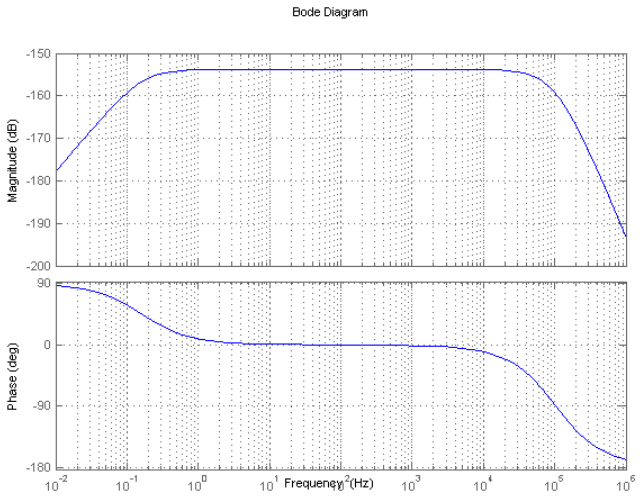

Figure 4.16: Bode diagram of FK-6330

The half power point of the coil is that frequency at which the output power has dropped to half of its mid-band value. That is a level of -3 dB, called also cut-off frequency. This occurs when the output voltage has dropped by $\frac{1}{\sqrt{2}}$ or 0.707, $20\log(\frac{1}{\sqrt{2}}) \approx -3.01dB$ and the power has dropped by half (1/2 or 0.5) (exact: $10\log(\frac{1}{2}) \approx -3.0103dB$. The bandwidth of the Rogowski transducer is the difference between the lower and upper half power points.

High frequency response As we can see from previous pictures, the upper point (high frequency) is determined by its resonant frequency. The self-inductance of the coil and its self capacitance form a resonant circuit. The higher the resonant frequency the better the high-frequency performance of the coil. Main parameters that affect the upper limit point are:[15]

- coil length, coil should be as short as possible
- mutual inductance, should be low
- output lead , it should be short to avoid extra capacitance
- presence of screen

Low frequency response The low-frequency response is determined by the design of the integrator used with the coil. Typically a response that is flat to within a few percent down to 1Hz is achievable. Coils with a low mutual inductance are not suitable for very low frequency measurements.[15]

4.6.1 Amplifier

The amplifier was modelized using PSPICE. The purpose was to calculate the amplitude and phase response of the circuit with a proper function available in the software. It is called AC Sweep. PSpice A/D calculates the small-signal response of the circuit to a combination of inputs by transforming it around the bias point and treating it as a linear circuit.
Non-linear devices, such as voltage- or current-controlled switches, are transformed to linear. In order to transform a device (such as a transistor amplifier) into a linear circuit, it is done the following:

1. Compute the DC bias point for the circuit.
2. Compute the complex impedance and/or transconductance values for each device at this bias point.
3. Perform the linear circuit analysis at the frequencies of interest by using simplifying approximations.

PSpice A/D automates this process. PSpice A/D computes the partial derivatives for non-linear devices at the bias point and uses these to perform small-signal analysis. The best way to use AC sweep analysis is to set the source magnitude to one. This way, the measured output equals the gain, relative to the input source, at that output.

That is the ideal response of the amplifier, taken from the data sheet for different values of the gain resistor G. Then, the modelling of the amplifier using PSPICE.

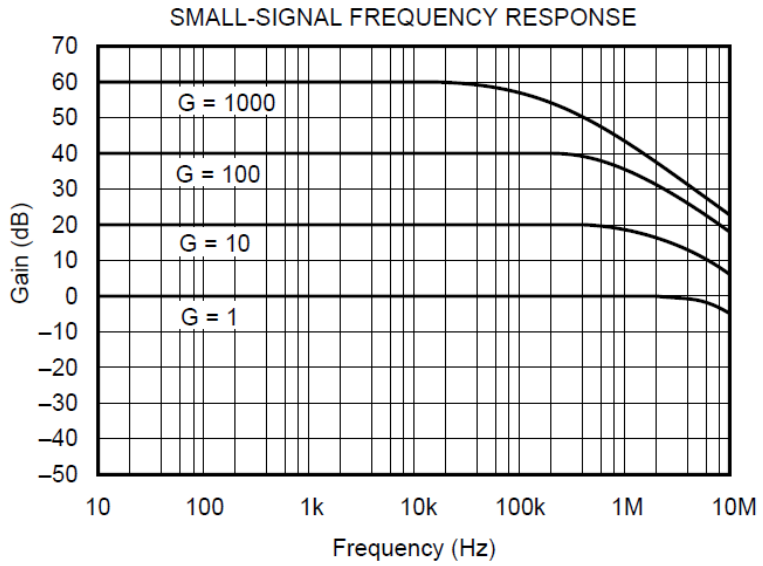

Figure 4.17: Frequency response of amplifier

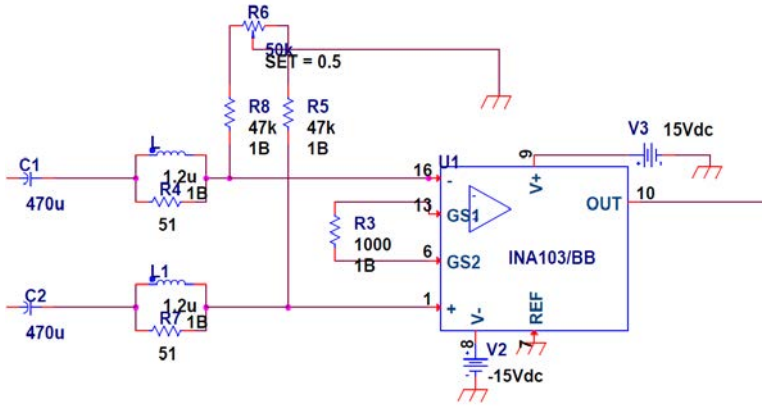

Figure 4.18: PSpice modelization of amplifier

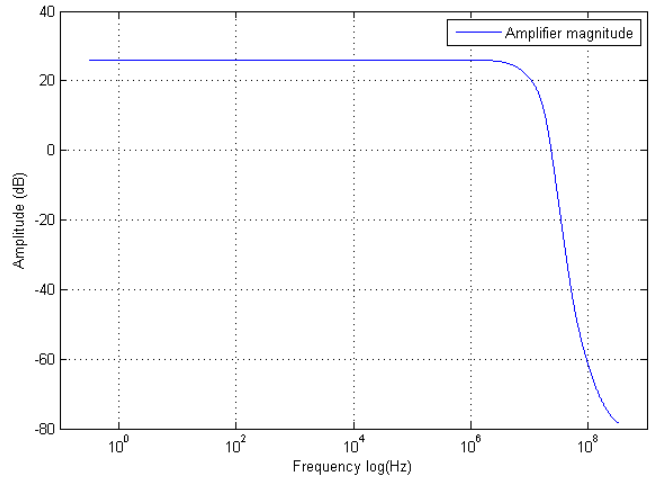

Figure 4.19: Magnitude amplifier response

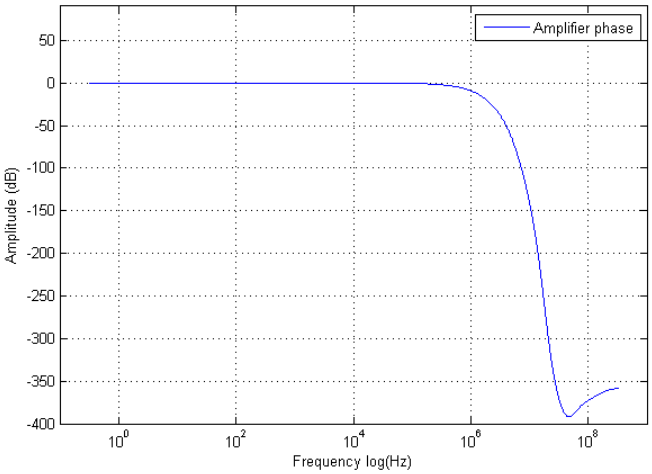

Figure 4.20: Phase amplifier response

Those are the comparisons between transducer and amplifier response.

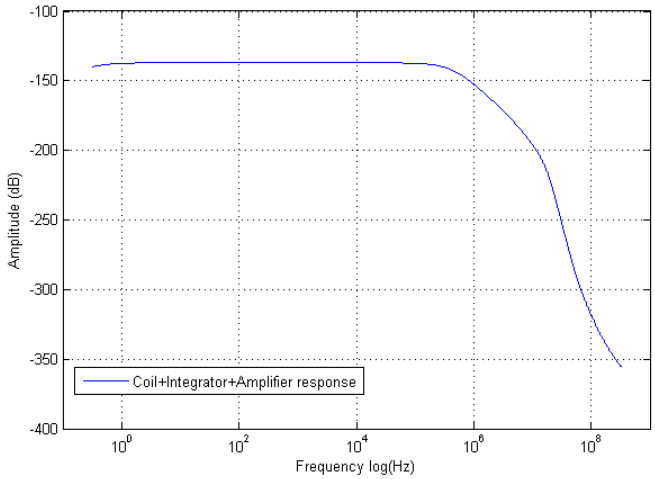

Figure 4.21: Magnitude amplifier and transducer response

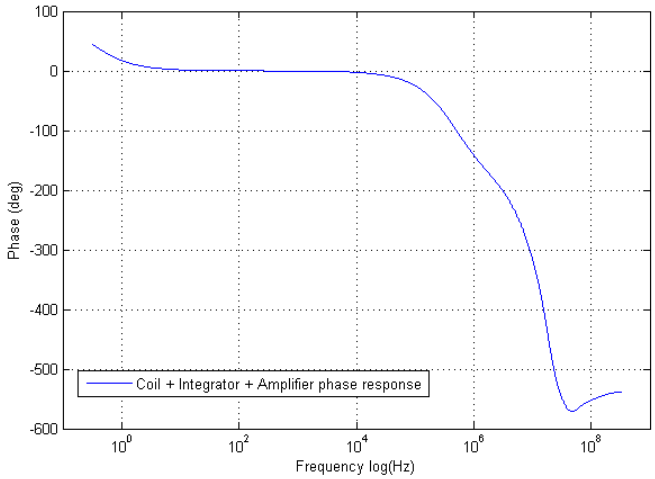

Figure 4.22: Phase amplifier and trasducer response

4.7 Analog filter implementation

From the transfer function of the coil and RC circuit and the transfer function of the amplifier (estimated) it is possible to obtain the total frequency response of the transducer. From that magnitude representation of the total frequency response, it is possible to estimate a filter which has the same frequency response as the transducer, especially the same bandwidth. Main requirements for a filter are:

- Bandwidth: 3-dB cut off frequency, the same as the transducer
- Slope: 40 dB/dec

This filter was estimated using an analog function, as represented in the following picture. As we can see, the filter well approximates the behaviour of the transducer in the pass-band area, while is less accurate in the transition area. However, or interest is to well preserve the signal in the passband area.

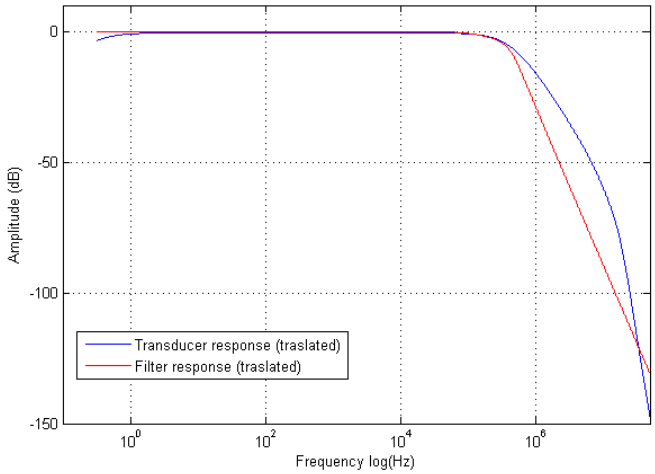

Figure 4.23: Analog Filter magnitude response

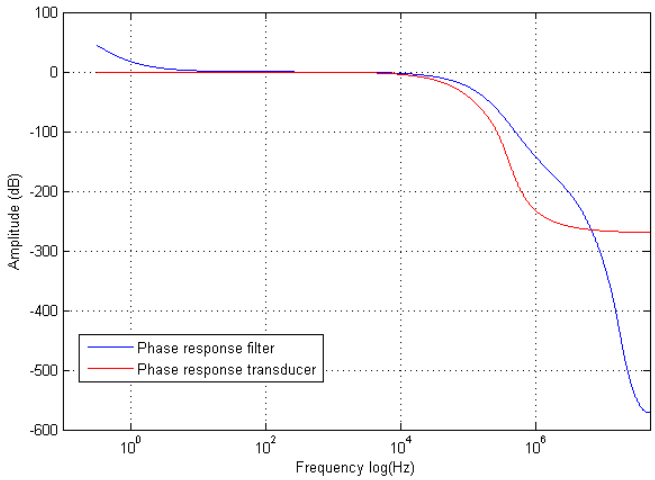

Figure 4.24: Analog filter phase response

4.8 Analog Butterworth filter Implementation

Butterworth belongs to the filter class called High-order or nth-order filters, because it has a shorter width of the roll-off (also called the transition band),compared to a simple first-order filter. The rate of roll-off and therefore the width of the transition band depends upon the order number of the filter so a simple first-order filter has a standard roll-off rate of 20dB/decade. High-order filters, such as third, fourth, and fifth-order are usually formed by cascading together single first-order and second-order filters.

The complexity or Filter Type is defined by the filters order, and which is dependant upon the number of reactive components such as capacitors or inductors within its design.

The frequency response of the Butterworth Filter approximation function is also often referred to as maximally flat (no ripples) response because the pass band is designed to have a frequency response which is as flat as mathematically possible from 0Hz (DC) until the cut-off frequency at -3dB with no ripples. Higher frequencies beyond the cut-off point rolls-off down to zero in the stop band at 20dB/decade or 6dB/octave. This is because it has a quality factor, Q of just 0.707.
The Butterworth filter provides the best Taylor Series approximation to the ideal lowpass filter response at analog frequencies $\Omega = 0$ and $\Omega = \text{inf}$; for any order N, the magnitude squared response has 2N-1 zero derivatives at these locations (maximally flat at $\Omega = 0$ and $\Omega = \text{inf}$). Response is monotonic overall, decreasing smoothly from $\Omega = 0$ to $\Omega = \text{inf}$. $H(j\Omega) = \sqrt{\frac{1}{2}}$ at $\Omega = 1$.

However, one main disadvantage of the Butterworth filter is that it achieves this pass band flatness at the expense of a wide transition band as the filter changes from the pass band to the stop band. It also has poor phase characteristics as well. The ideal frequency response is referred to as a brick wall filter, which corresponds to a rectangular window. The higher the Butterworth filter order, the higher the number of cascaded stages there are within the filter design, and the closer the filter becomes to the ideal brick wall response. In practice however, Butterworths ideal frequency response is unattainable as it produces excessive passband ripple.

Filter specification includes:

- Passband frequency ω_p, till cutoff frequency: normalized to half the sampling frequency (the Nyquist frequency). All of the filter design functions

operate with normalized frequencies, so they do not require the system sampling rate as an extra input argument. This toolbox uses the convention that unit frequency is the Nyquist frequency, defined as half the sampling frequency. The normalized frequency, therefore, is always in the interval between 0 and 1.

- Stopband ferquency ω_s
- Passband ripple: (A_{max}, in decibels)
- Stopband attenuation: (A_{min}, in decibels)

Design of Butterworth filter The design of a Butterworth filter is made as follows. We start from the typical lowpass second order transfer function which is defined as follows:

$$H(s) = \frac{K}{s^2(\frac{1}{\omega_n^2}) + s(\frac{2\sigma}{\omega_n}) + 1} \tag{4.45}$$

Putting

$$\sigma = \frac{1}{2Q} \tag{4.46}$$

we obtain

$$H(s) = \frac{K}{s^2(\frac{1}{\omega_n^2}) + s(\frac{1}{Q\omega_n}) + 1} \tag{4.47}$$

In the previous we have that:

- σ = damping factor
- Q = Q factor damping ratio
- undamped natural frequency, resonant frequency (not 3dB cutoff frequency)

It is possible to demonstrate that a Butterworth filter has two poles conjugate as $z_1 = -0.707 + j0.707$ and $z_1^* = -0.707 - j0.707$. Our requirements are:

1. Butterworth filter: $Q = 0.707$
2. Unity gain: K=1
3. Order: 2

4. Natural frequency: $0.3048MHz$

$$H(s) = \frac{1}{s^2(\frac{1}{\omega_n^2}) + s(\frac{\sqrt{2}}{\omega_n}) + 1} \tag{4.48}$$

The filter is obtained putting: $\omega_n = 0.3048MHz$.

Circuit design of Butterworth filter - Sallen-Key topology If we want to represent the filter using a circuit we can use the Sallen-Key topology.

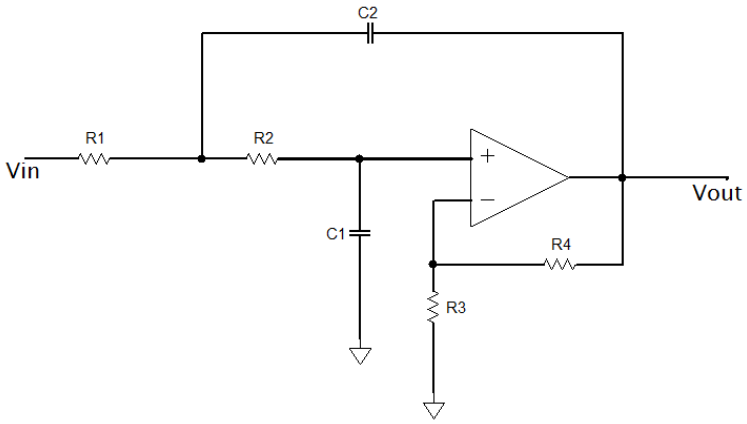

Figure 4.25: Sallen-Key topology

$$H(s) = \frac{\frac{R_3+R_4}{R_3}}{s^2(R_1R_2C_1C_2) + s(R_1C_1 + R_2C_1 + R_1C_2(-\frac{R_4}{R_3})) + 1} \tag{4.49}$$

Placing:

$$K = \frac{R_3 + R_4}{R_3} \tag{4.50}$$

$$\omega_n = \frac{1}{\sqrt{R_1R_2C_1C_2}} \tag{4.51}$$

$$Q = \frac{\sqrt{R_1R_2C_1C_2}}{R_1C_1 + R_2C_1 + R_1C_2(-\frac{R_4}{R_3})} \tag{4.52}$$

Remembering the conditions:

1. Butterworth filter: $Q = 0.707$

2. Unity gain: K=1
3. Order: 2
4. Natural frequency: $0.3048MHz$
5. $R_1 = R_2 = R$

We obtain, then:

$$R_4 = 0 \tag{4.53}$$
$$C_1 = \frac{1}{\sqrt{2}R\omega_n} \tag{4.54}$$
$$C_2 = \frac{\sqrt{2}}{R\omega_n} \tag{4.55}$$

Once chosen R and a natural frequency, it is possible to obtain directly C1 and C2. A circuit description is made:

$$V_1 = i_{C2}R_2 + V_{out} \tag{4.56}$$
$$V_1 = i_{out}C_2R_2s + V_{out} \tag{4.57}$$
$$V_1 = V_{out}(C_2R_2s + 1) \tag{4.58}$$

$$i_{C2} = i_{C1} + i_{R1} \tag{4.59}$$

$$\frac{V_{out}}{\frac{1}{sC_2}} = \frac{V_{in} - V_1}{R_1} + \frac{V_{out} - V_1}{\frac{1}{sC_1}} \tag{4.60}$$
$$sR_1C_2V_{out} = V_{in} - V_1 + sR_1C_1(V_{out} - V_1) \tag{4.61}$$

$$sR_1C_2V_{out} = V_{in} - V_{out}(R_2C_2s + 1) + sR_1C_1V_{out} - sR_1C_1(R_2C_2s \tag{4.62}$$

$$H(s) = \frac{\frac{1}{R_1R_2C_1C_2}}{s^2 + s(\frac{1}{R_2C_1} + \frac{1}{R_1C_1}) + \frac{1}{R_1R_2C_1C_2}} \tag{4.63}$$

The design obtained is called SallenKey topology: It is an electronic filter topology used to implement second-order active filters that is particularly valued for its simplicity.A SallenKey filter is a variation on a VCVS filter that uses a unity-gain amplifier (i.e., a pure buffer amplifier with 0 dB gain).

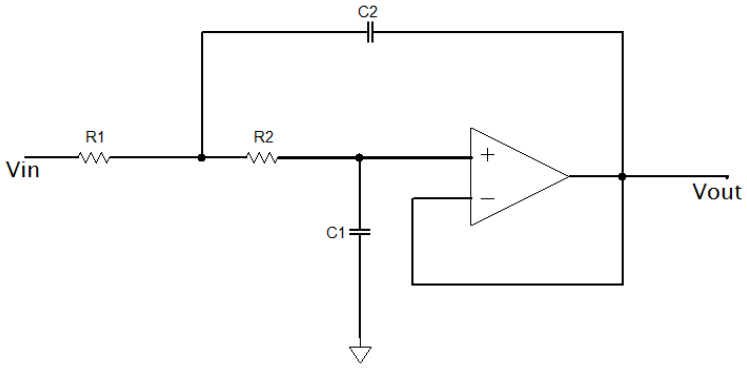

Figure 4.26: Sallen-Key topology when R1=R2 and G=1

As we can see, Butterworth approximates the real response much better than the simple anlog lowpass filter used before.

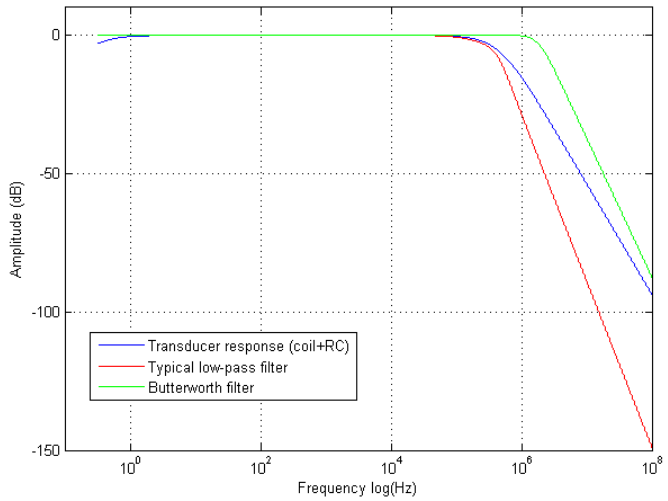

Figure 4.27: Analog and IIR magnitude response with trasducer response

The phase response is linear in the passband and has a small variation in transition from passband to stopband. This provides a very small phase delay which can be neglected.

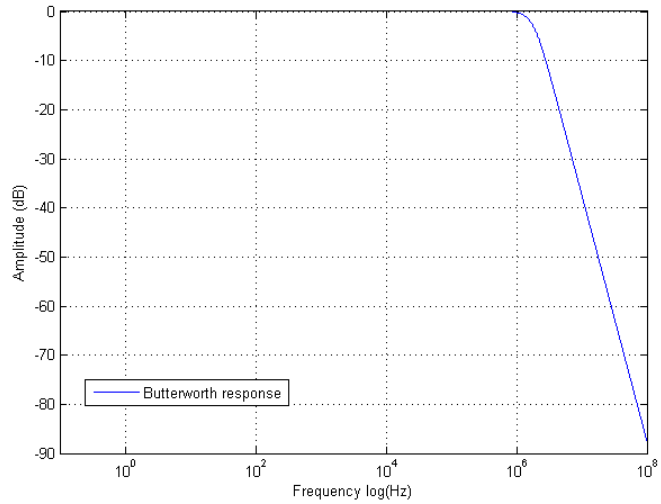

Figure 4.28: Butterworth magnitude response

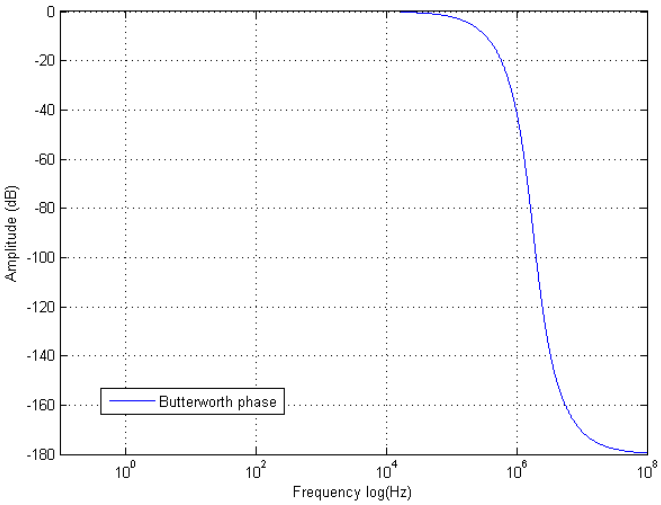

Figure 4.29: Butterworth phase response

Design of electronic circuit It is possible to represent the electronic implementation of the filter, which can be placed as a stage right downstream to the integrator circuit. In addition, there might be an electronic conversion of the signal into digital form (optocoupler) in order to avoid interferences between DAS and control room.

Cutoff frequency	0.3048 MHz
Order	2

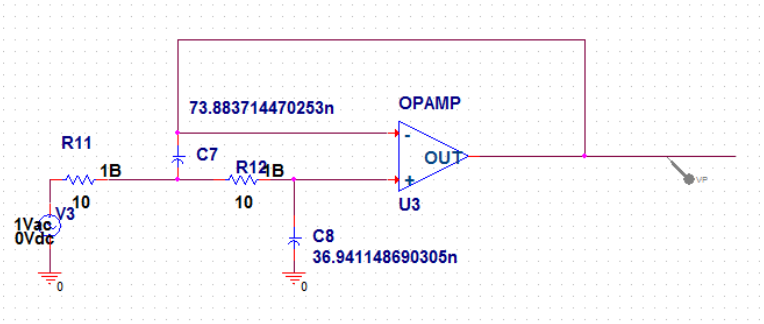

Figure 4.30: Butterworth filter in PSpice

The SIMSCAPE equivalent of the filter design has been used to filter all the following results.

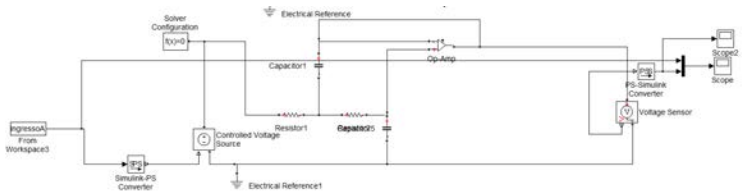

Figure 4.31: Butterworth filter in SIMSCAPE

Filter parameters:
Particular pratical aspects to take into account are:

- Given a specific corner frequency, the values of R and C are inversely proportional to each other. By making C larger R becomes smaller, and vice versa. Making R large may make C so small that parasitic capacitors cause errors. This makes smaller resistor values preferred over larger resistor values. [9]
- Capacitors: Avoid values less than 10 pF [9]
- Resistors: Values in the range of a few-hundred ohms to a few-thousand ohms are best [9]

Phase Linearity It's important to avoid distortion of the resulting signal, but filter used could partly have non-linear phase. If we consider its transfer function, with module

$$|H(w)| = G(w) \tag{4.64}$$

and phase

$$H(w) = \phi(w) \tag{4.65}$$

so that

$$H(w) = G(w)e^{j\phi(w)} \tag{4.66}$$

So, the complex signal, $e^{jw_1 t}$ is transformed, by the filter, in $G(w_1)e^{j(w_1 t+\phi(w_1))}$. So, if the phase is linear, then $\phi(w) = -t_0 w$ for a particular t_0. The ouput signal is then:

$$H(w) = G(w_1)e^{j\phi(w_1(t-t_0))} \tag{4.67}$$

So, the output signal is the same as the the input signal but shifted of a time t_0 , whatever is the frequency w_1. Out filter doesn't have the same linearity for all frequencies: that means that certain frequencies are shifted differently than others, creating distortion in the output signal. From the Bode plot, we see that the phase is not linear after the filter pole, and that could lead to a signal distortion. For this purpose, a SIMULINK simulation was made over an ideal D waveform to verify consequences of application of the filter. We see that the only consequence is a

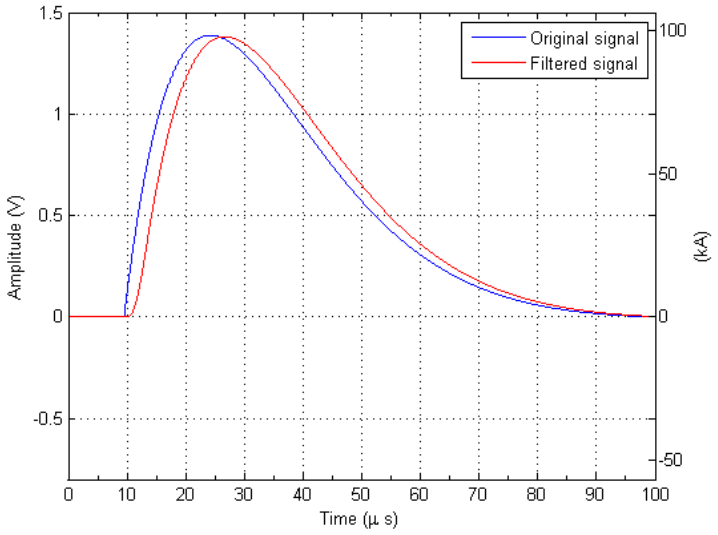

Figure 4.32: Filter application

time shif with no distortion of the signal.

	Relative error %
Rise time 10%-90%	1.28
Rise time 30%-90%	1.30
Fall time to 50%	0.29
Peak value	0.27

Response A good system must have a sufficient response speed in order to catch the rapid variations of the measured signal. That speed can be evaluated by the unit impulse response plot. Overshooting and ringing are important factors to take in consideration. The resistance in an RLC circuit will "damp" the oscillation, diminishing it with time if there is no driving AC power source in the circuit. So we can have those situations:

- Overdamping: ringing suppressed, what we want to obtain. The value of the damping factor σ can vary from 0 to 1. The more close it is to 0, the more ringing at time domain we have and the more high is the peak at ω_n in frequency domain. A value higher than 0.7 is considered acceptable for ringing suppression.
- Critically Damping: a circuit with a value of resistor that causes it to be just on the edge of ringing
- Underdamping: ringing happens. This is the condition studied in the previous section.

To avoid roll off in the signal output, especially at high frequencies signals, the damping resistance R_d must be fitted properly, according to the parameters. The damping resistance is the input impedance of the integrator. According to [8], the damping resistance is chosen so that, with a correctly damped coil, the -3dB roll-off point is at about the same frequency as the resonant frequency Unfortunately, damping a coil to give a flat amplitude response also has the effect of making the phase accuracy worse.

4.9 Butterworth filter in MATLAB

The previous method is equivalent to taking the MATLAB:

$$[z,p,k] = butter(n,Wn)$$

which allows to create a Butterworth filter from the n order and Wn cut-off frequency (normalized to half sampling rate).

4.10 Simulation of waveform produced by RLC laboratory circuit

The measured signal was also compared with a simulation of the current produced by the RLC circuit of the Laboratory. The RLC circuit for generation of D waveform is represented as folllows.

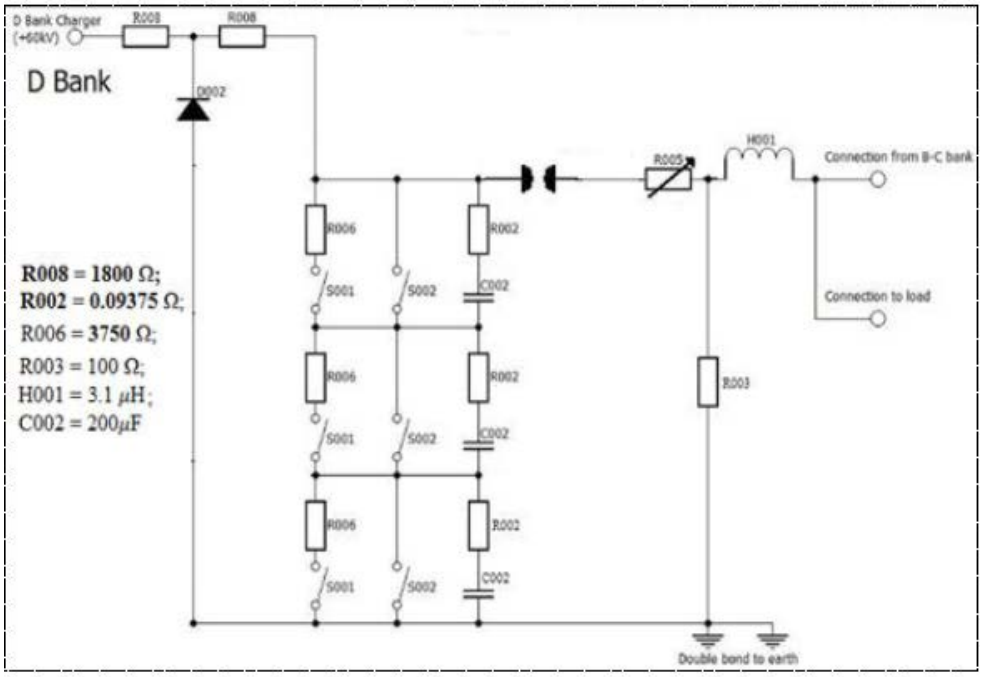

Figure 4.33: D waveform generator circuit

The transient in RLC circuit was simulated using the MATLAB Simulink Simscape package, which provides an environment for modelling and simulating physical systems spanning electrical domains. It provides fundamental building blocks from these domains that can be assembled into models of physical components, such as capacitors, resistors, inductors, pneumatic triggers and current transducers.
The physical signals are then converted into Simulink signals using a PS-Simulink Converter block, so they can be treated as normal MATLAB variables.

4.10.1 Description

Here is a picture of the Simscape model.

Component	Value	Others
Resistor1	0.09375 Ω	
Resistor2	0.09375 Ω	
Resistor4	0.09375 Ω	
Capacitor1	200 μF	Charged
Capacitor2	200 μF	
Capacitor3	200 μF	
Resistor3	0.08875 Ω	
Inductor	3.1 μH	

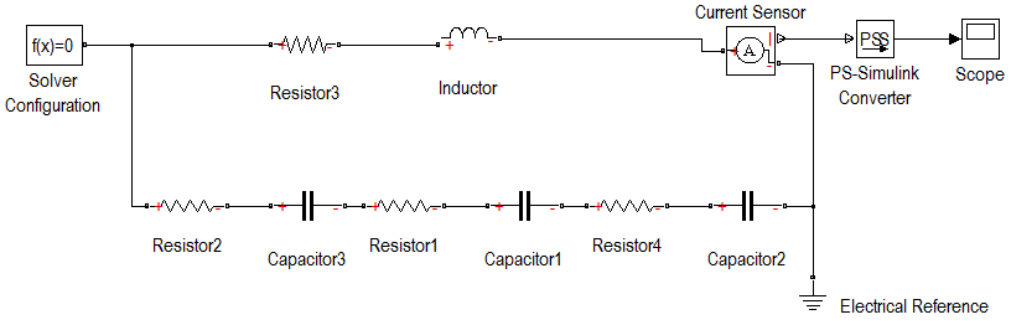

Figure 4.34: Simscape model

Resistor1,2,4 and Capacitor1,2,3 (R002 and C002) are part of the D waveform capacitor bank. The D-bank generator incorporates three sub-assemblies of series-connected 0.09375Ω resistors (Resistor1,2,4) with 200 F capacitors (Capacitor1,2,3), linked in series using long flat aluminium bars. These GAEP castor oil-impregnated capacitors are rated at 20kV and have Direct Current (DC) life of about 100 hours. The battery life is about 3000 charge/discharged cycles. Each capacitor has a single bushing having estimated equivalent series inductance of 40nH. Also, the rated voltage reversal is 20 % and maximum peak current rating is about 150kA, while the rated energy is roughly 50kJ.

Several HV 12.7cm diameter Linear Disc Resistors, each valued at 0.125 Ω 10 %, are combined uniquely to give an equivalent of 0.09375 Ω. This is achieved by connecting six discs in series across eight parallel branches.

Resistor3 represents the variable resistor (R005). It is implemented as three

stacks of resistors, which are combined appropriately to compensate for the test sample resistances. The resistances of stacks A, B, and C respectively are within the range of $0.125\Omega - 0.7708\Omega$, $0.1875\Omega - 1.1563\Omega$, and $0.375\Omega - 2.3125\Omega$. These three stacks are linked together in a parallel connection. Desired equivalent resistance can be achieved by adjusting flat conductive sheets on each stack, which have been designed to specific values. The value of Resistor3 is calculated considering the total resistance and subtracting the value of resistors 1,2,4. So, $Total_{resistance} - resistance_{1,2,4} = 0.37\Omega - (0.09375 * 3\Omega) = 0.37 - 0.28125 = 0.08875\Omega$.

As soon as the simulation starts, the capacitors discharge naturally through the circuit, simulating the discharge through short-circuited test rig.

The resulting current (D waveform) is measured by appropriate block. The physical signal from Simscape is converted to Simulink signal and then processed in MATLAB.

The inductor 'Inductor' (H001) represents the cumulative inductance of the circuit and is envisaged to be about 3.1μH. The major contribute to the total inductance is the HV bushing, that links the variable resistor stack and the test chamber, via eight 50 mm^2 H01N2-D welding cables at both input and return paths. However, within the test chamber, only six of these cables are actively connected to the test bed. Typically, the H01N2-D welding cable has a core made from Class 5 flexible plain copper conductors. The cable sheath is HOFR (Heat and Oil Resistant and Flame Retardant) with voltage rating of 450V for non-welding applications and thermal ratings between $-20C$ and $+85C$. At 100% duty cycle for a single cycle operation over a maximum period of 5 minutes, the implemented 50 mm^2 cable has a maximum loading capacity of 285A.

Here is a list of components which were not included in the simulation. They are part of the D waveform circuit but do not take part to the generation of the impulse.

- Capacitor charger. The 20kW TECHNIX SR60-P-20000 capacitor charger operates on 400V AC mains supply to deliver 0 - 60kV output voltage, at output current ranging from 0 - 500mA. Both voltage and current outputs are continuously adjustable from 0 to 100% full scale mode.

- Protection diodes. The diode represented is used to provide protection for the D-bank charger against any feedback from the charging circuit (sixty DSI 45-16A rectifier diodes). Each diode has a reverse blocking voltage (VRRM) of 1600V, with forward voltage (VFO) equals 0.85V; the root mean square (rms) forward current is rated at 70A, while the internal resistance of the diode is a negligible $90m\Omega$.

- Dumping circuit. S001, S002, R006 are used for dumping during charging/discharging operations. Dumps are represented by a resistor-switch combination (S001 and R006), while switch S002 is the short-circuit to earth. During capacitor charging, the pneumatically controlled switches S001 and S002 must be open. Upon capacitor discharge, dumps are closed firstly followed by the earthing switch. This delay is a safety consideration for ejection of excess charges within the system, whilst preventing arcing at the bronze-plated switch terminals.

- Pneumatic trigger. It assists the arc during direct effect testing of CFCs. The ram houses two electrodes, one on each side, and the arcing proceeds rather very rapidly. Consequent upon this, a blast of air is fed into the ram to cool the spark gap.

- R003 fault resistor. The fault load resistor acts to eject high current from the system if no-discharge occurs through the test sample. This HVR which is rated at peak voltage of 60kV can withstand impulse energy up to 1,500kJ. As with other HVRs, the fault load resistor is air-cooled and screwed to a plastic shelf for adequate insulation.

-	Unit	Ideal (equation)	Limits (ED-84)	Simulation
Peak value	kA	100	$\pm$ 10%	98.55
Integral action	A^2 s	0.25 x 10^6	$\pm$ 20%	
Duration	μ s	500	$\leq$ 500	81.88
Rise time (10% -90%)V_{peak}	μ s	1.42	$\leq$ 25	8.56
Rise time (30% -90%)V_{peak}	μ s	1.24	$\leq$ 25	7.22
Rise time to 10% V_{peak}	μ s	0.08		0.59
Rise time to 30% V_{peak}	μ s	0.26		1.93
Rise time to 90% V_{peak}	μ s	1.5		9.15
Rise time to 100% V_{peak}	μ s	3.18		14.78
Max slope di/dt	A/s	$10^1$1 at 0 μ s		
Slope di/dt at 0.25 μ s	A/s	1.4 x $10^1$1		
Fall time to 50% V_{peak}	μ s	34.48		36.90

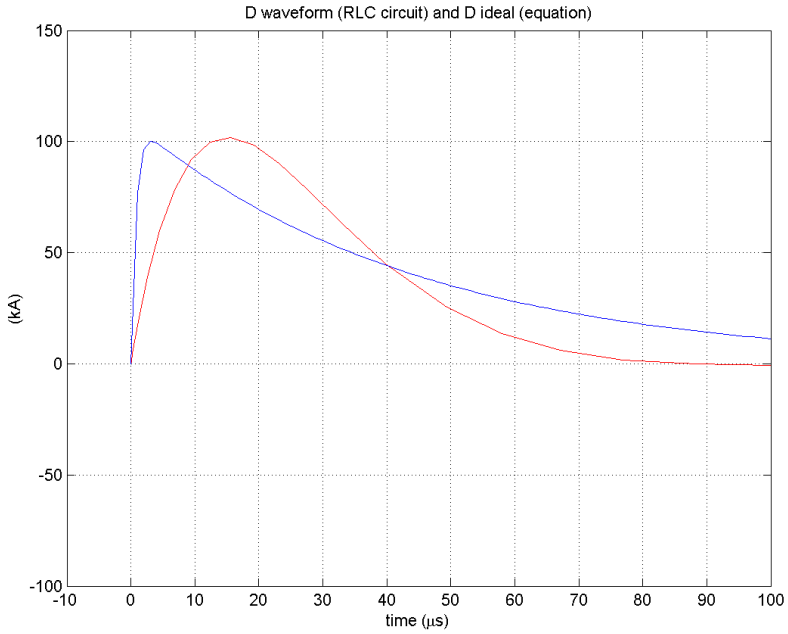

Figure 4.35: Comparison between D ideal waveform and simulated RLC

The different characteristics of the waveforms are due to the parameters of the RLC circuit.

4.11 Frequency domain analysis

4.11.1 Sampling issue

An analog signal is described by a function of time, say, x(t). The Fourier transform X() of x(t) is the frequency spectrum of the signal:

$$X(\Omega) = \int_{-\infty}^{\infty} x(t)e^{-j\omega t}dt \tag{4.68}$$

where Ω is the frequency in [radians/second]. The ordinary frequency f in [Hertz] or [cycles/sec] is related to Ω by

$$\Omega = 2\pi f \tag{4.69}$$

Sampling theorem: In the oscilloscope the analog signal x(t) is periodically measured every T seconds. Thus, time is discretized in units of the sampling interval T: $t = nT\ n = 0,1,2,..$

Considering the resulting stream of samples as an analog signal, we observe that the sampling process represents a very drastic chopping operation on the original signal x(t), and therefore, it will introduce a lot of spurious high-frequency components into the frequency spectrum which appears in a very regular fashion. Every frequency component of the original signal is periodically replicated over the entire frequency axis, with period given by the sampling rate: $f_s = \frac{1}{T}$

In the spectrum of the sampled signal, one cannot tell uniquely what the original frequency was. It could be any one of the replicated frequencies, namely, $f = f + mfs, m = 0, \pm 1, \pm 2,$ That is so because any one of them has the same periodic replication when sampled. This potential confusion of the original frequency with another is known as aliasing and can be avoided if one satisfies the conditions of the sampling theorem.

The sampling theorem states that for accurate representation of a signal x(t) by its time samples x(nT), two conditions must be met:

- The signal x(t) must be bandlimited, that is, its frequency spectrum must be limited to contain frequencies up to some maximum frequency, say f_{max}, and no frequencies beyond that.
- The sampling rate fs must be chosen to be at least twice the maximum frequency fmax,

$$f_s \geq 2f_{max} \tag{4.70}$$

that is, or, in terms of the sampling time interval

$$T \leq \frac{1}{2f_{max}} \tag{4.71}$$

The minimum sampling rate allowed by the sampling theorem, that is, $f_s = 2f_{max}$, is called the Nyquist rate. For arbitrary values of fs, the quantity fs/2 is called the Nyquist frequency or folding frequency. It defines the endpoints of the Nyquist frequency interval:

$$[-\frac{f_s}{2}, \frac{f_s}{2}] = Nyquistinterval \tag{4.72}$$

If we undersample, we may be missing important time variations between sampling instants and may arrive at the erroneous conclusion that the samples represent a signal which is smoother than it actually is. In other words, we will be confusing the true frequency content of the signal with a lower frequency content.

To calculate the Nyquist rate for our system it's useful to make these considerations:

- Rogowski transducer (Passive) allows signals up to 2.7 Mhz (-3dB point). So ideally frequencies much greater than 2.7 Mhz should not exist. However, it's still possible that noise superimposing in the cable could have higher frequency components.

- Active amplifier (output of integrator) limits output frequencies to 6 Mhz (-3dB point). That means that more higher frequencies would be cut off.

However the oscilloscope TDS 3034C is the main filter; For the used vertical scale (10mV/div to 1V/div) it has a bandwidth that reaches 300 Mhz (-3dB point). So, the ideal f_s would be $f_s = 600Mhz = 600MS/s$. The horizontal scale can be adjusted increasing the seconds per division (maximum limit is 2.5 GS/s @ 10 s/div).

T must be small enough so that signal variations that occur between samples are not lost. But how small is small enough? It would be very impractical to choose T too small because then there would be too many samples to be processed.

FFT Frequency range The range of frequencies covered in the output record from the FFT is 0 to 1/2 the sample rate of the acquired data record. For example, a sample rate of 20 MS/s (mega samples per second) would give an FFT range of 0 to 10 MHz. The value of 1/2 MS/s sample rate is often referred to as the Nyquist point.

Noise floor: The longer FFTs provide a lower noise floor. This is obtained increasing the number of points sampled. The cursor setting and the sample rate are the same for both figures.

Windowing: Windowing is a technique that compensates for some of the limitations of FFT analysis. The windowing operation consists of multiplying the time record by various weighting curves often named for their originators. The FFT operation is equivalent to curve-fitting a sum of complex sinusoids at discrete frequencies, to the observed data. The amplitudes and phases of these sinusoids are adjusted (computed by the FFT) to fit the observed data. If the number of sinusoids selected is equal to the data length (as in the FFT), the data can be fit exactly and uniquely. One limitation of using the FFT as a spectral estimator is that it cannot arbitrarily choose the frequencies of the sinusoids. The sinusoids are constrained to be at integer multiples of the sampling frequency divided by the record length (Sampling Frequency/Record Length). When a frequency component in a signal does not lie exactly on a bin, the FFT algorithm must assign a non-zero amplitude to many unrelated sinusoids in order to fit the time data exactly. The effect is often referred to as spectral leakage. This condition occurs more often when analyzing real-world signals. Since the algorithm assigns energy to these other components, the amplitude of the main component (the closest line to the actual signal frequency) tends to be underestimated. In addition, if there are smaller amplitude signals present in the data, they can be totally obscured by the leakage components.

The rectangular window is equivalent to multiplying all data record points by one. It generally gives the best frequency resolution because it results in the narrowest lobe width in the FFT output record. It gains frequency resolution at the expense of amplitude accuracy if the frequency of the signal being observed has a non-integer number of cycles in the FFT time record.

A rectangular window was chosen for the measured signal, because it is typically used for impulse response testing since the beginning points are usually zero and the data tapers to zero at the end of the record. The beginning points are zero because the impulse is normally placed in the center of the time domain record at the zero phase reference point. If phase is not important, the impulse can be placed at the beginning of the record. For this case, the window must be rectangular.

4.11.2 Discrete Time Fourier Transform (DTFT) and Discrete Fourier Transform (DFT)

In mathematics, the discrete-time Fourier transform (DTFT) is one of the specific forms of Fourier analysis. As such, it transforms one function into another, which is called the frequency domain representation, or simply the ”DTFT”, of

the original function (which is often a function in the time-domain). The DTFT requires an input function that is discrete.

The DTFT frequency-domain representation is always a periodic function. Since one period of the function contains all of the unique information, it is sometimes convenient to say that the DTFT is a transform to a "finite" frequency-domain (the length of one period), rather than to the entire real line.

The discrete-time Fourier transform (or DTFT) of a discrete set of real or complex numbers: x[n], for all integers n, is a Fourier series, which produces a periodic function of a frequency variable. When the frequency variable, ω, has normalized units of radians/sample, the periodicity is $2 * pi$, and the Fourier series is:

$$X(\omega) = \sum_{n=-\inf}^{\inf} x[n]e^{-j\omega n} \tag{4.73}$$

When the DTFT is continuous, a common practice is to compute an arbitrary number of samples (N) of one cycle of the periodic function X1/T:

$$X_d(k) = \sum_{n=0}^{N-1} x[n]e^{-j(\frac{2\pi}{N})kn} \tag{4.74}$$

where k goes [0,...,N-1].

In order to evaluate one cycle of xN numerically, we require a finite-length x[n] sequence. For instance, a long sequence might be truncated by a window function of length L resulting in two cases worthy of special mention: L N and L = IN, for some integer I (typically 6 or 8). For notational simplicity, consider the x[n] values below to represent the modified values.
The DFT and inverse DFT are implemented in Matlab by fft and ifft, respectively. In Matlab, Y = fft(x) returns the discrete Fourier transform (DFT) of vector x, computed with a fast Fourier transform (FFT) algorithm. Matlab also includes a functions fftshift and ifftshift that change the domain of the output or input, respectively, for fft and ifft from [0N-1] to [-N/2N/2-1]. If X() appears to be sampled too coarsely, then N should be increased, even if it means adding zeros to ends of the definition of x (know as zero padding). Doing a FFT one would like to insure that the power of the signal in the excluded (truncated) portion is insignificant.

With the Fourier transform analysis introduced above, it is possible to examine the frequency content of the signal. This would be useful for:

- Distinguish the noise component from the ideal signal; the signal is the one calculated from RLC circuit, as described in the previous section.

- Individuate the possible sources of noise, by comparing the frequency of the disturbs with known frequencies of components in the system. This has not been made
- Adopt specific shielding techniques against a particular frequency range of disturbs

4.11.3 Power Spectral Density PSD

From the average squared value it is possible to define then the power spectral density, normally used to examine the frequency content of a signal. For a certain interval of frequencies it is possible to apply the Perseval's theorem which states that:

$$\overline{x^2(t)_{\delta f}} = \int_{\delta f} S(f)df \tag{4.75}$$

to calculate the average squared value for a certain interval of feequencies. And this formula:

$$\overline{x^2(t)} = \int_0^{\inf} S(f)df \tag{4.76}$$

to calculate the same. The power spectral density S(f) is the Fourier transform of the autocorrelation of x(t).

$$S(f) = 2\int_{-\inf}^{\inf} \overline{x(t)x(t+\tau)}e^{j2\pi f\tau}d\tau \tag{4.77}$$

The MATLAB calculation of the PSD is obtained with this simplification. We consider a certain δf so small that S(f) can be considered constant in it. So, from Perseval we obtain that:

$$\overline{x^2(t)_{\delta f}} = S(f)\delta f \tag{4.78}$$

$$S(f) = \frac{\overline{x^2(t)_{\delta f}}}{\delta f} \tag{4.79}$$

So, the S(f) is calculated:

- Applying the Fourier transform to x(t) and obtaining X(f)
- Filtering with a rectangular filter the X(f) to obtain a δf sufficiently small.
- Measuring the RMS of X(f) = $\overline{x^2(t)_{\delta f}}$ in the small interval δf
- Obtaining S(f) as before

Chapter 5

Results

With reference of what explained in the previous chapter, here are the results of the tests:

5.1 D waveforms

5.1.1 Test 1 - Comparison between two different coils

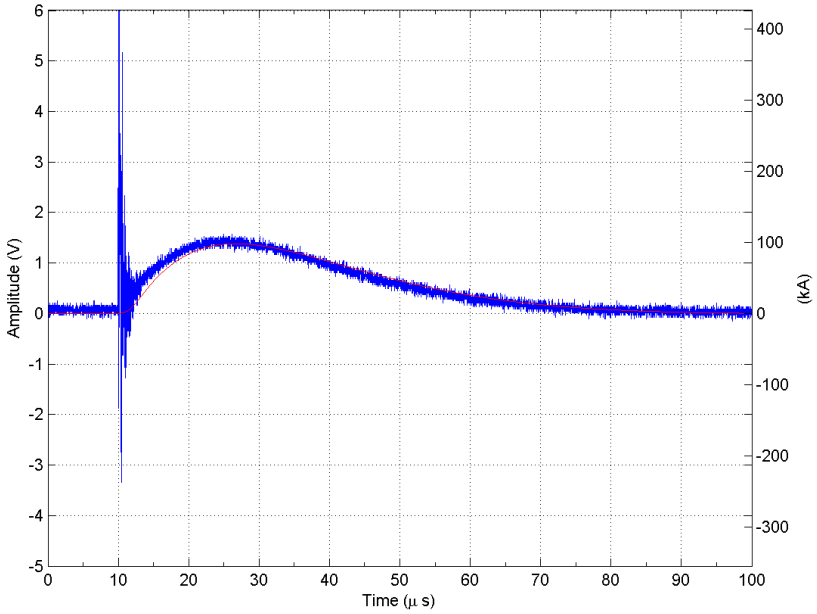

Figure 5.1: 55 kV - (FK-6328)

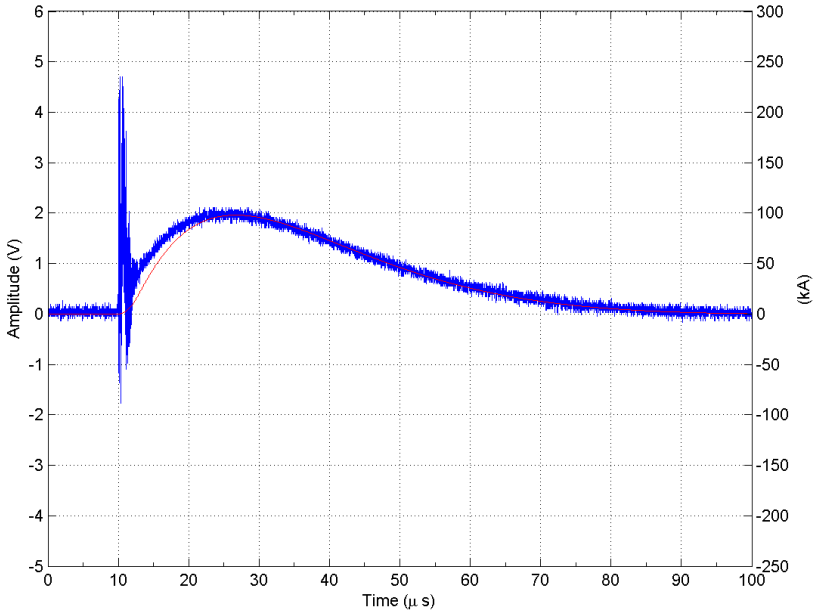

Figure 5.2: 55 kV - (FK-6330)

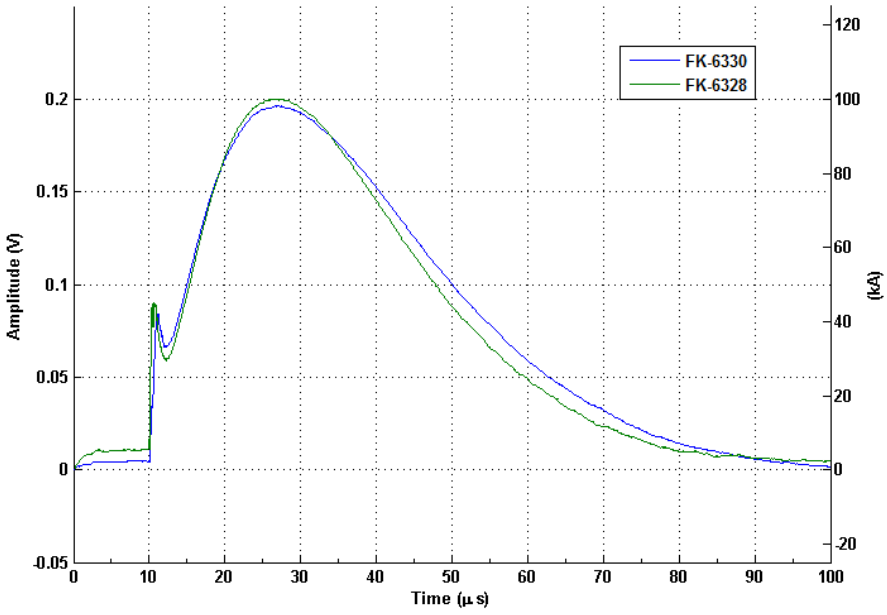

Figure 5.3: 55 kV -Filtered coils

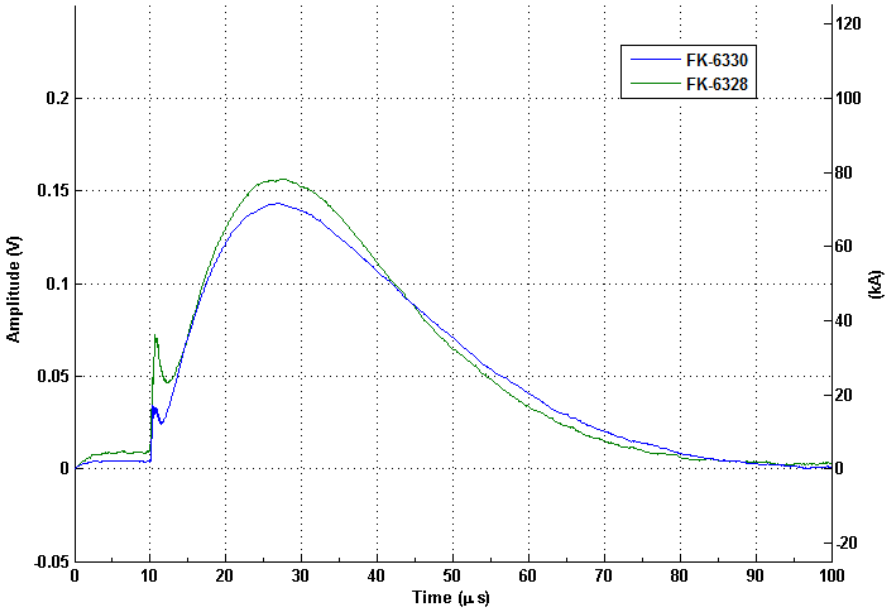

Figure 5.4: 40 kV -Filtered coils

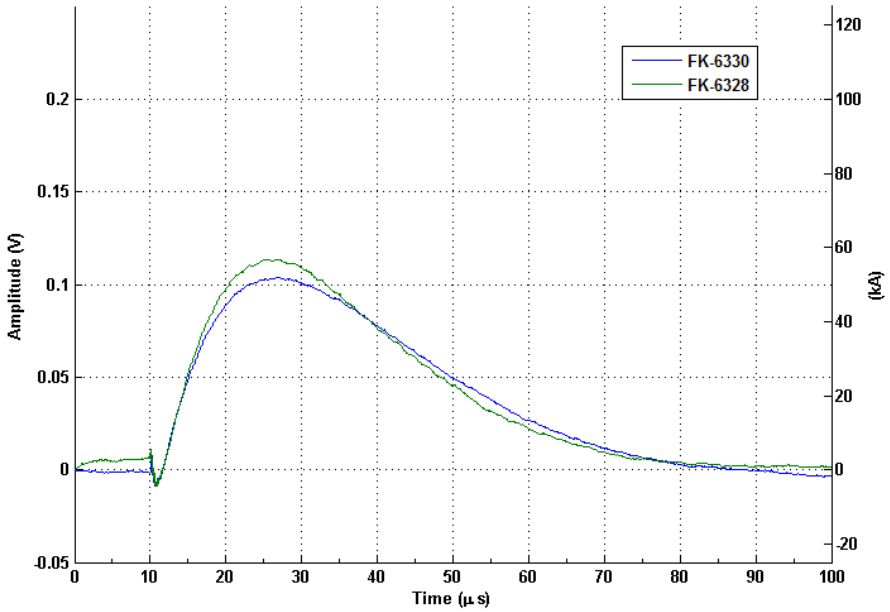

Figure 5.5: 30 kV -Filtered coils

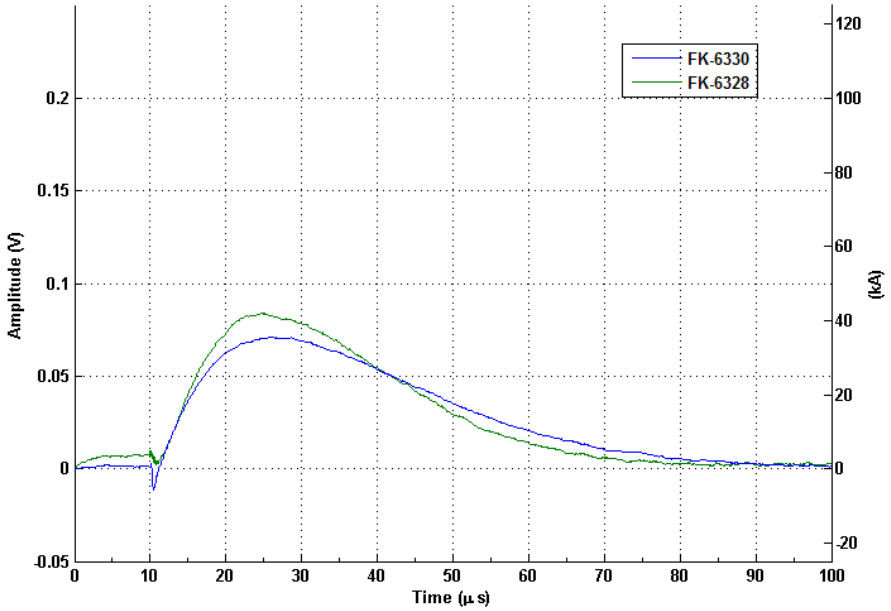

Figure 5.6: 20 kV -Filtered coils

In this section there are the relative errors between the FK-6328 and FK-6330 about the measured rise time, peak value and time to 50%. Tables used to calculate those errors are placed at the end of this book.

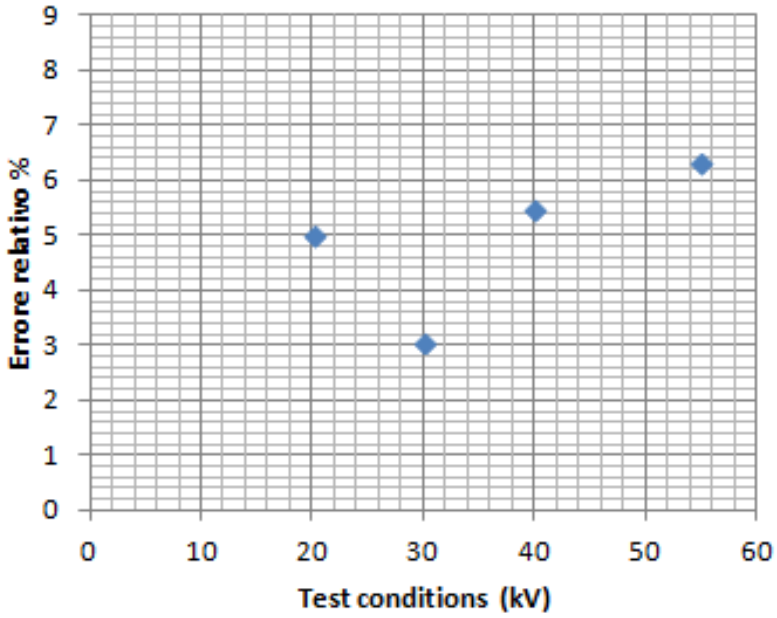

Figure 5.7: Rise time $(30\% - 90\%)$

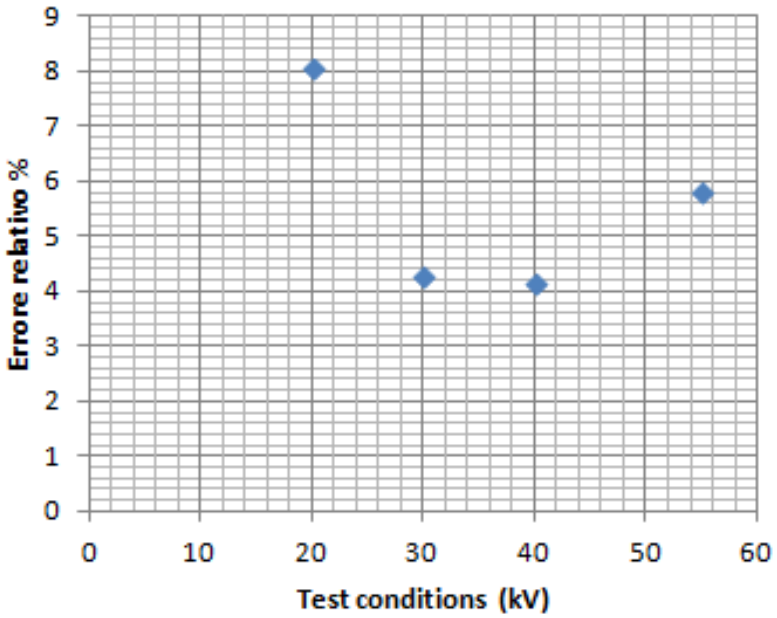

Figure 5.8: Peak value

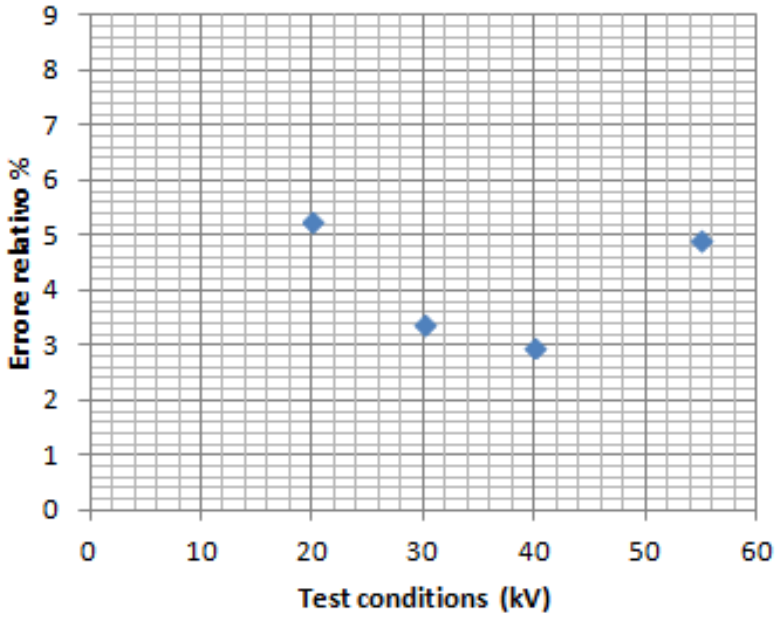

Figure 5.9: Time to 50%

5.1.2 Test 2 - Dependence on instrumentation position

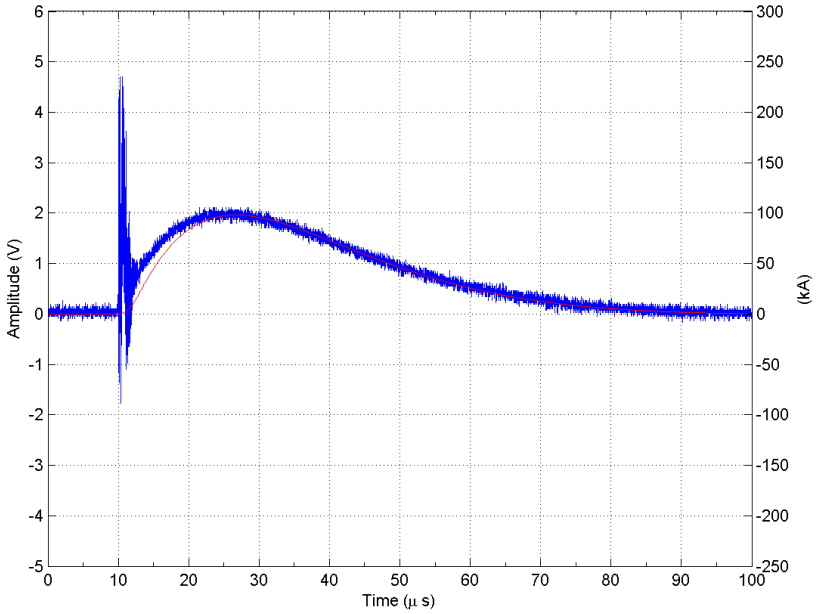

Figure 5.10: 55 kV - (FK-6330 (A))

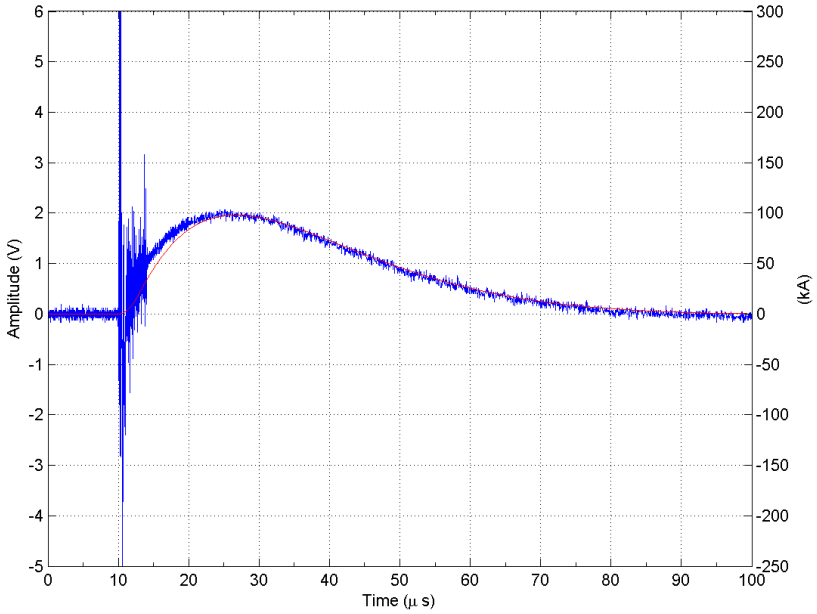

Figure 5.11: 55 kV - (FK-6330 (B))

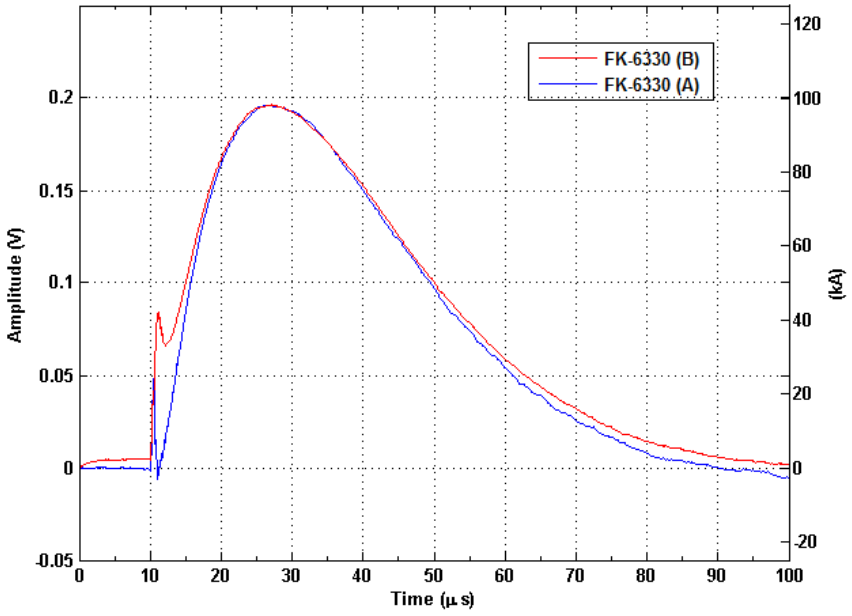

Figure 5.12: 55 kV -Filtered coils

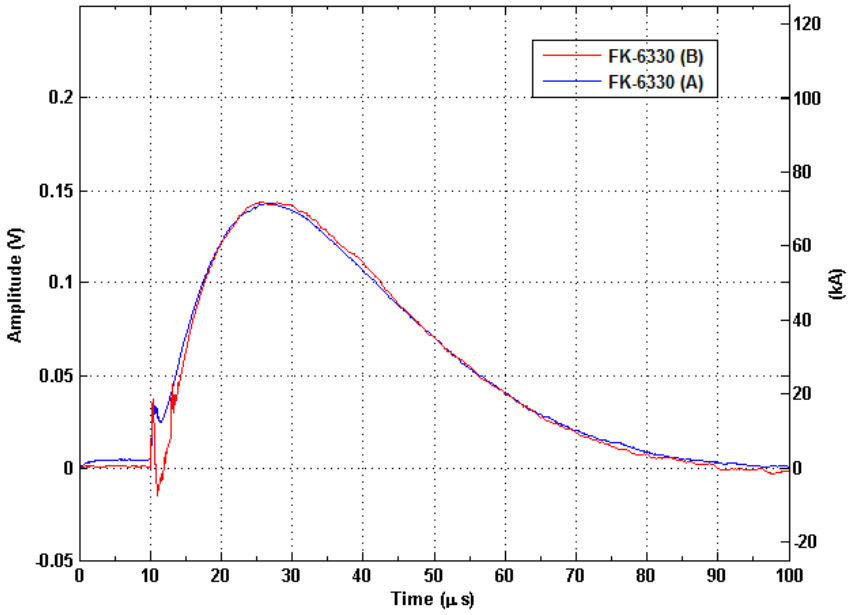

Figure 5.13: 40 kV -Filtered coils

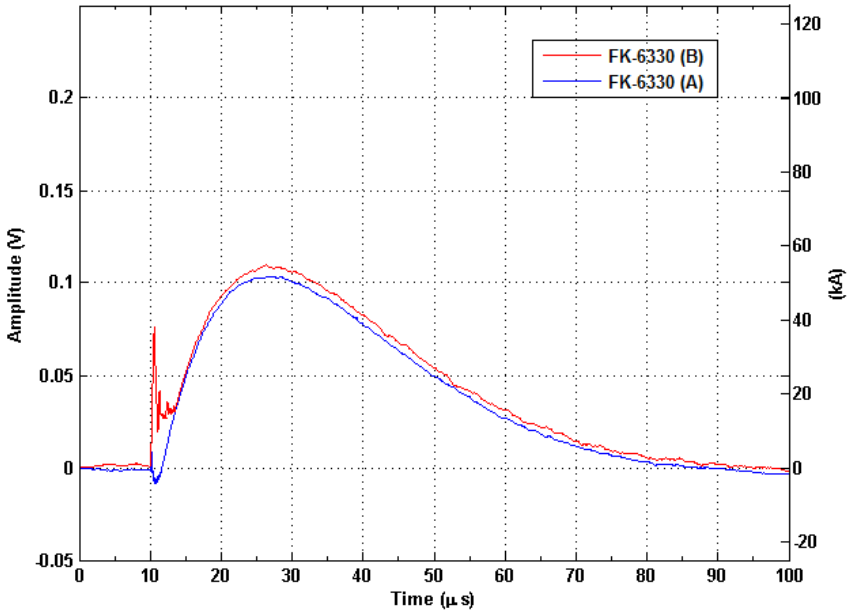

Figure 5.14: 30 kV -Filtered coils

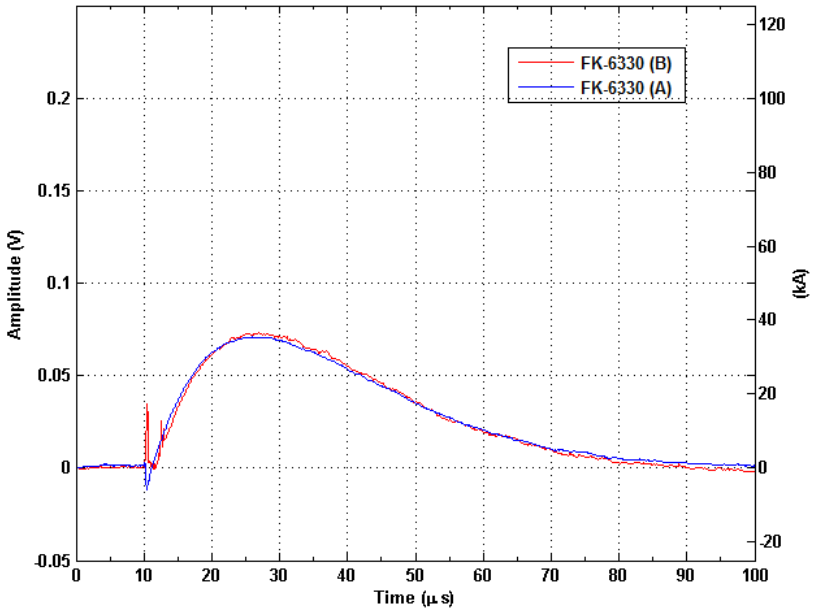

Figure 5.15: 20 kV -Filtered coils

5.1.3 Test 3 - Effect of screening

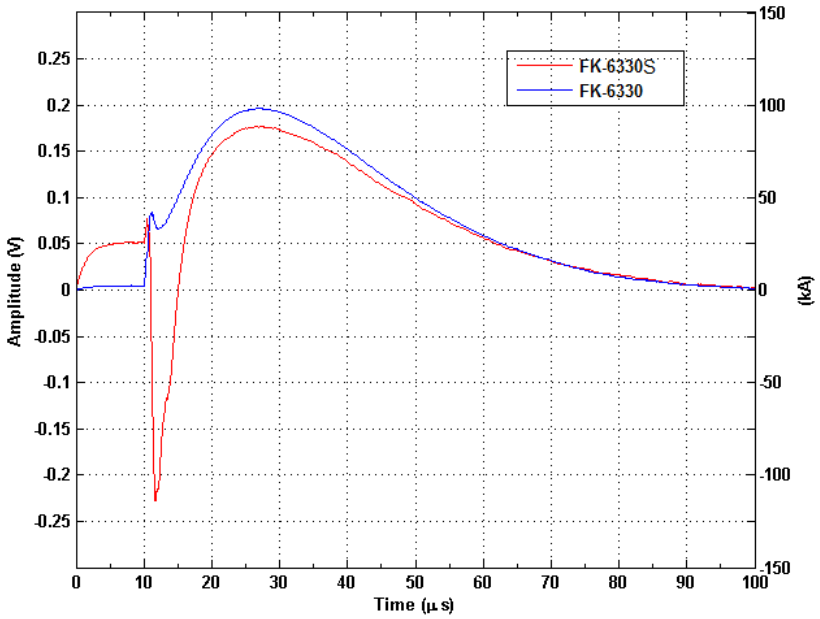

Figure 5.16: 55 kV -Filtered coils

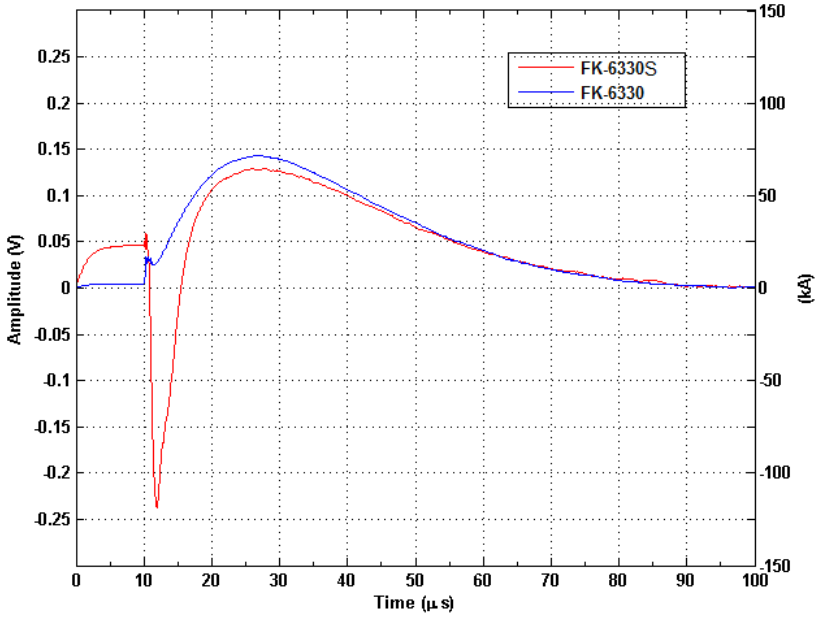

Figure 5.17: 40 kV -Filtered coils

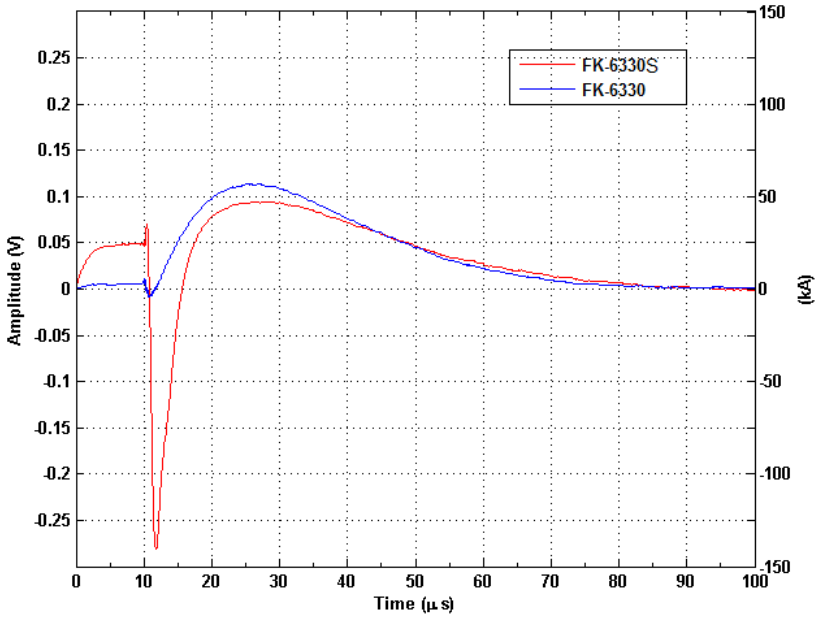

Figure 5.18: 30 kV -Filtered coils

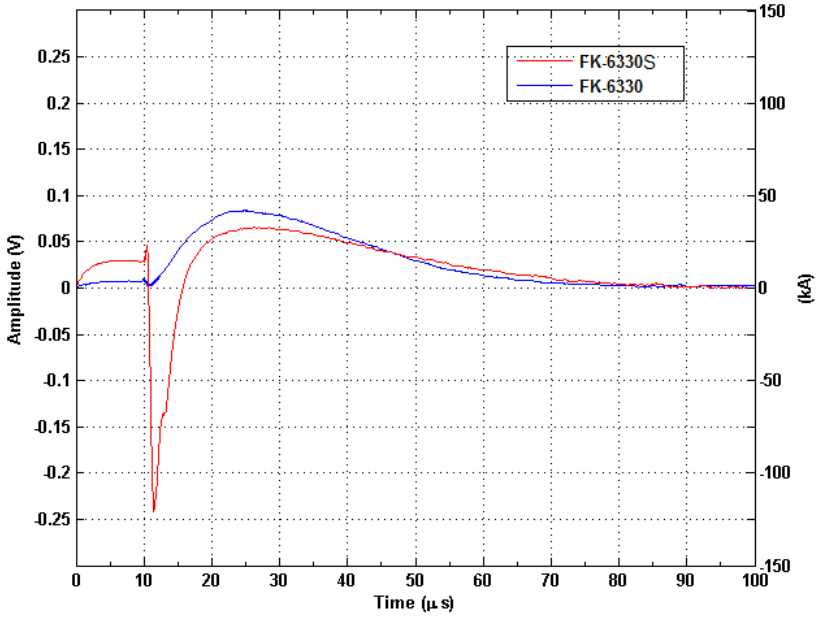

Figure 5.19: 20 kV -Filtered coils

5.1.4 Test 4 - Differential measurement

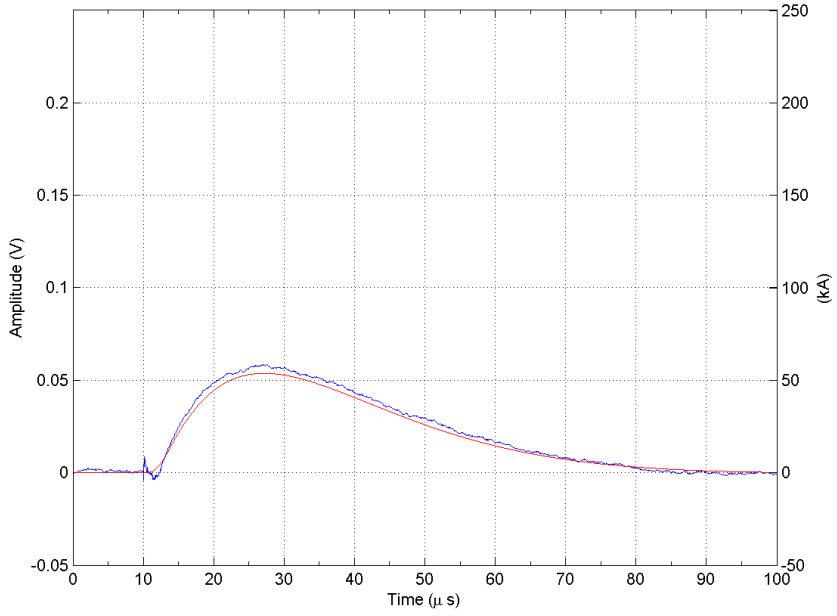

Figure 5.20: 55 kV - (FK-6328) 0

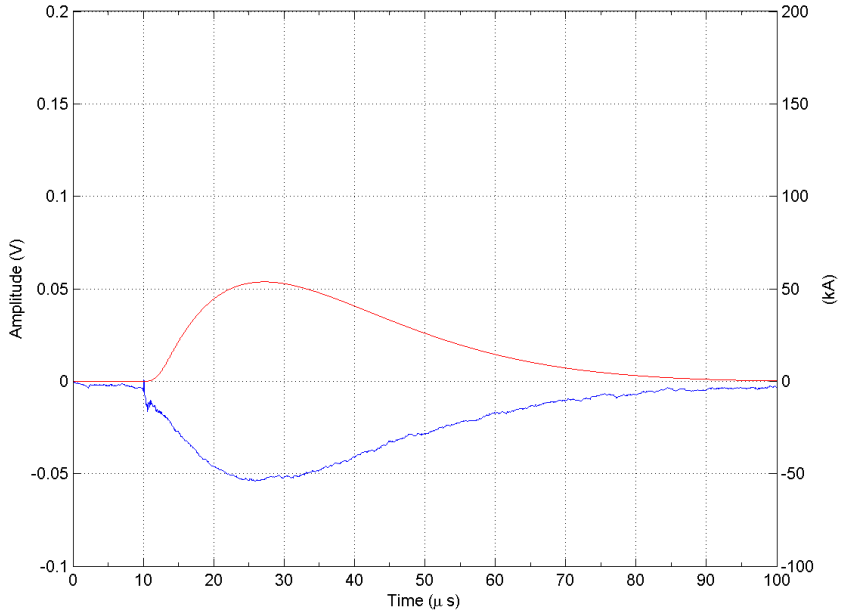

Figure 5.21: 55 kV - (FK-6328) 180

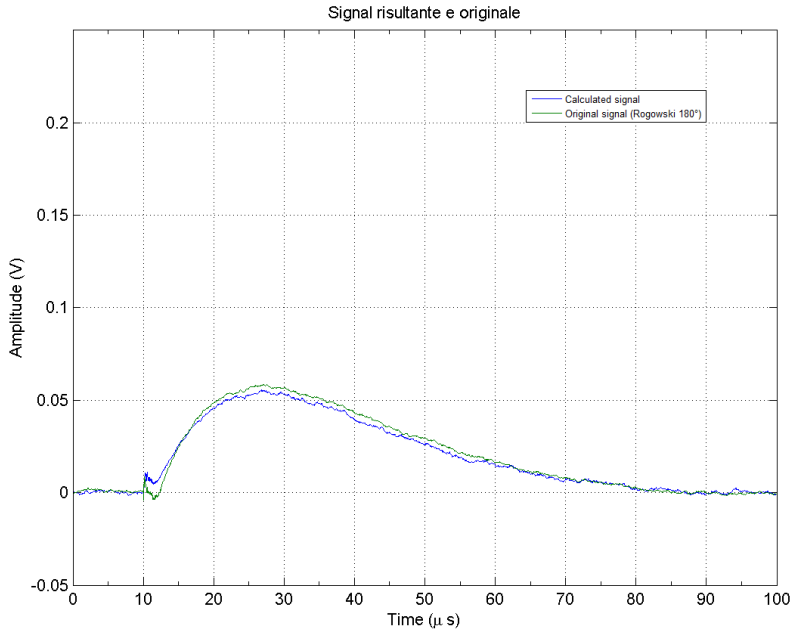

Figure 5.22: 55 kV - (FK-6328) Resulting signal

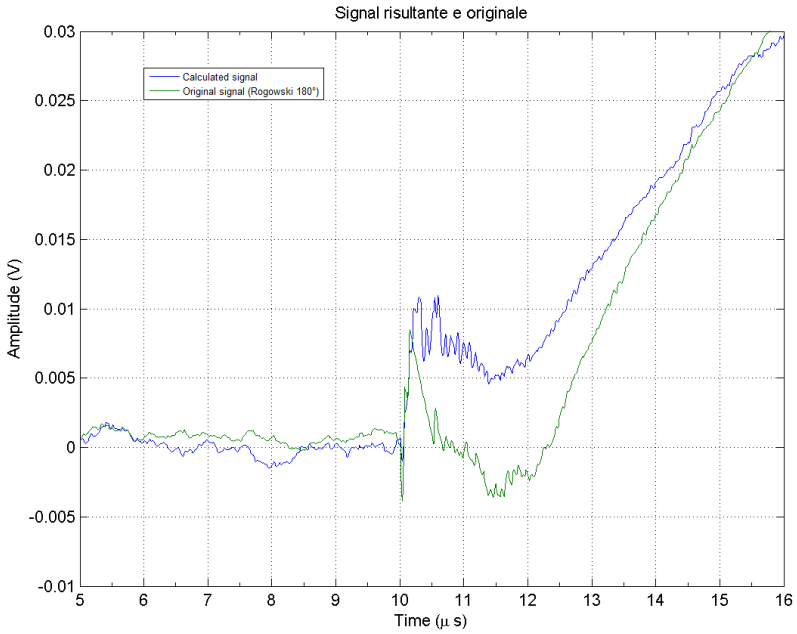

Figure 5.23: 55 kV - (FK-6328) Resulting signal

5.1.5 Test 5

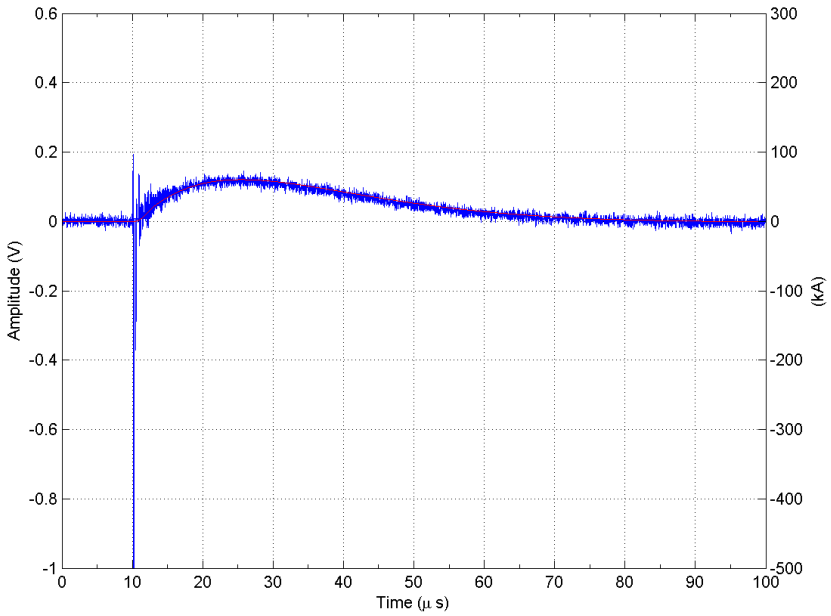

Figure 5.24: 30 kV - (FK-6328)

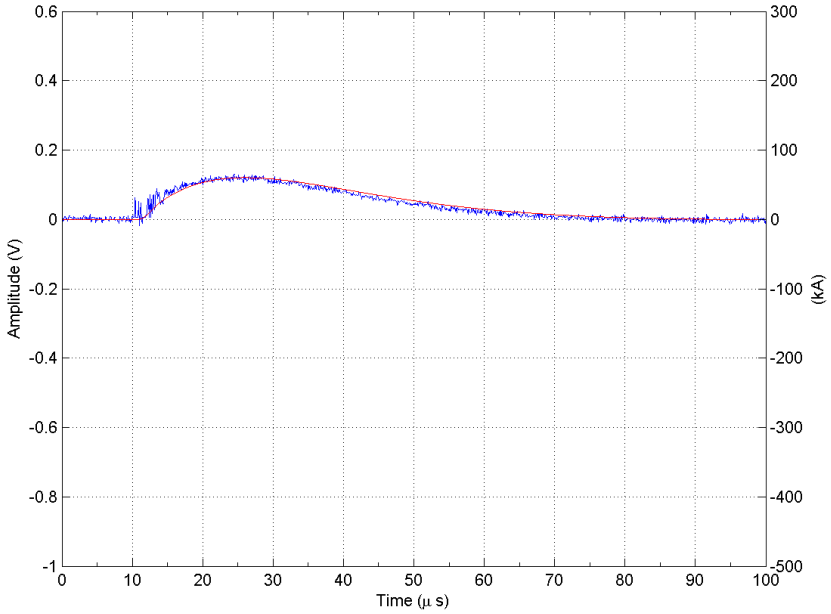

Figure 5.25: 30 kV - (FK-6328)

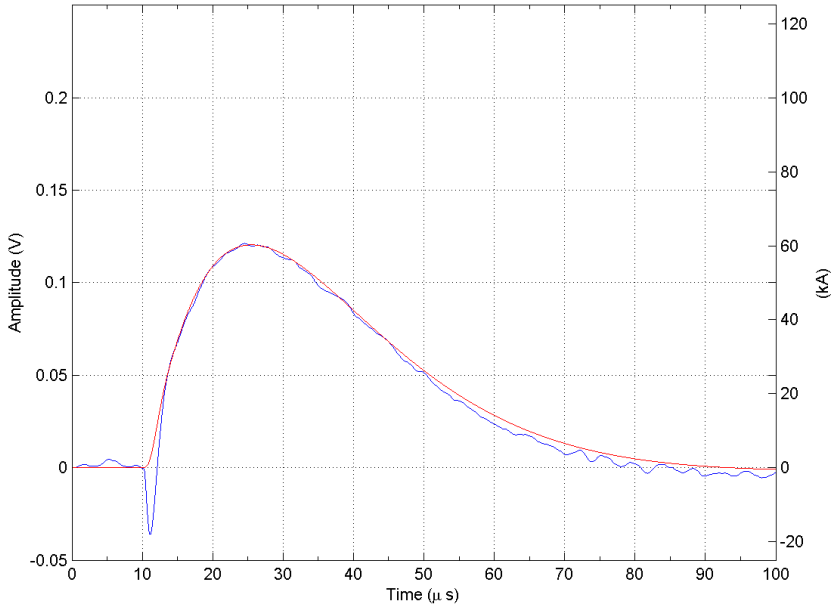

Figure 5.26: 30 kV - (FK-6328) Filtered

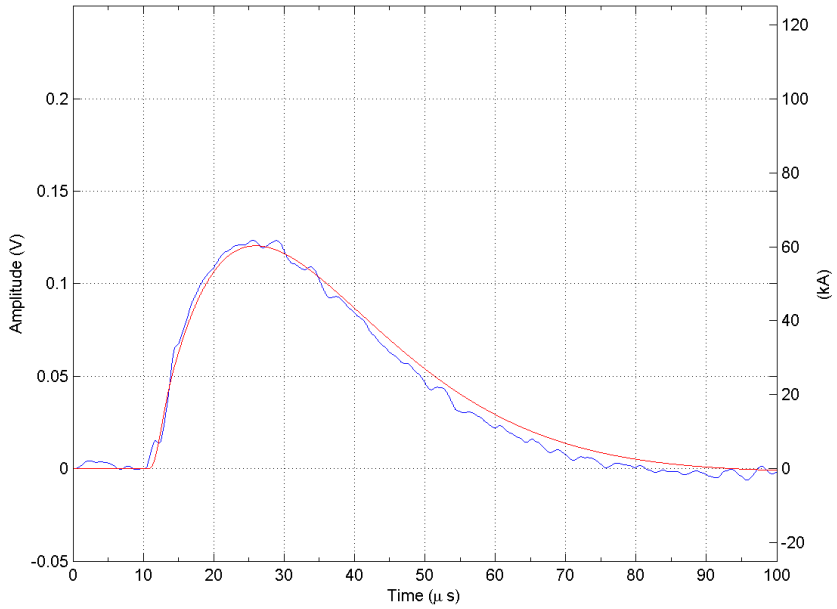

Figure 5.27: 30 kV - (FK-6328) Filtered

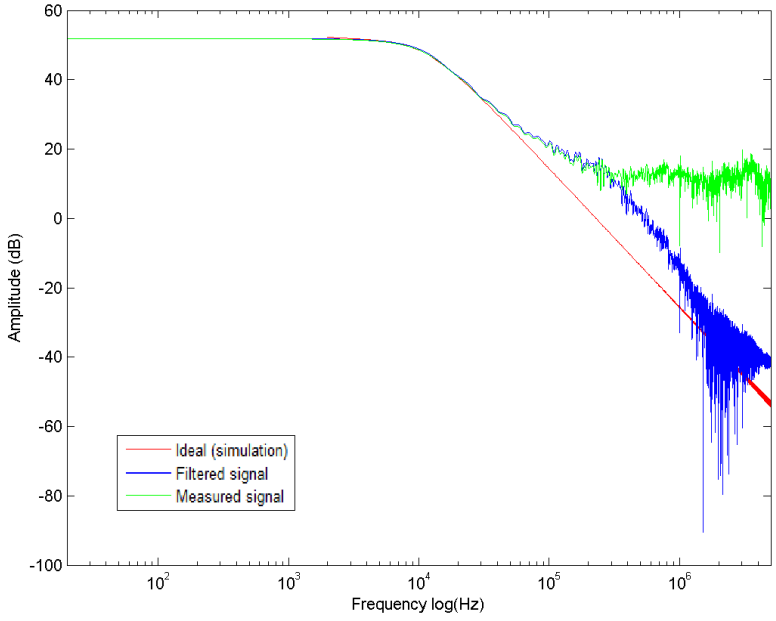

Figure 5.28: 30 kV - (FK-6328) Spectrum

5.1.6 Comparison with simulated waveform

Here there is a comparison between measured and simulated waveforms, using the configuration of Test 1.

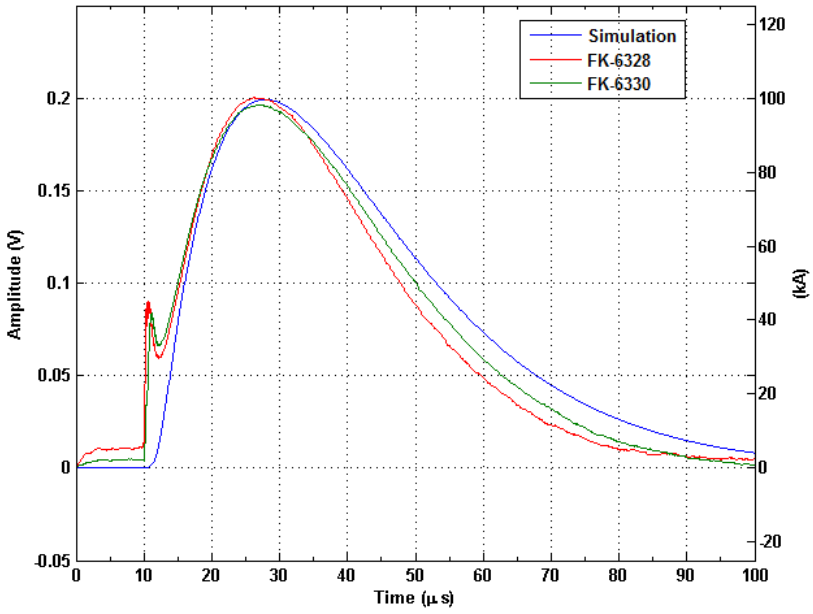

Figure 5.29: 55 kV- Measured FK6328, FK6330 and simulated waveform

5.2 Comments

5.2.1 Time domain analysis

From the previous figures we can see:

- Initial transient varies significantly with various tests and doesn't seem to be affected by the type of coil used (with/without screen) or by the conditions in which the test was made (55kV, 30kV).
- If we compare the pre-filtered and post-filtered waveform, we can see that filtering enhances the signal-to-noise ratio, allowing the signal to be viewed and compared with the simulated waveform.
- That means that the system is particularly affected by environment noise and may need to be screened more effectively.

5.2.2 D waveform

Here are discussed the results to the tests 1, 2 and 3.

- Measurements made by FK-6328 and FK-6330 (Test 1) differ for the waveform. This is confirmed by the study of the relative error which are between 3% and 8% for the rise time, time to 50% and peak value.
- This difference could be due to the characteristics of the coil FK-6328, which differ from the ideal model of Rogowski coil because it is flexible and has a larger diameter. This enhances the possibility of having a non uniform cross section S, non uniform turn density n, non orthogonality with measured conductor. In this situation , the pick up of magnetic fields from close conductors may be enhanced.
- In fact, measurements made with two similar coils FK-6330 (but different positions, Test 2) produce two waveforms which are very similar.
- From test 3 we see a very distorted signal from measurement from screened coil. That suggests that the screen used is not effective.
- So, measurements of waveforms are not affected by the position in the circuit of the coil but are affected by the type of coil used. Application of a screen to coil FK-6330 distorces the signal.
- The simulated waveform is the one we expect from the knowledge of base parameters of the Laboratory and surely respects the ED-84 standards on the rise time, peak value and fall time to 50%. The analysis shows that measured waveforms are compatible with the simulated one, so they respect ED-84 standards. Unfortunately, due to lack of precision of the simulated impulse (we only know some parameters), we can't make a numerical comparison between measured and ideal signals.

5.2.3 Initial spike

- In Test1, the initial noise occurs in the same way in both measurements. It is synchronous with the signal, and that supports the hypothesis that it is produced by the same circuit that produces the waveform. It may not be due to external instrumentation , power supply etc. which may produce an unsychronous noise.
- The problem is to identify in which way that noise couples with the signal. It may happen in the coil itself, in the cable, cable screen, in the passive integrator or amplifier, in the oscilloscope. The coupling mechanism may be

very difficult to identify: through earth connections, earth loops, magnetic, capacitive, electromagnetic, etc. Part of the noise may be part of the waveform (because it is measured by the coil) and part may be superimposed during measuring.

- One way to separate noise is to take measurements from two identical coils FK-6330 very close to each other on the same conductor but with one turned 180 degrees. We take the hypothesis that the noise couples in the same way in both coils. After making the difference of the two opposite signals, the common mode noise may be cancelled. This is the principle on which Differential Rogowski Coils work.

- We see also from test 2, that initial noise depends on ground connection point and coil position since both coils are identical but connected in two different points.

- The conclusion is that the initial noise is synchronous with the signal and is partly due to coupling and partly is measured. It also depends on the ground connections. Further informations may be obtained with a CT measurement.

5.2.4 Frequency domain analysis

Following there is a comparison between the RLC simulated signal frequency spectrum and the real measured in the following tests.

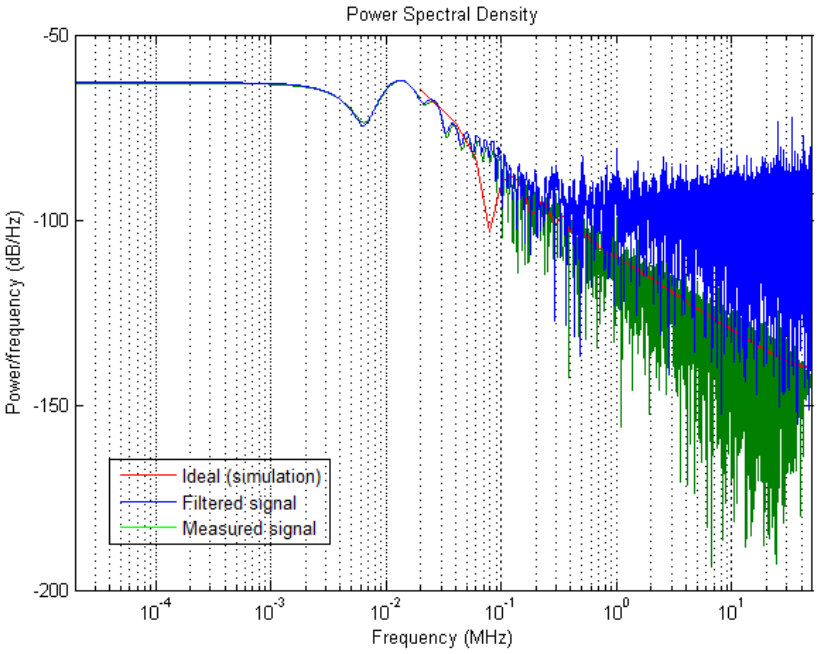

Figure 5.30: 55 kV - (FK-6330) PSD

We may distinguish those two parts:

1. Measured bandwidth: means the frequencies which are between 0 Hz and half of the sampling frequency (Nyquist frequency) which is 50 MHz.

2. Transducer bandwidth: means the set of frequencies between 0.161 Hz and 0.228 Mhz (or 0.233 MHz) , depending on coil type). This is the actual bandwidth of the current transducer.

From the previous pictures we can say that:

- The simulated signal is entirely comprised inside the transducer bandwidth and that suggests that it is an appropriate transducer for measuring this impulse.

- Inside transducer bandwidth, there is a portion where signal prevails over the noise (where the measured signal coincides with the simulated one). There is also a portion where the noise is preponderant.

- Outside transducer bandwidth, from 0.228 MHz (or 0.233 MHz), no significant signal should be measured. In the PSD it is possible to identify the white noise which has a constant power spectral density in the frequency

domain. When the diagram starts to rise in the low frequency area, then the white noise is not more preponderant.

- Any disturb as the initial spike visible in time domain would be concentrated into few spikes in frequency domain too, because it would be dominant into certain frequencies. However, due to high white noise, it is not possible to define which frequencies are dominant.
- From the previous results we can see that a great part of the background noise must be contained into this portion of spectrum. Also the initial transient is placed into this portion.

Chapter 6

Proposed solutions for signal quality and noise reduction

6.1 Improvement of the transducer shielding and bonding

However, to guarantee a better performance and to respect the indications [14], it is possible to improve the earthing system with the following solutions:

1. **Enclosure performance:** According to the results of the tests, we must adopt enclosure for instrumentation which comply with EMI standards and ensure a protection of at least the bandwidth range of the supposed noise ($>$ 100 kHz). For these frequencies a SE of at least 40 dB should be ideal.

2. **Cable shielding performance:** Also cables should be screened against radiated noise of frequencies above 100 kHz and with SE $>$ 40 dB. Simulations showed that some materials can reach this value

3. **Integrator module:** The integrator module needs to be re projected, especially for what concerns the amplifier section. Also, the passive output of the FK-6328 is highly distorted. This could be due to a bad measurement of the coil or to a distortion introduced by the passive section of the integrator module. The FK-6330 demonstrated to be more accurate and produced a less distorted signal.

4. **Reduce the impedance of earth wires:** While at DC or low frequencies, cable impedance is constant and purely resistive, at low-medium frequencies impedance rises as long as the inductance dominates. This effect is mitigated by the proximity of the cable to the reference plane.[14] When

the frequency rises to a point which the wire length becomes an appreciable fraction of the wavelength (it becomes resonant) the cable must be treated with transmission-line theory. In general, the impedance of a length of wire connected at one end to an earth reference plane reaches a resonant maximum when its length is a multiple of a quarter wavelength, and falls to a resonant minimum at multiples of a half wavelength. [14] Geometry and proximity to the plane can affect the position of the resonant peaks but not their order. Also, if any of those resonant peaks coincides with a susceptible or emissive frequency of the equipment, surprising and unpredictable variations in equipment performance will be brought about simply by moving such a wire by a few centimetres.
It is useful to adopt particular type of connections to avoid decoupling of the apparatus from earth with consequences on functional ground effectiveness. Using short fat straps instead of wires to connect oscilloscope to functional ground: they have lower impedance and normally help to reduce the entity of resonances and push them in high frequencies. [14] The best would be to use short wide metal plate with multiple bonds.

5. **Backplate:** Using backplate instead of directly connecting the earth wires from apparatus to the stud in the cabinet wall. A better solution would be to use a zinc backplate mounted inside the enclosure and bonded at every corner to the enclosure metal floor. The integrator would have its metal housing directly bonded to backplate, as described by METHOD C in [14]. The oscilloscope instead would be connected by short wide strap (described before) to a captive nut in the backplate, as described by METHOD B in [14].
   To ensure good conductivity, metal mating surfaces must be conductive, clean, free from contaminants and protected from corrosion. Rely solely on the body of a bolt or other mechanical fixing may not be good for rf as directly mating surfaces. The pressure of fixing should be enough to ensure a gas-tight joint between the two mating surfaces,, to help prevent corrosion. [14]

6. **Enclosure earth connection:** The best would be to have a connection at each corner of its frame, according to [14].

7. **Separate SRPP:** For the control of voltage differences in the earth structure at higher frequencies at the same level of power, or at higher powers for the same frequency, the mesh size needs to be smaller. With the different types of apparatus having been segregated according to weather they are noisy or sensitive, the building should then be partitioned into areas with different earth mesh sizes, depending on the earthing needs of each [14].

6.2 Use of Current Transformers

To solve the problem of the low SNR and to have a comparison with another transducer type, it would be useful to introduce a Current Transformer. Current monitors are able to measure pulses, transients and continuous signals. They do not measure steady-state dc current. We have to deal with a pulse measurement.

6.2.1 Differences between CTs and Rogowski Coils

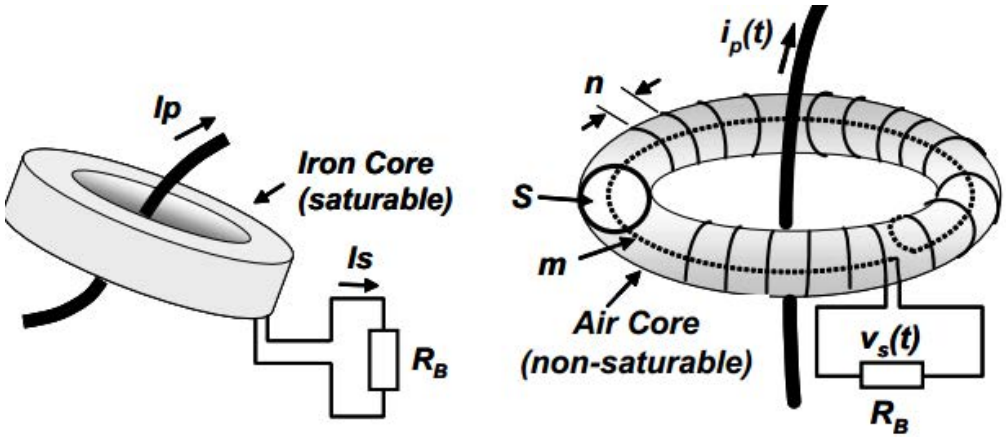

Figure 6.1: CT and Rogowski coils

- **Magnetic core** The main difference between Rogowski Coils and CTs is that Rogowski Coil windings are wound over an (non-magnetic) air core, instead of over an iron core.
- **Saturation and phase/magnitude errors** as a main consequence of the previous, Rogowski Coils are linear since the air core cannot saturate. In CTs, magnetizing current Ie introduces amplitude error and phase error. Since the CT iron-core has a non-linear characteristic it saturates at high currents, or when a DC component is present in the primary current. When the CT saturates, the magnetizing current increases and the secondary current produced decreases (ie. CT ratio error increases).
- **Output** the mutual coupling between the primary conductor and the secondary winding in Rogowski Coils is much smaller than in CTs. Therefore, Rogowski Coil output power is small, so it cannot drive current through low-resistance burden like CTs are able to drive. Rogowski Coils can provide input signals for microprocessor-based devices that have a high input

resistance; therefore, these devices measure voltage across the Rogowski Coil secondary output terminals.

- **Output type** unlike CTs that produce secondary current proportional to the primary current, Rogowski Coils produce output voltage that is a scaled time derivative di(t)/dt of the primary current. Signal processing is required to extract the power frequency signal. Why does it happen?

- **Disturbs** As Rogowski Coils use a non-magnetic core to support the secondary windings, mutual coupling between the primary and secondary windings is weak. Because of weak coupling, to obtain quality current sensors, Rogowski Coils should be designed to meet two main criteria: the relative position of the primary conductor inside the coil loop should not affect the coil output signal, and the impact of nearby conductors that carry high currents on the coil output signal should be minimal. The first criteria can be achieved when: This can be achieved if the windings are:

  1. on a core that has a constant cross-section S,
  2. perpendicular to the middle line m (dashed line in Figure 2-2 that also represents return wire through the winding), and
  3. built with constant turn density n.

The equivalent circuit for a CT and Rogowski coil are:

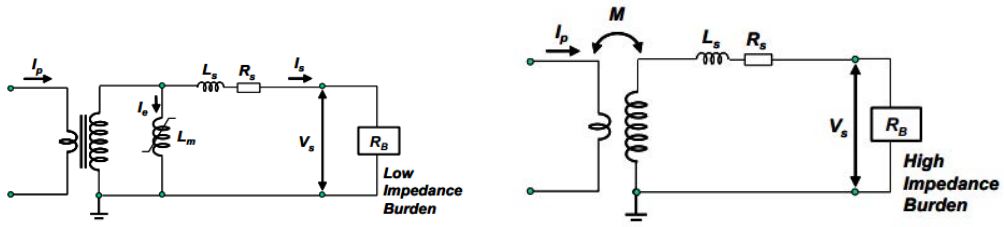

Figure 6.2: CT and Rogowski coil equivalent circuits

If we consider a CT equivalent circuit in which ferromagnetic losses are neglected, then it turns to be similar to Rogowski equivalent circuit, with the same transfer function.

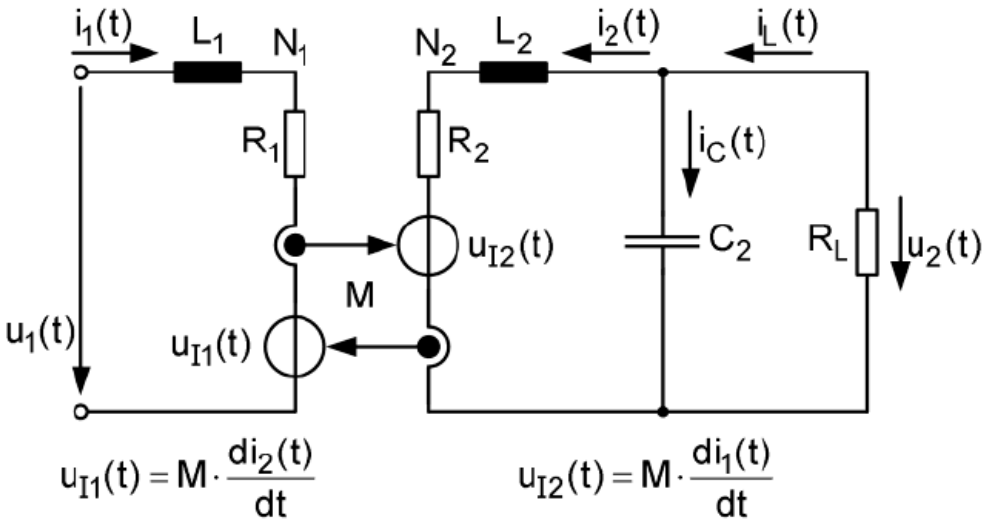

Figure 6.3: CT equivalent circuit

The differences between a CT and a Rogowski coil, for what concerns the transfer function are:

- CT is low resistance terminated, so the TF will be constant between a low corner frequency f_{low} and a high frequency f_{high}. in this case, the frequency looks like a combination of low and high pass filter (bandpass filter).The voltage across the resistor R_L is directly proportional to the current to be measured.

- In Rogowski coil, where a high resistance termination is placed, f_{low} and f_{high} frequencies get the closer the resistance is. With high resistance the damping is low and there is only the resonance frequency f_{res}. In this case, The magnitude has a constant gradient of 20dB/dec and the phase is constant almost up to the resonance frequency. The change in phase is sharper the higher the value of R_L is or the lower the damping factor gets.

6.2.2 CT implementation

Main parameters to take in consideration for the choice of a CT are:

- **Maximum peak current:** This value is based primarily on the voltage-breakdown rating of the connector used. For instance, a 500-volt rating on the connector gives a 5000-ampere peak current rating for a 0.1 volt-per-ampere current monitor.

- **Maximum current-time product and biasing:** All Pearson Current Monitors use ferromagnetic cores which can become saturated by the dc component (average value) of the current (Idc), or by the current-time product (I*t) of the pulses. In case of a pulse the It product is calculated as $I_{maxpeak} * t_{max} = (100000)A * (0.0002)s = 20A * s$ Since the output of the monitor is sustained by the changing flux level in the core, magnetic saturation will degrade performance. As a function of increasing Idc, the effective permeability of the core decreases, causing the droop rate and low-frequency cut-off point to increase. Also, the available flux swing is decreased, reducing the maximum viewable I*t. When viewing a pulse, the output voltage will drop to zero when the integrated value of current with respect to time causes the flux level to reach saturation. The monitor will recover after the applied current returns to zero and the flux returns to its remanent value. [8]

- **Minimum rise time:** The rise-time of the pulse to be viewed should be longer than the rating of the current monitor to avoid excessive overshoot and ringing. The useable rise time of a current transformer is defined with respect to a transition from one current level to another. If the difference between the levels is defined as 100%, then the rise time is the interval from 10% to 90% of the transition. When a fast-rising current transition is applied to a current transformer, it is typical for the output to either overshoot and ring, or rise more slowly than the input current pulse. If the overshoot or ringing amplitude is less than 10% of the transition, the output is considered usable. Therefore, the fastest 10 to 90% transition that causes no more than 10% overshoot and ringing is known as the usable rise time. If the output does not overshoot or ring, then the output voltage rise time becomes the usable rise time. In choosing a current monitor, the specified usable rise time should be less than the rise-time of the current pulse to be viewed. [8]

- **Size:** See figure below. The values are compatible with the place where the CT is to be installed: the top portion of the return conductor in the test rig inside test chamber.

- **Output termination:** An often asked question concerns terminating the output of the monitor with a resistor. Since the monitor can be modelled as a voltage source in series with 50 Ohms, the addition of an external terminating resistance will decrease the output of the unit. For example, a 50 Ohm external termination would reduce the output to one-half.

The model found to meet all previous requirements is the PEARSON 1423 Current Monitor.

Parameter	Required	FK-6328	FK-6330	PEARSON 1423 CT
Max Peak Current [kA]	> 100	1000		500
Current*time [A*s]	> 20			75
Rise time [ns]	< 1420			300
Low frequency 3dB cutoff [Hz]	-	0.161	0.161	0.161
High frequency 3dB cutoff [MHz]	-	0.228	0.233	1.2

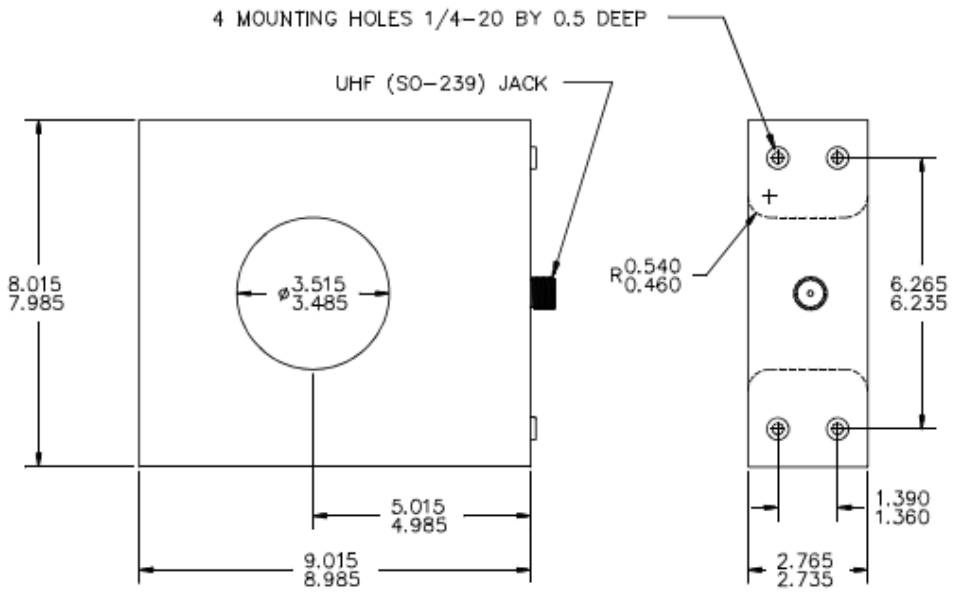

Figure 6.4: PEARSON 1423 CT

'Required values' are based on the standard ideal waveform. It is supposed that the generated waveform by RLC circuit requirements are automatically satisfied. Frequency cut-offs are approximate.

Main advantages of the use of a CT are:

- **Output Sensitivity:** A higher output sensitivity will give a better signal that withstands from background noise. This will especially solve the problem of the low signal produced by the passive output of the integrator. The CT model chosen (see table) has a sensitivity 10 times greater than the passive output of the fk-6328 and 5 times greater that the passive output of fk-6330.

	Coil FK-6328	Coil FK-6330	PEARSON CT 1423
Passive Output	$1*10^{-6} \div 2*10^{-6}$	$2*10^{-6} \div 4*10^{-6}$	$1*10^{-3}$
Active Output	$1*10^{-5} \div 5*10^{-5}$	$2*10^{-5} \div 1*10^{-4}$	

Table 6.1: Sensitivity [V/A]

'Min' values are obtained with LO-LO settings of switches on the integrator module. 'Max' values are obtained with HI-HI settings.

- **No integrator module:** The current transformer does not need an integrator circuit to work and this simplifies the instrumentation complexity and the earth connections. The Ct could be directly connected to an oscilloscope. The higher sensitivity would eliminate also the needing of an amplifier circuit which is the main source of the previous noise problems.

- **Electrostatic Shielding:** All Pearson Current Monitors are double shielded or single shielded. In some models, the outer shield (case) is automatically grounded when the threaded mounting holes are used with metal screws through a grounded bracket. In others the shield is grounded through the cable braid to the oscilloscope. This is a very important feature because it guarantees to have a transducer especially made for high voltage and high noise environment. Is also eliminates the need to build a shielding screen, as we did for Rogowski coils, which has no specifications and has not been tested for EMI shielding properties. However, to meet the requirements for protection from potential radiated noise from 100 kHz (SE $>$ 40 dB), we must follow also the procedures described in the previous section for enclosure.

- **Cabling and shielding:** The CT comes with a UHF (SO-239) cable. Again, to meet the requirements for protection from potential radiated noise from 100 kHz (SE $>$ 40 dB), we must follow also the procedures described in the previous section for cables.

- **Accuracy and Droop:** The standard accuracy for a Pearson Current Monitor is within +1%, -0% of the nominal sensitivity. This accuracy applies to the mid-band response. Droop is the maximum amount to be expected at current levels above a few amperes. Its value for the chosen Ct is $0.7\%/ms$. At low current levels, low initial core permeability may cause higher droop values and a corresponding increase in the low-frequency -3 dB point for some models. Exceptions due to droop and monitor rise-time (low and high frequency cut-off) are particular to each model and are treated separately

in the specification sheet. Rise time is short, ranging between 1 and 100 nanoseconds (10-90% levels) in most cases. [8]

Main disadvantages of using a CT would be:

- **Bandwidth:** The proposed PEARSON 1423 CT has a smaller bandwidth compared with the FK-6328 and FK-6330 coils, especially for what concerns the higher -3dB point. However, it is still possible to use PEARSON 4418 CT with the biasing to achieve a better bandwidth.
- **No Clamping:** The circuit must be opened to insert the CT because it is not clamped. The solution is to place the CT into the test room around the return conductor in the test rig, where both Rogowski coils are placed in TEST 2. The CT could be inserted from the electrode where the circuit is open.

Chapter 7

Conclusions

The study previously done has underlined that the measured signal from Rogowski coil is highly affected by noise which reduces the signal-to-noise ratio (SNR). In this way it is impossible to see the waveform of the impulse and this is of main concern for the study of lightning effects on composite materials.

A good measurement requires that the signal is 'clean' so it is possible to study its rise time, time to 50% and peak value.

A first solution is proposed by numerically filtering the signal. This was done using a Butterworth filter and has helped to increase significantly the SNR. Also a circuit design (Sallen-Key) was proposed to implement the filter permanently after the integrator.

It was demonstrated that the measured waveforms are compatible with ED-84 standards and with a Simulink simulation of the generating circuit.

By comparison between measured waveforms it was possible to determine that measurements differ from a coil (FK-6328) to the other (FK-6330). The hypothesis is that the FK-6328 coil is not working in ideal conditions due to its bigger diameter and floppy shape. Further studies may be done by moving the coil with respect to the conductor to see the consequences on the waveform.

The noise peak (spike) in the initial instants of the signal is synchronous with the signal itself and that is because it is produced by the circuit that generates the impulse. It was demonstrated that this spike varies with respect to the coil position in the circuit and ground connection of the instrumentation.

The problem was to identify the way of coupling with the signal. For this

reason, a test was performed by analysing and comparing the output of two Rogowski coils placed in opposite directions. The results showed that the spike is partly due to the signal and partly to a common-mode noise.

At the end, an alternative solution was proposed in order to substitute the Rogowski coils. PEARSON CT 1423 current monitor was chosen as the model, meeting all requirements on saturation, peak value, hole diameter, bandwidth, accuracy and droop. It allows to produce a significantly increased signal which is supposed to be less affected by low SNR. It does not require and integrator nor amplifier nor filter, allowing to simplify measurement circuits and reduce sensitivity to external noise.

Bibliography

[1] Weiyang Wu Baocheng Wang, Deyu Wang. A rogowski coil current transducer designed for wide bandwidth current pulse measurement. *Power Electronics and Motion Control Conference IEEE 6th International*, Wuhan, 17-20 May 2009, pp.1246-1249.

[2] Adeuyi Oluwole Daniel. *Carbon Composite Materials for aerospace applications*. PhD thesis, Cardiff University, 2012.

[3] Donald W. Yauch David E. Shepard. An overview of rogowski coil current sensing technology. *Grove City (Ohio),LEM DynAmp Inc.*, 2010, pp.1-25.

[4] Kai-Sang Lock Elya B. Joffe. Grounds for grounding: A circuit to system handbook. *Hoboken, Wiley-IEEE Press*, 2010, pp.1-200.

[5] EPCOS. Surge arrester 2-electrode arrester (m51-c90x). *Munich*, 2010, pp.1-3.

[6] Bakran Hain. New rogowski coil design with a high dv/dt immunity and high bandwidth. *Power Electronics and Applications (EPE) 15th European Conference*, Lille, 2-6 Sept 2013, pp. 1-10.

[7] Ray Hewson. The effect of electrostatic screening of rogowski coils designed for wide-bandwidth current measurement in power electronic applications. *Power Electronics Specialists Conference IEEE 35th Annual*, 20-25 June 2004, pp. 1143 - 1148 Vol.2.

[8] Pearson Electronics Inc. Selecting a pearson current monitor. *Palo Alto*, 1991.

[9] Jim Karki. Active low-pass filter design. *Dallas, Texas Instruments*, 2002.

[10] Wolfgang Langguth. Earthing and emc fundamentals of electromagnetic compatibility (emc). *Hemel Hempstead-Brussels*, 2006, pp.15-16.

[11] J. Sanz M. Argueso, G. Robles. Measurement of high frequency currents with a rogowski coil. *Instrumentation and Measurement Technology Conference Proceedings*, Warsaw, 1-3 May 2007, pp.1-4.

[12] D.N. Woodland1 P.N. Murgatroyd. Geometrical properties of rogowski sensors. *IEE Colloquium on Low Frequency Power Measurement and Analysis*, Savoy Place, 2nd November 1994, pp.1-5.

[13] Tektronix. Tds3000c series digital phosphor oscilloscopes. *Beaverton*, 2007, pp.55-100.

[14] Keith Armstrong Tim Williams. Emc for systems and installations. *Oxford, Newnes*, 2000.

[15] David Ward. More about flexible coils. *Harrogate, Rocoil Limited*, 2010, pp.1-5.

[16] Li Hui Yan Bing, Wang Yutian. Research of measurement circuits for high voltage current transformer based on rogowski coils. *Sensors and Transducers, IFSA Publishing*, Hebei (China), February 2014, pp. 35-39 Vol. 165.